eman ta zabal zazu

Universidad del País Vasco
Euskal Herriko Unibertsitatea

Departamento de Fisiología
Facultad de Medicina y Enfermería

The role of transcription factor KLF15 in the etiopathogenesis of biliary cancer: new diagnostic, prognostic and therapeutic strategy

Tesis presentada por

NUNO ANDRE DA SILVA PAIVA

Donostia – San Sebastián

2022

eman ta zabal zazu
Universidad del País Vasco
Euskal Herriko Unibertsitatea
biodonostia
osasun ikerketa institutua
instituto de investigación sanitaria

The role of transcription factor KLF15 in the etiopathogenesis of biliary cancer: new diagnostic, prognostic and therapeutic strategy

Tesis presentada por

Nuno André da Silva Paiva

Para la obtención del título de doctor en

***Investigación Biomédica* por la**

Universidad del País Vasco/Euskal Herriko Unibertsitatea

Tesis dirigida por

Dr. D. Jesús María Bañales Asurmendi

Dr. D. Pedro M. Rodrigues

The project exposed in this thesis was performed at Biodonostia Health Research Institute under the supervision of Dr. Jesús Mª Bañales Asurmendi and Dr. Pedro M. Rodrigues. Likewise, Dr. María Begoña Ruiz Larrea, on behalf of the Faculty of Medicine and Nursing of the University of the Basque Country (UPV/EHU), supported this dissertation.

Nuno André da Silva Paiva was the recipient of a Ph.D. fellowship (*SFRH/BD/147362/2019)*) from *Fundação para a Ciência e a Tecnologia, I. P.* (Portuguese Government, Portugal). This work was funded by Diputacion Foral de Guipuzcoa (2020-CIEN-000067-01) and by Instituto de Salud Carlos III (SCIII; FIS Project PI21/00922).

berrikuntza + ikerketa + osasuna eusko fundazioa
fundación vasca de innovación e investigación sanitarias

Acknowledgments (Agradecimientos)

I would like to thank my supervisors, Dr. Jesús Bañales and Dr. Pedro Rodrigues, for having given me this opportunity to do my doctoral thesis in their group, as well as help me grow professionally and personally thanks to their experience and dedication. To Txus I want to thank his trust and support, as well as his resolution and determination in undertaking this project. To Pedro, the reason I was able to be here doing this today, I owe my eternal gratitude. More than a supervisor, more than a friend, you were family when I was so far away from home and you didn't let me feel so alone. I would not have traveled to another country and changed my whole life if I didn't trust you the way I did. Obrigado de coração, Chico. I would also like to thank Dr. Luis Bujanda for always having a helping help available.

I would also like to thank the FCT for the scholarship granted for this project, as well as the Universidad del País Vasco (UVP/EHU) and Instituto de Investigación Sanitaria Biodonostia for allowing me full dedication to this research.

To all my "Hepato" lab mates, who made it so that these 4 years went by less painfully, more joyfully, and always with a story or a smile to share. I have to thank you all for the time I got to spend with you. Matxus, thank you for your kindness and generosity in giving a helping hand when needed. Ibone, "a minha mãe de viagem", thank you for her honest smile and for her patience when speaking with me despite all the "tonterias" I always said. Aitor, thank you for your always ready smile and for making everyone feel at ease in your presence. And thank you for never mocking me in the beginning when I was still trying to speak Spanish at my own pace. Álvaro, thank you for the incredible number of bad jokes that it should be humanly possible for you to know and for always be able to bring me back up after a rough day with your genuinely positive spirit. Laura, thank you for the laughs in every spare time we had, for always having a solution for any problem we had, for being the perfect travel company and for teaching me how to dance like a guy should! Anne, thank you for your joy! It's not always easy to present ourselves to the world a certain way, sometimes we do it to protect others rather than ourselves. A smile can hide much sorrow, but also shows immense courage and strength. Enara, Irune and Maider, the most recent additions, but not less important! I wish you all the best and thank you for having shared a bit of my path and having filled it with a little bit more color. Ainhoa, thank you for all the mind-blowing and genuinely interesting conversations about almost everything, from gender equality to non-binary and heteronormativity, scientific rigor and ethics, to (etc…). Thank you as well for all the kinds of dance lessons we had, even the breakdancing ones on the disgusting floor of the lab! Pui Yuen, thank you for being one of my first friends here and for making me feel welcome. Thank you for all the crazy, inappropriate and extremely funny conversations we always had. But also, the

deep serious conversations that helped in the tough times. Thank you for turning me into a runner, we still have to race together someday! Aloña, Aloñi! Thank you for your happy energies and for the shots of Patxaran! We knew we could always count on you, because of the amazing person you are, and you can count on us to help you whenever you need. Irene, sis! Mana! What would “Irenu” be without you? Thank you for your annoyingly high motivation and your unique personality and sense of humor. A little improvement could be done in musical, but we can’t have it all, can we? Thank you for being an honorary Olaizola, it’s an honor! Javi, I have to thank you for everything. For the patience in dealing with me while I took so many Nuno’s in the cell culture room. For teaching me how to play “a pala”. For helping me buy my first electric guitar! For sharing so many interests with me in games, sports and music. For being one of the first people who gave a chance to the guy who barely spoke during the first 2 months in the lab. Thank you for allowing me to call you my friend.Paula, la jefa! The person I probably bothered the most in the lab. I don’t even know if I have to apologize more than what I have to thank for. Thank you for your saint-level patience and for having helped me every step of the way. Couldn’t have done it without you, for sure. Thank you for the conversations on music and movies, on teaching about culture and not making me feel bad about my poor Spanish diction for not being able to say the r’s. Thank you for everything! Jon, you’re not Hepato, but in spirit you are! Thank you for having been a part of this with me and for making it impossible to be in a bad mood around you. Thank you for your attempts at teaching me Euskara and for your friendship!

To my friends back home, who supported me through the fog of distance and difficulties of everyday normal life. Filipe, thank you for always being there, through thick and thin. You are my family, not by blood, but by my own choice. Life put us in each other’s path and I am thankful for the support you have given me. Victor, thank you for always taking the time to talk to me and hear me when I am going through something difficult, even when you are in similar shoes to mine with your PhD. I will never be able to thank you enough. You are one of the best people I have had the luck of meeting and I am glad I can call you my friend.

A special thank you to Isabel Cordeiro for creating the artwork for the book cover. A design made by a true artist, with such a special meaning to me and that I found a way to share in new forms.

To my family, the foundation that allowed me to sustain myself during these years and reach the end of this process, I have to thank them my life.

Aos meus pais, nunca teria ultrapassado todos estes desafios sem o vosso amor e apoio constante. Peço desculpa pela preocupação e noites mal dormidas que vos causei. Tudo o que alcancei até hoje vos devo a vós. Amo-vos muito!

Ao meu irmão, Miguel, obrigado pelo teu apoio incondicional. Saber que posso contar contigo quando preciso dá-me a força necessária para enfrentar qualquer desafio. Desculpa se às vezes a minha falta de confiança em mim mesmo leva a que te possa decepcionar. Prometo que este novo caminho que estou a percorrer te vai deixar orgulhoso do irmão que tens, que te ama muito!

To Kathleen, my wife, the love of my life. If you hadn't come into my life when you did, I don't know if I would have had the strength to carry on by myself through what was being asked of me. Having you to come home to at the end of the day was the only thing that made me hold on for dear life throughout most of this path. Without your support, your love, your smile to keep me from crashing down, none of this would have been possible. This is all thanks to you. I love you.

Abbreviations

3D	Three dimensional
5-FU	5-fluoroacil
ABC	ATP-binding cassette
ATP	Adenosine triphosphate
BSA	Bovine serum albumin
CA19-9	Carbohydrate antigen 19-9
CAF	Cancer-associated fibroblasts
CAR	Chimeric Antigen Receptor
CCA	Cholangiocarcinoma
CDK1	Cyclin-dependent kinase 1 (Cdc2)
CDC25A	Cell division cycle 25 homolog A
cDNA	Complementary DNA
CEA	Carcinoembryonic antigen
Cis	Cisplastin
CK19	Cytokeratin 19
COX-2	Cyclooxygenase-2
CT	Computed tomography
DAB	3,3-diaminobenzidine
dCCA	Distal CCA
eCCA	Extrahepatic CCA
ECM	Extracellular matrix
EGF	Epidermal growth factor
EGFR	Epidermal growth factor receptor
EMT	Epithelial-mesenchymal transition
EpCAM	Epithelial cell adhesion molecule
ERBB2	Erb-b2 receptor tyrosine kinase 2
ERCP	Endoscopic retrograde cholangiopancreatography
FBS	Fetal bovine serum
FDA	Food and Drug Administration
FGFR	Fibroblast growth factor receptor
GAPDH	Glyceraldehyde-3-phosphate dehydrogenase
Gem	Gemcitabine
GemCis	Gemcitabine and cisplatin combination
GO	Gene ontology
H&E	Hematoxylin and eosin
HBV	Hepatitis B virus
HCC	Hepatocellular carcinoma
HCV	Hepatitis C vírus
HDAC	Histone Deacetylase
Hh	Hedgehog
HRP	Horseradish peroxidase
HSC	Hepatic stellate cell
IBDU	Intrahepatic bile duct unit
iCCA	Intrahepatic CCA

ICI	Immune Checkpoint Inhibitor
IDH	Isocitrate dehydrogenase
i.e.	Latin: *id est* (it is)
IF	Immunofluorescence
IG-iCCA	Intraductal-growing iCCA
IgG	Immunoglobulin G
IHC	Immunohistochemistry
IL-6	Interleukin 6
iNOS	Inducible nitric oxide synthase
IP	Immunoprecipitation
KIF11	Kinesin-like protein KIF11
LUAD	Lung Adenocarcinoma
MDR1	Multidrug resistant protein 1 or P-glycoprotein
MF-iCCA	Mass-forming iCCA
MOC	Mechanism of chemoresistance
MRI	Magnetic resonance imaging
mRNA	Messenger RNA
MRP	Multidrug resistance-associated protein
mTORC1	Mammalian target of rapamycin complex 1
NAFLD	Non-alcoholic fatty liver disease
NFκB	Nuclear factor kappa-light-chain-enhancer of activated B cells
NBD	Normal bile duct
ncRNA	Non-coding RNA
NEM	N-ethylmaleimide
NHC	Normal human cholangiocytes
NCID1	Notch intracellular domain 1
NK	Natural killer
P/S	Penicillin-streptomycin
PBC	Primary biliary cholangitis
pCCA	Perihilar CCA
PCNA	Proliferating cell nuclear antigen
PDGF	Platelet-derived growth factor
PI-iCCA	Periductal-infiltrating iCCA
PLD	Polycystic liver disease
PSC	Primary sclerosing cholangitis
qPCR	Quantitative polymerase chain reaction
RIPA	Radio-immunoprecipitation assay
ROS	Reactive oxygen species
RTK	Receptor tyrosine kinase
SOX9	(Sex-determining region Y)-box transcription factor 9
SOX17	(Sex-determining region Y)-box transcription factor 2
SDS	Sodium dodecyl sulfate
SDS-PAGE	Sodium dodecyl sulfate polyacrylamide gel electrophoresis
SLC	Solute carrier

SN	Surrounding normal
SS	San Sebastian
T_0	Time zero
TAA	Tumor-associated antigen
TACE	Transarterial chemoembolization
TAMs	Tumor-associated macrophages
TARE	Transarterial radioembolization
TBS-T	Tris-buffered saline with 0.1% Tween® 20
TCGA	The Cancer Genome Atlas
TGF-β	Transforming growth factor β
TIGER	The Thailand Initiative in Genomics and Expression Research
TME	Tumor microenvironment
TSA	Trichostatin A
UMAP	Uniform Manifold Approximation and Projection
WB	Western blot
WNT	Wingless
WT	Wild type
XRCC5	X-ray repair cross complementing 5 (Ku80)

Table of content

Table of figures and tables

Figures

Tables

Introduction

I.1. The liver and the biliary tree

I.1.1. Physiology

The liver is the largest internal organ in the human body, being of pivotal importance in the maintenance of physiological homeostasis.[1] The liver performs multiple and complex metabolic functions including carbohydrate, lipid, bile acid and amino acid metabolism, and is deeply involved in the synthesis and secretion of plasma proteins into the bloodstream (e.g., albumin, transferrin, fibrinogen, apolipoproteins, among others.[2] Bile production and secretion constitutes a vital function of the liver, being essential for biliary clearance of organic and inorganic solutes, as well as for nutrient digestion and absorption in the gut.[3] The liver receives a dual blood supply (i.e., from both the hepatic portal vein and the hepatic artery), being exposed to a high number of toxic compounds. In this matter, the liver has the ability to metabolize potentially harmful biochemical byproducts generated in the human body (e.g., bilirubin or ammonia), consequently contributing to their secretion and clearance.[2,4] Thanks to the unique regenerative capability of the liver, hepatic functions are maintained even after extensive liver damage or partial resection, ensuring the proper control of whole-body homeostasis.[5]

I.1.2. Macroscopic and microscopic anatomy

At the anatomical level, the liver is structured into two large lobes (i.e., right and left) and two small central ones (i.e., quadrate and caudate), which are mostly covered by a fibrous layer, known as the Glisson's capsule.[2,6] The liver parenchyma is organized in thousands of hexagonal units designated as hepatic lobules (**Figure I.1**).[2] Each hepatic lobule represents the functional and structural unit of the liver, consisting of a central vein from which hepatocytes radiate, forming linear cords towards a portal triad, which is constituted by the connective tissue surrounding branches of the hepatic artery, the portal vein and the bile duct (**Figure I.1**).[6] Oxygen, nutrients, bile acids and hormones delivered by venous and arterial blood from the terminal branches of the portal vein and hepatic artery, respectively, reach the lobule's central vein by seeping through the hepatic sinusoids (**Figure I.1**).[2] In a similar manner, hepatocyte-secreted bile reaches the bile duct branches at the portal triad through a network of canaliculi.[2] The sinusoidal capillaries are situated between the cords of the hepatocytes separated by a narrow perisinusoidal space (also known as the space of Disse), which comprises reticular fibers

and nutrient-rich blood plasma. Of note, direct contact between sinusoidal capillaries and hepatocytes is important to improve the metabolic exchanges.[2]

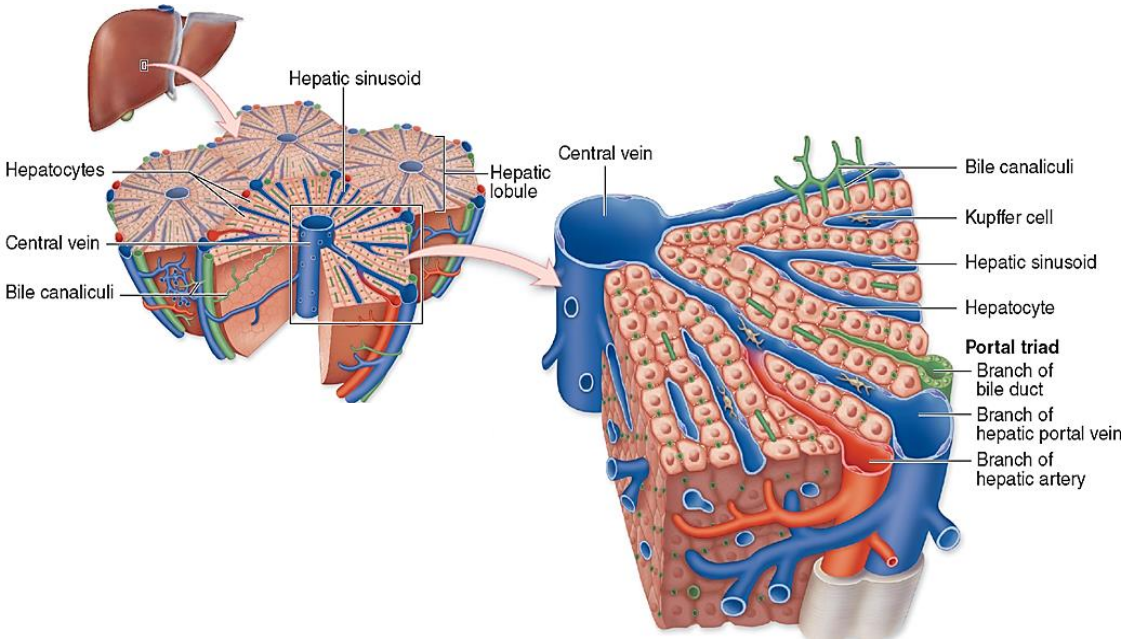

Figure I.1. Microscopic structure of the liver. The liver is ordered in hexagonal hepatic lobules composed of lines of hepatocytes radiating from the central vein outwards to the portal triads. (Adapted from Mescher AL, 2013)[7]

Different parenchymal and non-parenchymal cells coexist within the liver and coordinate the hepatic functions at multiple levels.[1,2] Hepatocytes and cholangiocytes are the two main epithelial cell types in the liver. Roughly, 70-80% of liver volume consists of parenchymal hepatocytes, which are responsible for most of its metabolic functions, while cholangiocytes, the epithelial cells lining the bile ducts, represent only 3-5% of total liver cell number, even though they carry out crucial functions in bile transport and modification.[1,2] Non-parenchymal hepatic include the liver resident macrophages, also known as Kupffer cells, hepatic stellate cells and sinusoidal endothelial cells, among others, which are involved in immunological, fibrogenic and metabolites and gases exchange processes, respectively.[1,2]

I.2. The biliary tract

I.2.1. Anatomy

The biliary tract is comprised of numerous ducts lined by cholangiocytes that regulate the production, composition and transport of the bile from the liver to the duodenum. As previously mentioned, primary bile is secreted from the hepatocytes into the canaliculi

(i.e. a narrow tubular space between the apical membranes of two adjacent hepatocytes) and is subsequently collected by the canals of Hering, reaching the ductule-canalicular junction.[8] These specialized channels serve as the anatomical and physiological transition from the hepatocyte-lined canaliculi to cholangiocyte-lined ductules (<15 µm), which ultimately form the biliary tree (**Figure I.2**).[8,9] These small structures converge sequentially at the portal space to form the interlobular ducts (15-100 µm), progressively enlarging and forming septal ducts (100-300 µm), area ducts (300-400 µm) and segmental ducts (400-800 µm).[8,9] The bile collected from the right and left lobes is then drained to the corresponding hepatic ducts (>800 µm), which are considered the limit of the intrahepatic biliary tree.[8,9] Ultimately, the bile flows through the extrahepatic biliary tree (i.e., common hepatic duct, cystic duct, gallbladder, and common bile duct) reaching

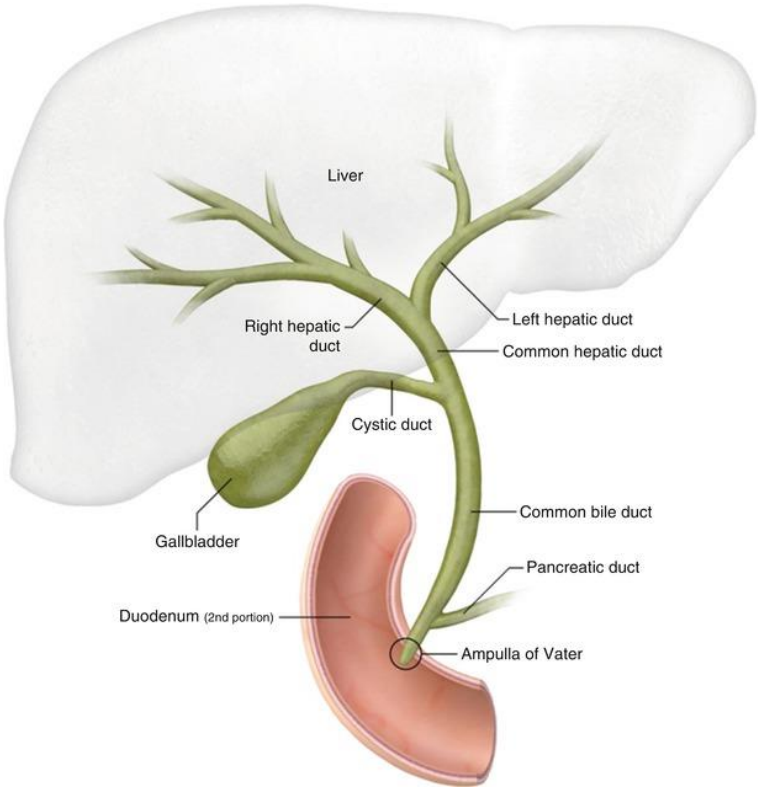

the duodenum (**Figure I.2**), where it facilitates lipid digestion and absorption.[8,9]

Figure I.2. Biliary tract architecture. The biliary tract consists of a network of intrahepatic and extrahepatic tubular ducts where the hepatocyte-secreted bile is modified and transported to the duodenum.[10]

I.2.2. Cholangiocytes

Cholangiocytes constitute a small proportion of all liver cells but play a very important role in health and disease. Biologically, these epithelial cells are essential for normal liver function and are key in regulating hepatocyte-derived bile composition, facilitating biliary

salt reabsorption, and contributing to its fluidification and alkalinization. Multiple transmembrane carriers (i.e., aquaporins, transporters and exchangers) are usually found at both the apical and basolateral membranes of cholangiocytes, being involved in the regulation of bile composition and biliary bicarbonate secretion,[3,11–13] as well as in the protection of those cells from harmful or toxic agents.[14,15]

Additionally, cholangiocytes contain a primary cilium, which is a microtubule-based organelle that protrudes from the apical plasma membrane into the ductal lumen.[16–18] This structure possesses mechano-, chemo- and osmo-sensory properties that allow the detection of changes in bile flow and composition, thus modulating bile formation.[19,20] Importantly, the basal body within the primary cilium derives directly from the mother centriole necessary to form the mitotic spindle,[21] which implies a relevant function of this organelle in the control of cholangiocyte cell cycle progression and proliferation.

I.2.3. Cholangiopathies

Biliary diseases, also designated as cholangiopathies, encompass a large group of chronic liver diseases that target primarily cholangiocytes.[13] Cholestasis, chronic inflammation, ductular reaction and fibrosis appear to be common events among biliary disorders. Cholangiopathies are generally classified in different categories according to their etiology in: a) immune-mediated [such as primary biliary cholangitis (PBC)[22] or primary sclerosing cholangitis (PSC)],[23] b) infectious (e.g., *Cryptosporidium parvum*, *Opisthorchis viverrini*, *Clonorchis sinensis*),[24] c) genetic [e.g., polycystic liver disease (PLD),[25] cystic fibrosis[26] or Alagille's syndrome],[27] d) vascular (post-ischemic cholangiopathies),[28] e) neoplastic [e.g., biliary tract cancer or cholangiocarcinoma (CCA)], f) drug-induced [e.g., amoxicillin/clavulanic acid, carbamazepine, 5- fluorouracil (5-FU), among others],[29,30] or g) idiopathic (e.g., biliary atresia, idiopathic childhood/adulthood ductopenia).[13] Despite being considered rare diseases, cholangiopathies account for substantial morbidity and mortality, being a major indication for liver transplantation.[22,31,32] Therefore, elucidating the molecular mechanisms underlying the development and progression of these diseases is essential to find potential therapeutical targets.

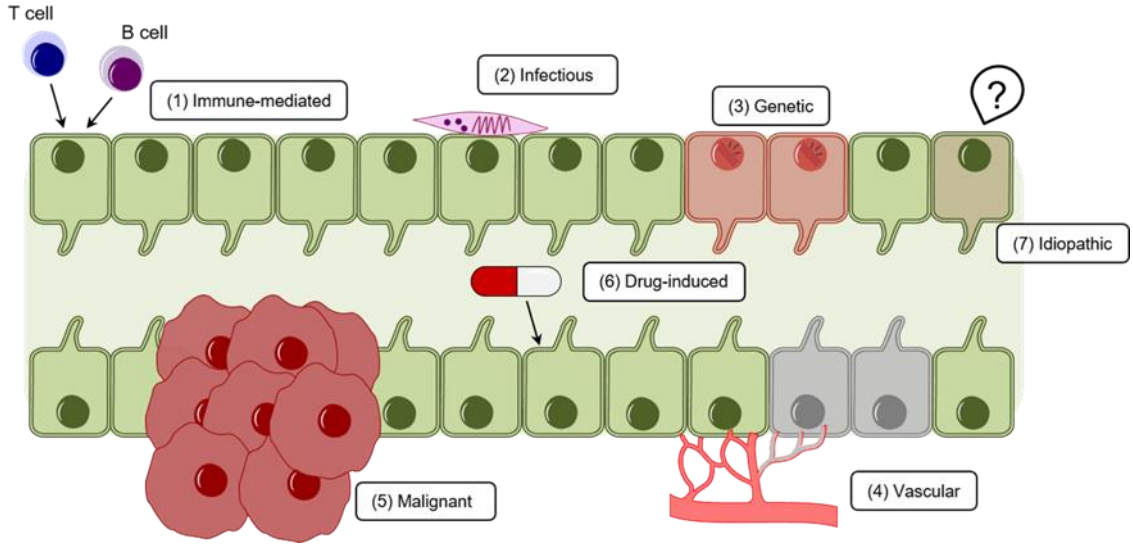

Figure I.3. Classification of cholangiopathies according to their etiology. Cholangiopathies are chronic liver diseases that affect cholangiocytes and are categorized as (1) Immune-mediated, (2) Infectious, (3) Genetic, (4) Ischemic, (5) Malignant, (6) Drug-induced and (7) Idiopathic.

I.3. Cancer of the biliary tree: cholangiocarcinoma

I.3.1. General Features

Cholangiocarcinoma (CCA) comprises a heterogeneous group of malignancies occurring along the biliary tree. These tumors may emerge from the malignant transformation of the epithelial cells lining the bile ducts, although it can also derive from peribiliary glands, hepatic stem cells or even hepatocytes undergoing transdifferentiation.[33] CCA is the second most frequent primary liver tumor (~15%), after hepatocellular carcinoma (HCC), and represents ~3% of all gastrointestinal cancers, contributing to approximately 2% of all cancer-related deaths yearly and being a major health problem worldwide. CCAs are highly desmoplastic tumors, characterized by an extensive tumor microenvironment (TME), mostly composed of cancer-associated fibroblasts (CAFs), a complex group of inflammatory cells including macrophages, neutrophils, natural killer (NK) cells and T cells which supports the epithelial proliferation of malignant cholangiocytes, consequently fueling tumor growth.[34]

I.3.2. Classification

Taking into consideration the anatomical origin, CCAs are classified into intrahepatic (iCCA), perihilar (pCCA) and distal (dCCA).[35,36] iCCAs can emerge from any portion of the intrahepatic biliary tree, from the smallest branches, called bile ductules, to the

second-order bile ducts, also known as segmental bile ducts (**Figure I.4**). They account for 10-20% of all CCA malignancies, making them the least common of the three subtypes. pCCAs, previously designated as Klatskin tumors due to their characterization by Klatskin in 1965, can occur between the second-order right and/or left hepatic bile ducts and the insertion of the cystic duct into the common bile duct.[37] Comprising 50 to 60% of all cases, pCCAs are the most typical subtype of CCA. Lastly, dCCAs can be found in the common bile duct, below the cystic duct to the ampulla of Vater, where the bile duct and the pancreatic duct connect, and account for 20-30% of all bile duct cancers. Up until recently, pCCAs and dCCAs had been collectively referred to as extrahepatic cholangiocarcinomas (eCCAs), although such nomenclature is now strongly discouraged.

Each anatomic subtype is associated to different risk factors, genetic aberrations, growing patterns, clinical presentations, diagnostic strategies, therapeutic options, prognosis, and clinical management, thus representing independent entities.

According to their pattern of growth, iCCAs can be further subdivided, into mass-forming (MF-iCCA), periductal infiltrating (PI-iCCA) and intraductal growing (IG-iCCA) tumors, although mixed growth patterns have also been described (**Figure I.4**).[38] MF-iCCAs are characterized by a mass of tumor cells affecting both the biliary duct and the liver parenchyma.[39] By contrast, PI-iCCAs grow longitudinally along the wall of large bile ducts, leading to progressive wall thickening and narrowing development,[36,40,41] while IG-iCCAs present a papillary growth pattern towards the duct lumen.[40,42] On the other hand, pCCAs and dCCAs largely present as poorly defined sclerosing tumors and, less frequently, as papillary tumors, exhibiting similar growth patterns to PI- and IG-iCCAs.[35,43,44]

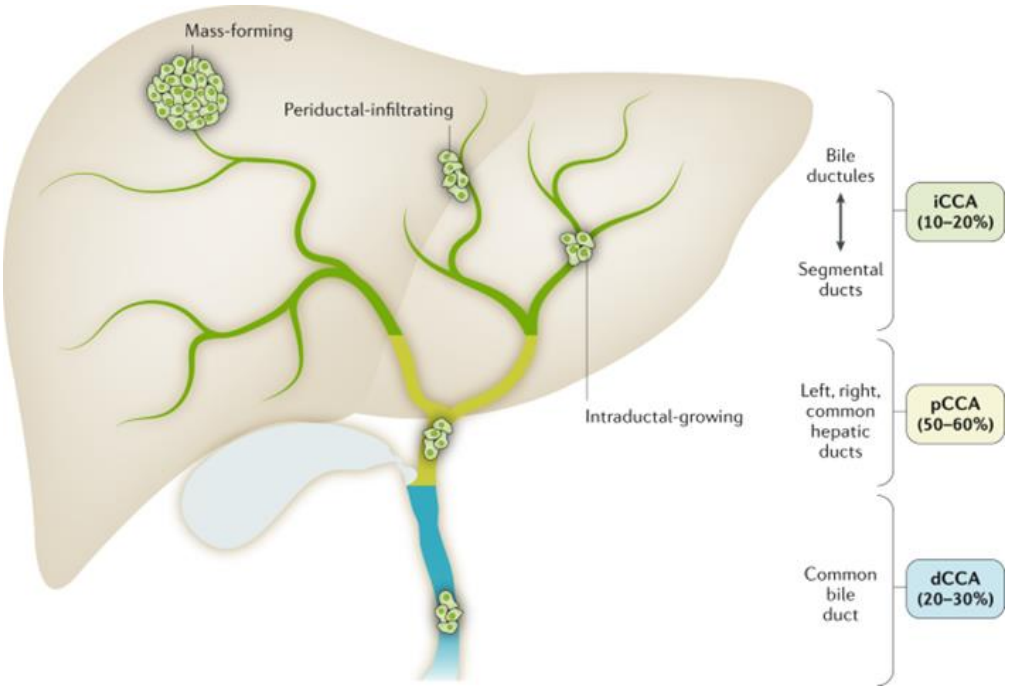

Figure I.4. CCA classification. Depending on their anatomical site of origin, CCAs are classified as intrahepatic (iCCA), perihilar (pCCA) or distal (dCCA). iCCAs can also be classified into mass-forming, periductal infiltrating or intraductal growing according to their growth pattern.[36]

Histologically, pCCAs and dCCAs are predominantly mucinous adenocarcinomas or papillary tumors,[41,45] while iCCAs are more heterogeneous, showing several histological variants. In this regard, two major histological subtypes of iCCA are normally identified according to the level or size of the affected bile duct. Thus, small bile duct (mixed) iCCAs appear as a small-sized tubular or acinar adenocarcinoma with nodular growth invading the liver parenchyma, with minimal or no mucin production.[46–50] In comparison, the large bile duct (mucinous) type affects large intrahepatic bile ducts and is characterized by mucin-producing columnar tumor cells arranged in a large-duct or papillary architecture.[47,51–53] The difference between small and large bile duct types not only has histopathological implications but also distinguishes iCCA subtypes with different clinicopathological and molecular features.[47,48]

I.3.3. Epidemiology

The global epidemiological trends of CCA over the past decades show an increase in both incidence (0.3-6 per 100,000 inhabitants per year)[54–56] and mortality (1-6 per 100,000 inhabitants per year) throughout the last decade.[36,57–59] Despite being still considered a rare tumor in most Western countries (<6 cases per 100,000 people), the

geographical distribution of CCA globally is asymmetrical, with Southeast Asian countries, such as China, South Korea, Thailand and Japan, presenting significantly higher incidence rates.[36,58,60]

Asymmetrical trends in CCA were also seen among its different subtypes, in the last decades. Recent reports show an increased incidence of iCCA and an opposite tendency for eCCA, implying a potential improvement in iCCA identification due to advances in diagnostic techniques and/or changes in related risk factors.[61] Nevertheless, possible explanations for this phenomenon can be complex and the reported incidence rate fluctuations have to be interpreted with a degree of caution. In fact, previous coding systems (including ICD-10) lacked an independent code for pCCA, the most common type of CCA, being sometimes classified as either iCCA or dCCA.[62]

In a similar way, the annual mortality rates caused by CCA have a heterogeneous distribution worldwide, with Latin America, Lithuania and the Czech Republic showing the lowest mortality rates (<2 deaths per 100,000 people) and Japan, Hong Kong and Austria registering the highest (>4 deaths per 100,000 people) (**Figure I.5**).[36,59] CCA mortality in countries/regions showing the highest incidence rates, such as South Korea, Taiwan, China and Thailand, has yet to be reported, so futures studies regarding this are necessary.

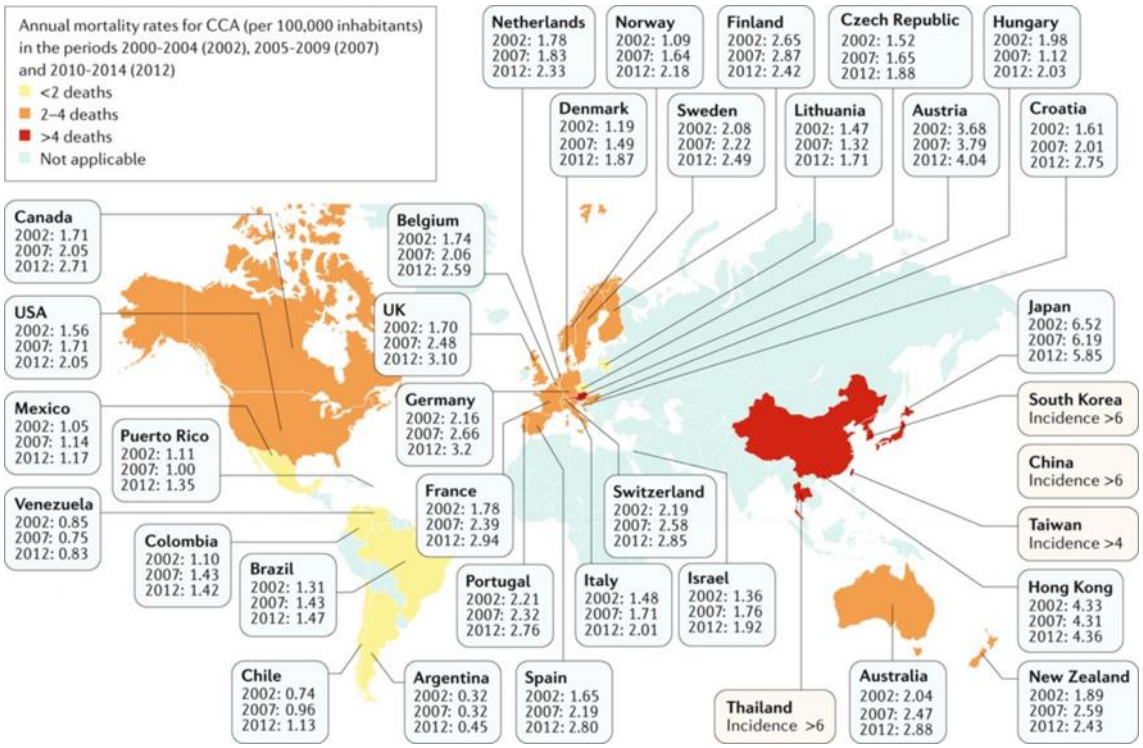

Figure I.5. Age-standardized annual mortality rates of CCA worldwide.[36] Mortality rates including iCCA, pCCA and dCCA are reported, from 2000 to 2014. Yellow-filled countries/regions indicate low mortality (<2 deaths per 100,000 people), orange-filled countries/regions indicate mortality between 2 and 4 deaths per 100,000 people and red-filled countries/regions indicate high mortality (>4 deaths per 100,000 people). Incidence is displayed in highly prevalent CCA regions where mortality rates were not reported.

I.3.4. Risk Factors

The etiologies of most CCAs are unknown; however, several risk factors with different degree of predisposition for the development of CCA have been established.[58,63] The presence of certain biliary pathologies are known risk factors. Choledochal cysts, a congenital condition in which a cystic dilatation of the intrahepatic and/or extrahepatic biliary tree occurs,[64] is a rare inherited disease more prevalent in Asian populations that can predispose for the development of CCA at a young age (mean age of 30 years), with slightly more predisposition for eCCA (**Figure I.6**).[63] The presence of calculi (i.e., gallstones) all along the biliary tree and the common bile duct can also result in added risk of developing CCA,[63] with hepatolithiasis (i.e., presence of calculi within the intrahepatic biliary tree) being more frequent in Asia than Western countries and having a strong association with iCCA.[65]

Primary sclerosing cholangitis (PSC) is a chronic cholestatic and immune-mediated disorder of unknown etiology, where there is a development of multifocal fibroinflammatory biliary strictures that might lead to intra- and/or extrahepatic bile duct

obstruction.[66] It is highly associated with CCA, being the lifetime risk of CCA development for patients with PSC 400-fold higher than the general population with 10-20% of these patients presenting CCA during their lifetime.[67] In parallel, Caroli's disease is a rare autosomal recessive congenital condition characterized by non-obstructive saccular or fusiform dilatation of larger segmental intrahepatic bile ducts.[68] It also predisposes for CCA development, being one of the strongest risk factors associated with both iCCA (38-fold higher risk) and eCCA (97-fold higher risk).[69]

In addition, viral infections due to hepatitis B (HBV) and hepatitis C virus (HCV), as well as liver fluke parasites, such as *Opisthorchis viverrini* and *Clonorchis sinensis*, have been reported to augment the risk of CCA development (**Figure I.6**). This can also explain the disparity in the geographical distribution of CCA incidence rates, as liver fluke parasites are endemic to Southeast Asia, and also a high prevalence of HBV and HCV infections in Asia is observed.[55,70–72]

Other types of liver disorders can raise the risk of CCA. Cirrhosis, which has already been established as a risk factor for HCC, has also been found to increase the odds of CCA development, predominantly towards iCCA (**Figure I.6**).[63] Hereditary hemochromatosis, a disorder in which the body suffers an iron overload, leading to secondary tissue damage in several organs, including the liver,[73] was found to increase the risk of iCCA development (2.07-fold), with no association found for eCCA.[69]

Diseases affecting other parts of the gastrointestinal (GI) tract have also been shown to increase the risk for CCA development. Inflammatory bowel disease (IBD) is a form of chronic inflammation of the GI tract which encompasses two conditions, Crohn's disease, and ulcerative colitis (UC). It is suggested that the inflammatory conditions generated in the digestive tract can lead to bile duct inflammation, leaving patients with IBD at risk of developing CCA, being this association stronger in the case of patients with UC (**Figure I.6**).[55] However, since 70-80% of patients with PSC have concomitant UC, the association of IBD with CCA may be dependent on the presence of PSC, making it necessary to prove the direct impact of IBD on increasing CCA risk.[55] Chronic pancreatitis is a disorder consisting of episodic pancreatic inflammation leading to considerable fibrosis, resulting in chronic pain, as well as both exocrine and endocrine insufficiency of the pancreas.[74] It was positively associated with CCA, with more prevalence towards eCCA (OR=6.61) than iCCA (OR=2.66).[69]

Metabolic and endocrine disorders are also included as CCA risk factors, although due to their frequent co-occurrence, the independent impact of the overlapping conditions on the risk increase needs furthers clarification. Type 2 diabetes has been extensively

shown to be associated with increased risk of CCA development.[69,75] Non-alcoholic fatty liver disease (NAFLD), which is the most prevalent cause of chronic liver disease in Western countries,[76] has also been described as predisposing for CCA development, particularly iCCA (**Figure I.6**).[77,78] Obesity, being a major public health issue due to its prevalence in modern society, has been analyzed for associations as an independent risk factor for CCA. However, results have been controversial, as there is disparity between geographical regions, with a positive association with CCA in Western countries that does not seem to be observed in Asian populations.[79–82] A recent study including populations from both of the previous geographical areas did not find any association with either type of CCA.[63]

Exposure to certain toxins and compounds (Thorotrast,[83,84] asbestos,[85,86] 1,2-dichloropropane,[87] dioxins or nitrosamines[36]) has also been associated with CCA (**Figure I.6**). On the other hand, life-style behaviors can also present themselves as significant risk factors due to their higher prevalence.[36] Such a case is heavy alcohol consumption, which is strongly associated with both iCCA (OR=3.15) and eCCA (OR=1.75).[63] Tobacco smoking is also moderately associated with CCA development risk.[88]

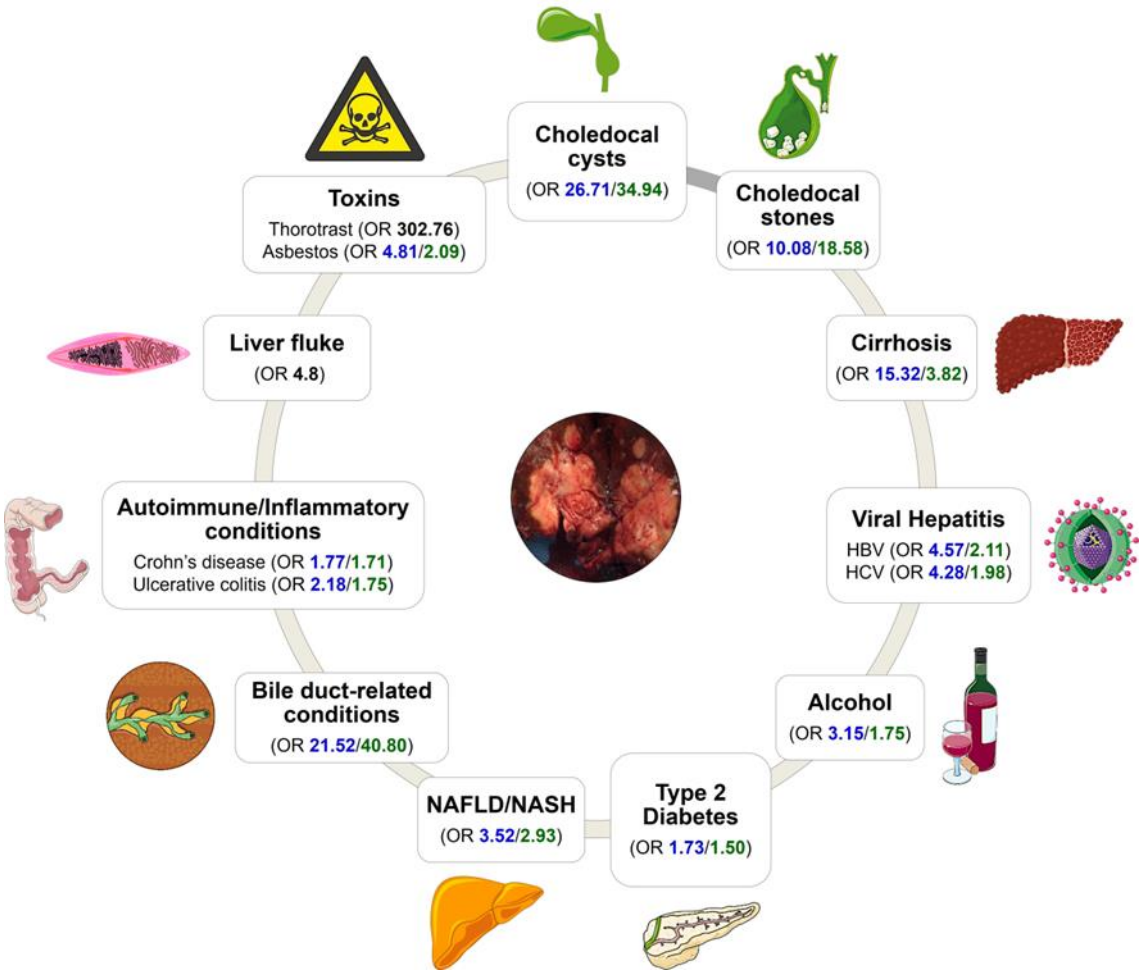

Figure I.6. Risk factors for iCCA and eCCA. Blue ORs are assigned to iCCAs while green ORs refer to eCCAs. Black ORs report the risk for CCA regardless the anatomical origin of the tumor. HBV, hepatitis B virus; HCV, hepatitis C virus; NAFLD, non-alcoholic fatty liver disease; NASH, non-alcoholic steatohepatitis; OR, odds ratio.[78]

I.3.5. Clinical presentation: diagnosis and prognosis

CCAs are generally asymptomatic in early stages, being usually diagnosed at advanced phases (~70%), when disease is already widespread. Although there are no specific symptoms associated with early CCA development, abdominal pain, malaise, fatigue, pruritus, severe weight loss and/or jaundice, among others, might appear during tumor progression.[89,90]

Diagnosis is usually conducted by a combination of different methods, as no single method other than biopsy followed by histological/cytological analysis is sufficient to give a definitive diagnosis in most cases.[60,89] Complementary minimally- and non-invasive methods are employed in parallel to biopsy/histology/cytology, as they can also bring added value in other aspects such as prognosis or response to treatment.[91–93]

Serum levels of biliary tract-excreted products such as bilirubin, alkaline phosphatase (ALP), gamma-glutamyl transpeptidase (GGT), 5'-nucleosidase or cholesterol often increase in patients with CCA, due to the obstructive cholestasis generated, forcing bile into the bloodstream, and causing jaundice and pale stools. However, the most common markers for liver damage, alanine transaminase (ALT) and aspartate transaminase (AST) can remain normal, particularly in the early stages of tumor development and in the absence of cirrhosis.[89] Carbohydrate antigen 19-9 (CA19-9) and carcinoembryonic antigen (CEA) are unspecific tumor markers broadly used, which are found to be increased in patients with CCA under advanced stages.[93] Unfortunately, they lack the sensitivity and specificity needed for early diagnosis, since at early CCA tumor stages, their levels rarely go above the diagnostic cut-off value (37 IU/mL for CA19-9; 5 IU/mL for CEA), discrediting any possible usefulness for early screening. Also, other non-malignant bile duct conditions can increase CA19-9 serum levels.[94] In addition, 7% of the general population do not express the CA19-9 epitope (*i.e.*, Lewis antigen negative individuals), limiting even more its diagnostic usefulness.[94,95] By themselves, these serum tumor markers are insufficient for diagnosis, but can complement imaging methos in supporting a possible CCA diagnosis.

However, when considering their prognostic value, it was shown that high levels of CA19-9 in patients with resectable tumors was associated with worse post-operative survival.[92,96] In a similar manner, it was shown that CEA serum levels could independently predict post-operative survival upon resection in patients with iCCA.[97,98] Regarding predicting response to treatment, CA19-9 serum levels below 1000IU/mL have been associated with improved response to gemcitabine-based therapy, with an over 50% reduction during treatment being reported as a good prognosis indicator.[99] This shows that, although lacking in diagnostic accuracy, specially at early stages, these tumor biomarkers still have use for their prognostic value.

In terms of imaging methods, standard protocol involves non-invasive abdominal imaging to visualize the liver to detect suspicious masses, followed by cholangiography imaging of the bile duct. The diagnostic accuracy of this approach is affected by tumor size, anatomical location and tumor growth patterns.[91] Ultrasonography (US) can identify bile duct dilatation and obstruction. This method has a high detection rate for iCCA, although with a risk of misclassification between iCCA and HCC, due to the anatomical location.[100] For extrahepatic biliary malignancies, it is highly accurate at identifying dCCA, while pCCA identification proves to be more difficult.[101] Computed tomography (CT) scanning is seen as the imaging standard for CCA characterization. While large masses and ductal dilatation can be detected for tumor size measurement, in the cases

of lesions smaller than 1 cm, or in the presence of cirrhosis or abnormal morphological features, the characterization of the tumor is more difficult.[101]

Magnetic resonance imaging (MRI) possesses comparable diagnostic accuracy and characterization capability to CT scanning.[102] With this approach, more comprehensive imaging protocols that not include the liver but also the biliary tree and pancreas can be applied to discard other malignancies such as pancreatic adenocarcinoma.[103] In this way, MRI gives the possibility of performing magnetic resonance cholangiopancreatography (MRCP).

Positron emission tomography (PET), particularly ^{18}F-fluorodeoxyglucose PET (^{18}FDG-PET), is a reliable method for accurate CCA tumor detection, dissemination screening and distinction between malignant and benign structures. Nevertheless, it can result in false-positives in cases such as biliary inflammation, or false-negatives, with cases of misdiagnosis of mucinous tumors. Due to this, it is currently more geared towards disease staging and tumor recurrence rather than diagnosis.[104]

Cholangiograms allow direct imaging of the bile ducts, which is sometimes necessary for confirmation of CCA presence. In the clinical settings, endoscopic retrograde cholangiopancreatography (ERCP) and MRCP are the standard cholangiography methods, with percutaneous transhepatic cholangiography (PTC) becoming more popular.[105] Both ERCP and PTC make it possible to obtain tumor material for histologic/cytologic studies. Unlike the previous, MRCP is a non-invasive imaging technique for the accurate assessment of biliary system. In addition, ERCP also allows to place stents for relieving bile duct obstruction when the affected area is close to the small intestine.[106]

Biopsy with histological analysis confirmation remains the only unequivocal way to obtain a CCA diagnosis, for staging of the disease and to detect specific genetic abnormalities that could guide the course of treatment.[60,89] Sample collection method depends on tumor location, and biopsy sensitivity depends on multiple factors, such as tumor location, size, clinician expertise and representativeness of the collected sample.[89] Its main limitation is sensibility, which due to the quality and quantity of the cytological samples being reduced, does not allow for a negative cytological result to automatically exclude the presence of CCA.[60,107] As an alternative, fluorescence *in situ* hybridization (FISH) polysomy test in cytology samples has been shown to improve the sensitivity for detection of malignancy while maintaining high specificity.[108]

Late diagnosis, combined with the high aggressiveness and chemoresistant nature of these tumors, leads to poor patient prognosis, with 5-year survival rates between 7-20%

and with median overall survival (mOS) below 12 months.[36,109–111] With surgical resection being the main potentially curative option, achieving a successful course of treatment still depends on the success of the surgery and lymph node invasion.[111] Recurrence after surgery is a common event in CCA, being reported in 49% to 70% of cases, and with relapses occurring fairly early, usually 2 to 3 years post-surgery.[60,112,113]

I.3.6. Molecular mechanisms of pathogenesis

Biliary tumorigenesis requires the combination of multiple complex mechanisms to drive malignant transformation of cholangiocytes. Among them, sustained proliferation, death evasion, neo-angiogenesis, as well as the development of invasive and colonizing capabilities are some of the main hallmarks of CCA cells,[114] which are regulated by genetic, epigenetic and molecular alterations.[36]

I.3.6.1 Genetic and Epigenetic modifications

Several studies, using whole and targeted DNA sequencing approaches, have highlighted the genomic complexity of CCA tumors. In this regard, although CCA tumors were shown to be highly heterogeneous at the genomic level, several mutations in genes necessary for cell growth promotion (KRAS, BRAF, SMAD4, FGFR1-3, EGFR, NOTCH, WNT), DNA rearrangements and genomic instability (TP53, CDK1NA, CCND1, ATM, ROBO2, BRCA1 and BRCA2), de-ubiquitination (BAP1) and chromatin remodeling (ARID1A, ARID1B, ARID2A, SMARCA4, PBRM1, MLL2, MLL3, KMT2C).[36] Additionally, mutations dysregulating the Wnt/β-catenin (such as *RNF43*[115,116], *AXIN1*, *APC*, *CTNBB1*[117]) or PI3K signaling networks (such as ROS tyrosine kinase fusions)[118] have been reported.

Although displaying shared mutations, the distinct CCA subtypes present different genomic profiles. Thus, FGFR-fusions together with TP53, KRAS, IDH1/2 and BAP1 mutations are the most common genetic alterations in iCCAs, while PRKACA and PRKACB fusions, as well as mutations in ELF3 preferentially occur in p/dCCAs.[119,120] Integrative genomic studies have also aimed to stratify CCA human tumors based on prognosis.[121,122] In this regard, mutations in TP53 or KRAS have been associated with higher tumor recurrence and lower OS in patients with CCA upon surgical resection,[120] compared to patients with IDH mutations or patients without mutations in any of those 3 genes. Additionally, although most CCA tumor mutations are somatic, a proportion of

patients (5-10%) harbor germline mutations in BRCA1/2, ATM or BAP1, which can predispose to CCA development.[123,124]

At the epigenetic level, dysregulated DNA methylation, histone modifications and abnormal non-coding RNA (ncRNA) expression can also trigger the disproportionate transcription of a number of genes capable of sustaining malignant cell transformation without modifying the DNA sequence.[125,126] Integrative genomic and epigenomic studies have been able to stratify and identify different CCA clusters based on their transcriptomic and DNA methylation profiles. A previous study reported four distinct clusters of CCA, with distinct mutational and even epigenetic dysregulation patterns, such as targeting of either the CpG islands or CpG shores.[127] Another study described four iCCA subgroups also through integrative analysis, finding prognostic value between the different transcriptomic and DNA hypermethylation profiles.[128] At the level of histone modifications, histone deacetylases (HDACs) play a role in chromatin organization by regulating histone acetylation. Although these modifications have been less studied in CCA, HDACs have been shown to be upregulated in CCA, correlating with worse prognosis.[129,130]

With ncRNAs accounting for most of human RNA, they were bound to play a regulatory role within the cell. Among them are included microRNAs (miRNAs or miRs) and long non-coding RNAs (lncRNAs). In CCA, they have been shown to affect many of the hallmark processes of tumorigenesis, from cancer proliferation to metastasis and EMT, through aberrant expression of ncRNAs such as oncogenic miR-21[131] and miR-191[132] or tumor suppressor miR-34a[133] and miR-122[134]. Ciliary loss, an event that happens in cholangiocytes upon malignant transformation, can also be affected by miRNA dysregulation.[135]

I.3.6.2 Signaling and molecular networks

CCAs often emerge during prolonged biliary inflammation and cholestasis, which provide a rich environment of pro-inflammatory cytokines, growth factors and toxic bile acids, thus contributing to cholangiocarcinogenesis.[36,136,137] This setting likely generates aberrant signaling pathways, leading to uncontrolled cellular proliferation, survival, angiogenesis and invasion, in turn promoting CCA development and sustaining its progression (**Figure I.7**). Transcriptomic profiling of CCA tumors identified two subclasses of iCCA: the “inflammation” (38%) and “proliferative” (62%) subtypes, characterized by the activation of immune-mediated and oncogenic pathways, respectively.[121] Among the pro-inflammatory cytokines sustaining CCA growth and

progression, interleukin 6 (IL-6) is a major player, being involved in the activation of the JAK/STAT3, ERK1/2 or the mitogenic p38 signaling pathways, enhancing tumor proliferation and growth.[138–141] On the other hand, different signals [e.g., inducible nitric oxide synthase (iNOS) activation, bile acids, oxysterol, among others) may induce the expression of inflammatory mediator cyclooxygenase-2 (COX-2), causing uncontrolled proliferation and preventing apoptosis through prostaglandin E2-mediated AKT mechanisms.[142–145]

Multiple signaling networks participating in biliary development during embryogenesis, including Notch, Wnt/β-catenin, Hedgehog (Hh) or Hippo/YAP, re-activate during liver repair or in an inflammatory setting.[146] In CCA, a significant overactivation of the Notch, Wnt/β-catenin and transforming growth factor-β (TGF-β) pathways was observed in comparison to HCC, which suggests a major role of these developmental pathways during cholangiocarcinogenesis.[147]

The Notch pathway mediates biliary repair, growth and hepatocyte transdifferentiation into cholangiocytes during carcinogenesis.[148,149] Overexpression or abnormal expression of the Notch receptors has been observed in all types of CCA (i.e., iCCA, pCCA and dCCA),[150–153] with receptors Notch 1, 3 and 4 being associated with poor survival, [150,152] while Notch 2 correlates with low grade tumor differentiation.[150] iCCA development has been achieved in mouse models through experimental overexpression of Notch intracellular domain 1 (NICD1) in hepatocytes.[148,154] Using another mouse model of CCA that involves activated forms of AKT and YAP proto-oncogenes, it was shown that AKT/YAP-induced CCA development derived from hepatocytes, in a manner strictly dependent on Notch signaling pathway *in vivo*.[155] By deleting *Notch2* in that animal model, the induced tumors changed from a malignant iCCA phenotype to hepatocellular adenoma-like lesions, while inactivation of *Notch1* did not cause any phenotypical alterations. This showed that in AKT/YAP-induced iCCA formation, it is Notch2, and not Notch1, that plays a major and necessary role in hepatocyte-derived cholangiocarcinogenesis.[155] Inhibiting this pathway is a prospective therapeutic strategy, with several drugs being developed for this purpose that can target distinct points along the signaling cascade. The main groups of drugs currently in or that underwent clinical trials which target the Notch pathway would be γ-secretase inhibitors,[156–160] which are able to block the proteolytic cleavage of Notch receptors to disable the signaling, anti-Notch receptor antibodies,[161,162] which antagonize each specific receptor paralogue without some of the off-target effects of chemical drugs, and anti-DLL4 antibodies,[163,164] which target the transmembrane Delta-like ligand 4 (DLL4), a ligand of the Notch receptors.

Additionally, the bulk of CCAs present increased Wnt/β-catenin signaling, in part due to the activated macrophage-mediated release of Wnt ligands,[165,166] but also as a result of mutations in genes such as *AXIN1*, *APC* and *CTNBB1*[117] or hypermethylation of the gene promoter of several inhibitors of this pathway such as *SOX17*, *WNT3A*, *DKK2*, *SFRP1* and *SFRP2*,[167,168] altogether modulating cell growth and survival.[117] Similarly, studies report the activation of Hh signaling in CCA through overexpression of pathway components that include PTCH1 and GL1[169] or of the Hh ligand Sonic hedgehog protein (SHH),[170] in between 40-90% of the samples analyzed.[169,170] This pathway could be induced by myofibroblast[171] or hepatic stellate cell (HSC)-secreted platelet-derived growth factor BB (PDGF-BB),[172] enhancing cell proliferation, migration and invasion. On another end, the Hippo/YAP signaling pathway is known to modulate organ size, cell proliferation and apoptosis.[173] In CCA, upregulation of the protein YAP has been described.[174–178] It had been observed that high YAP expression was associated with lower RFS rates, with the 1-year and 3-year RFS rates for the low YAP group being 63.9% and 41.2%, respectively, and the 1-year and 3-year RFS rates for the high YAP group being 37.3% and 17.4%, respectively.[177] Other studies obtained at similar conclusions, associating higher YAP expression with worse clinicopathological parameters, such as histological differentiation, tumor staging and metastasis, and poor OS.[176,178] In spite of the rarity of genetic alterations of the YAP pathway,[179] up to 14% of CCAs present mutations in ARID1A, which encodes for a subunit of the chromatin remodeling complex SWI/SNF, which in turn reduces YAP transcriptional activity.[180]

Receptor tyrosine kinase (RTK) signaling activation is a common phenomenon among all CCA subtypes. Overactivation of EGFR1, ERBB2 and MET RTK signaling has been reported in CCA and is associated with worse prognosis.[121,122] RAS-MAPK and PI3K-AKT-mTOR pathways prompted by RTK signaling, resulting in enhanced proliferation, apoptosis evasion and increased tumor growth.[113,121,122,181] Moreover, chromosomal fusion rearrangements in FGFR2 occur, particularly in iCCAs. In this way, molecular alterations in RTK signaling pathways constitute suitable therapeutic targets.

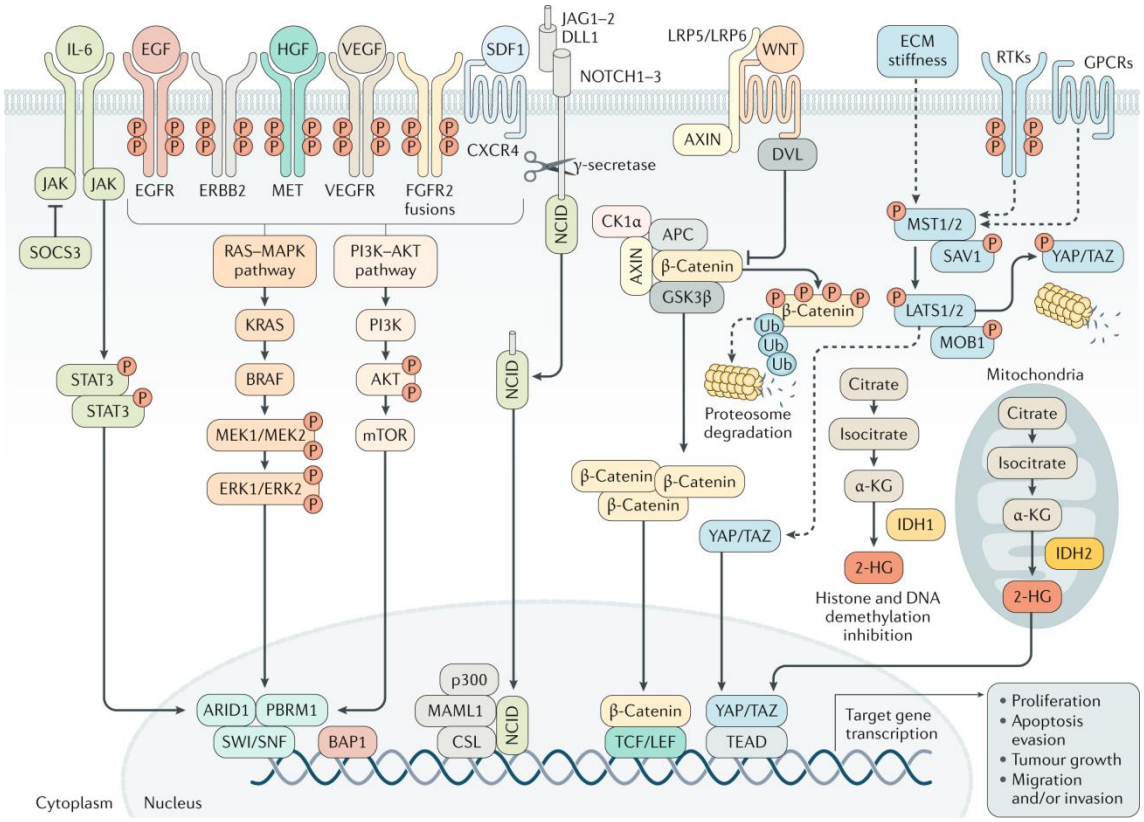

Figure I.7. Signaling pathways driving cholangiocarcinogenesis. CCA development, growth and progression involve complex molecular processes that include the interaction between extracellular ligands and increased expression of abnormally activated cell surface receptors that lead to the dysregulation of signaling pathways, ultimately enhancing cell proliferation, survival, migration or invasion. The most frequently mutated genes resulting in overactivation of some of these pathways are KRAS, BRAF, ARID1, PBRM1, BAP1, IDH1 and IDH2. Abbreviations: 2-HG, 2-hydroxyglutarate; ECM, extracellular matrix; RTK, receptor tyrosine kinase.[36]

I.3.7. Therapeutic strategies

The late diagnosis, combined with the highly chemoresistant behavior of these tumors strongly compromise the access and outcome of the current available therapeutic options, thus contributing to their discouraging prognosis. Currently, surgical resection of the tumor or liver transplantation remain as the only potentially curative options for CCA. The eligibility of patients with CCA for surgical resection is conditioned by their clinical status, tumor extension as well as the presence/absence of metastasis or locally-advanced disease.[182] Still, most patients present advanced unresectable tumors, therefore, less than one third undergo complete resection.[182] Aside from that, with relapse upon surgical resection being frequent and patients presenting short 5-year survival rates,[60,109–113,183] there is need to identify patients at risk of recurrence and to find effective adjuvant therapies. In this regard, the BILCAP study, a chemotherapy-based phase III clinical trial, reported benefits in terms of OS and RFS when employing

capecitabine as adjuvant therapy in biliary tract cancers.[184] Based on the favorable results obtained, international guidelines recommend capecitabine as an adjuvant therapy after curative resection of CCA.[184] Liver transplantation for CCA remains controversial, and even though different retrospective multicenter studies have reached promising results concerning disease-free survival (DFS) or OS rates for very small tumors (<2-3cm),[185–188] liver allograft supply and life-long immunosuppression are serious limitations of this strategy.

In unresectable cases, palliative treatment remains the only option. Robust data obtained from the phase III ABC-02 and the phase II BT22 trials support the use of first-line gemcitabine and cisplatin combination (GemCis) chemotherapy in patients with advanced CCA.[189,190] Once resistance to first-line therapy is acquired, FOLFOX (folinic acid, 5-FU and oxaliplatin) has shown potential benefit as second-line therapy for CCA.[191] Additionally, more intensive approaches with triple chemotherapy are currently under investigation as first-line chemotherapeutic strategies.[192,193] Locoregional therapies such as transarterial chemoembolization (TACE), transarterial radioembolization (TARE) and liver chemosaturation are also promising therapeutic options,[194–196] but evidence supporting their efficacy is modest and further studies confirming the benefits are needed.

Trying to set the standard for precision medicine, the currently explored treatment options are based on the mutational signatures driving CCA. Several ongoing clinical trials are evaluating multiple compounds targeting specific genetic modifications, such as IDH1/2 mutations, FGFR alterations, RTK fusions or EGFR, MET and ERBB2 mutations.

Pemigatinib, a small molecule inhibitor of FGFR1, FGFR2 and FGFR3, was the first targeted therapy for the treatment of CCA to be approved by the FDA.[197–199] Previously applied in the treatment of other malignancies, such as myeloid/lymphoid neoplasms, it received approval in April 2020 for the treatment of adults patients with f previously treated, unresectable, locally advanced or metastatic CCA and presenting FGFR2 fusion or other type of genetic rearrangement.[198,200] Following it, in 2021, a second FGFR inhibitor designated infigratinib was approved for use in patients with CCA presenting the same genetic alterations as for the previous one treated, unresectable locally advanced or metastatic tumors.[201–203] Derazantinib is another example of a pan-FGFR inhibitor currently in phase II clinical trials for advanced or unresectable iCCA presenting FGFR2 gene fusion.[204] Other molecules of the same type currently undergoing clinical

trials include erdafitinib, which has been already approved for urothelial carcinoma,[192,205,206] and futibatinib.[207]

Another common genetic modifications available as therapeutic targets in CCA are IDH1/2 mutations, for which ivosidenib, a small molecule inhibitor of IDH1, has already been approved by the FDA as of August 2021, for the treatment of adult patients with inoperable, locally advanced or metastatic hepatocellular IDH1-mutated CCA.[208–210] Dasatinib and Enasidenib are examples of other IDH1/2 inhibitors in early clinical trial stages for patients with advanced IDH1/2 mutated CCA.[211]

With the MAPK cascade being another potentially targetable pathway that frequently suffers from mutations or dysregulations in CCA, another small molecule inhibitor, designated dabrafenib, capable of inhibiting mutated BRAF, has been approved by the FDA as of July 2022, in combination with trametinib, an inhibitor of MEK1/2, for the treatment of $BRAF^{V600E}$-mutated unresectable, recurrent, locally advanced or metastatic CCA in adult patients.[212,213]

With such targeted approaches, comes the need for comprehensive and detailed molecular profiling of each case, to choose the most appropriate therapeutic strategy for the genetic/molecular background of the patient.[78] FoundationOneCDx (F1CDx) is a next-generation sequencing diagnostic test approved by the FDA with the capability of examining 324 cancer genes in solid tumors to identify patients who can benefit from specific courses of treatment.[214] Its precision and reproducibility in detecting FGFR2 fusions or rearrangements were examined and validated in CCA in the pemigatinib clinical trial FIGHT-202.[215] Upon validation through concordance analysis between F1CDx and an externally validated RNA-based NGS (evNGS) test, F1CDx achieved a reproducibility and repeatability of 90-100%.[215] Another approach is recovering the circulating tumor DNA (ctDNA) in the bloodstream for analysis of genomic alterations that could prove beneficial in the choice of treatment course, which is especially useful when tumor tissue is not available or not easily obtainable. In a study, they compared the accuracy of genomic profiling of blood-derived ctDNA from patients with CCA by NGS against tumor tissue sample profiling and genomic database analysis.[216] It was observed that ctDNA testing by NGS was comparable to the standard profiling in tissue samples, with the frequencies of single nucleotide variation in ctDNA being comparable to the ones observed for tissue samples in commonly mutated genes, such as TP53 (35.1 vs. 40.4%) and KRAS (20.1 vs. 22.6%), making it a viable alternative to tumor biopsies for patients with metastatic biliary malignancies.[216]

Immunotherapy, which involves the modulation of the immune system, either through suppression or activation, for the treatment of the disease, is seen as the vanguard of precision medicine, making it also appealing as an anti-cancer therapeutic option in CCA. Immune checkpoint inhibitor (ICI) therapy is the main and most common type of immunotherapeutic approach under research. For CCA, there are no approved immunotherapy options patients, but there are already several treatments undergoing clinical trials.[217–222] Among them, durvalumab, an anti-programmed cell death 1 (PD-1) receptor human monoclonal antibody, has already been through phase III clinical trials (TOPAZ-1; NCT03875235), showing significant improvements in OS of patients as a first-line combination therapy with gemcitabine plus cisplatin for advanced biliary tract cancer, with a 24-month estimated OS of 24.9% for durvalumab compared to 10.4% with the placebo.[222] It is pending approval by the FDA upon review of the results of the clinical trials.[223] Apart from this, it is also under research for other courses of treatment, with clinical trials running treatments such as durvalumab with tremelimumab, a human monoclonal antibody against CTLA-4,[224] or triple combination therapies such as gemcitabine and cisplatin plus durvalumab with tremelimumab[225] or a combination of durvalumab, tremelimumab and paclitaxel.[226] Other antibodies focusing on PD-L1 blockade are undergoing clinical trials for advanced CCA, such as pembrolizumab[220] and nivolumab.[221]

Chimeric antigen receptor (CAR)-modified T cells are yet another possible therapeutic approach. By modifying a given receptor or set of receptor on the host immune cells to recognize a specific tumor-associated antigen (TAA), the principle is to be able to prime the immune system to recognize the tumor cells more easily and that way destroy them by itself.[227] Some advances have been made in trying to apply CAR-T cell immunotherapy in CCA in the last decade,[217,228] with some phase I trials running for the use of CAR-T cells in treating EGFR-positive[218] and HER2-positive patients[219] with advanced CCA.

I.4. Krüppel-like factors

I.4.1. General features and physiological roles

Krüppel-like factors (KLFs) include a family of highly conserved and widely expressed transcription factors involved in a multitude of physiological and pathological processes in humans. Initially identified through its *Drosophila melanogaster* homologous protein Krüppel, currently holds 18 known members, all containing three cysteine and histidine (C_2H_2) zinc finger motifs (**Figure I.8**), characteristic to this family of proteins, which allow

them to recognize GC-rich DNA binding sequences and regulate gene expression through repression or transactivation.[229,230] They recruit coactivator and corepressor proteins to add an extra layer of modulation to its KLF-mediated mechanisms of transcriptional regulation.[229,230] The last member of the family to have been discovered, KLF18, has only been predicted through bioinformatic analysis, with very little being known about it.[231,232]

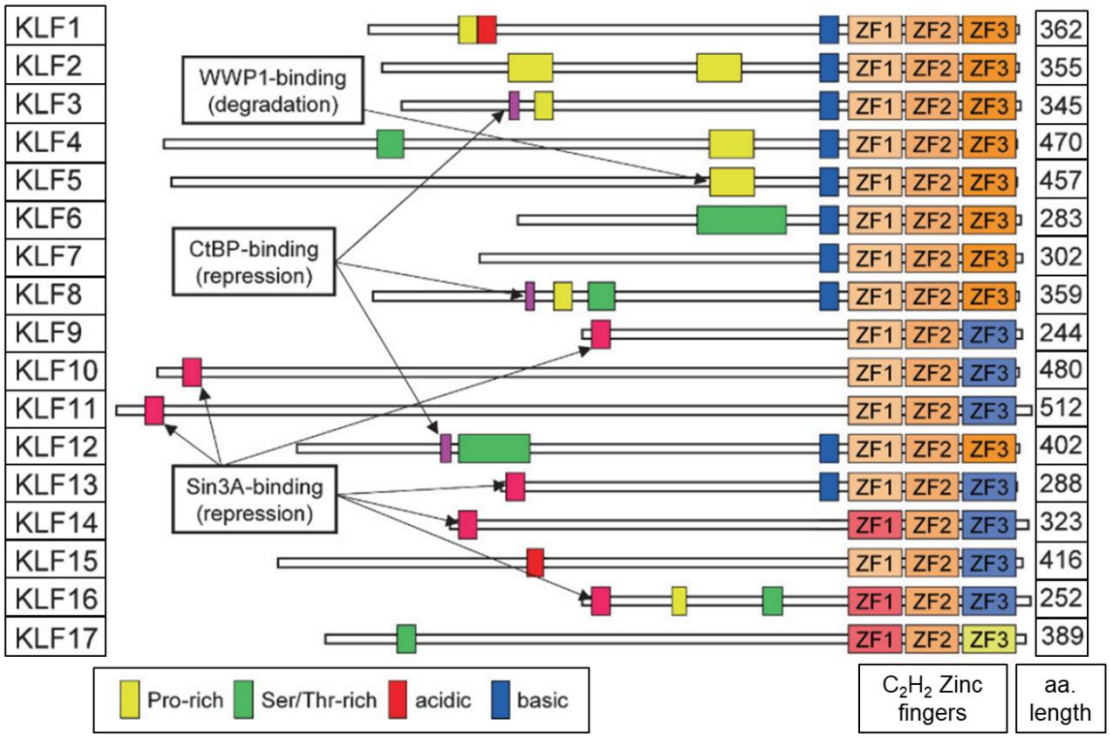

Figure I.8. Members of the human Krüppel-like factor family. The structure of each KLF protein (apart from KLF18) is depicted. The three C2H2 zinc fingers are shown as ZF1, ZF2, and ZF3. Pro-rich, Ser/Thr-rich, acidic, and basic regions are represented in yellow, green, red, and blue rectangles, respectively. CtBP-binding regions and Sin3A-binding regions are indicated by arrows. (Adapted from Nagai, 2009)[230]

Their roles and functions extend to most of the organ system, including cardiovascular,[233,234] hematological,[235] respiratory,[236,237] digestive,[238,239] and immune systems.[240] KLF4, initially referred to as gut-enriched KLF (GKLF) for being found highly expressed in intestinal epithelia at the time of its discovery,[241] despite being expressed in a variety of different tissues such as thymus, cornea, cardiac myocytes and lymphocytes,[242–245] it has multiple different roles. In the gut, it has been shown to be necessary for correct intestinal epithelial cell morphology, regulating their proliferation, differentiation and polarity.[239] In the heart, KLF4 can modulate the expression and activity of myocardin, having a potentially beneficial antihypertrofic effect in the context of cardiac hypertrophy.[234] KLF2, also known as lung-KLF (LKLF), for being identified in lung tissue

when it was first discovered,[246] has been shown as crucial for the maintenance of a pool of peripheral T cells, being necessary to license mature T cells present in the thymus for migration and circulation through the secondary lymphoid tissues.[247]

In developmental biology, they also play an important part, being necessary for organogenesis of various tissues.[237,248–252] KLF1, also designated erythroid-KLF (EKLF), the first member of the protein family to be discovered, earned such a designation due to the mouse and human forms only being expressed in erythroid cells of the yolk sac, fetal liver, spleen, and bone marrow.[253,254] Additionally, it has been shown to be essential for the correct maturation of embryonic red blood cells into definitive erythrocytes, regulating processes such as cell membrane structural integrity, hemoglobin synthesis and blood group antigens.[250] KLF7, also known by its early name of ubiquitous KLF (UKLF), as upon its discovery it was found to be widely expressed at low levels in adult tissues.[255] This transcription factor has been shown to play a prevalent role in neuronal morphogenesis, more specifically in the differentiation and neurite outgrowth of olfactory sensory neurons.[252]

Their importance extends even further, also impacting the pathophysiology of many organs, with reports of KLFs being connected to heart failure and cardiac hypertrophy in cardiac muscle,[256,257] to atherosclerosis in the endothelium,[258,259] to renal fibrosis and interstitial inflammation in the kidney,[260–262] to diabetes in the pancreas,[263–265] and to obesity and dyslipidemia in adipose tissue,[263,266–269] among others.

I.4.2. Pathophysiological role in cancer

Some of the main cellular processes regulated by many of the members of the KLF family are growth, proliferation, differentiation, and development.[270–272] For this reason, they are known to be inadvertently involved in malignant transformation in various types of tissues. Since their regulatory activity can be either towards promoting or inhibiting expression of the target gene depending on the coactivators and/or corepressors with which they coordinate, they can have the role of tumor suppressors or oncogenes in different contexts and different tissues.[273–275]

KLF8, one of the relatively more recent additions to the KLF family, has been connected with regulating many hallmarks of cancer,[276] being intimately related with oncogenic transformation. In a study on breast cancer, it was observed that KLF8 induced EMT and improved the motility and invasive capability of the cells, modulating their morphology and epithelial and mesenchymal protein markers.[275] It was shown to directly bind and

repress the promoter of *E-cadherin*, and silencing KLF8 through RNA interference restored E-cadherin expression and hindered the invasive capability of the cells.[275] KLF17, another one of the more recently discovered members of this transcription factor family,[277] has been shown to have an opposite role to the formerly member in breast cancer, acting as a negative regulator of EMT and metastasis.[274] It was reported that ectopic expression of KLF17 led to impaired metastization capability of breast cancer cells and, conversely, KLF17 suppression promoted cell invasion and EMT. Additionally, it was demonstrated that KLF17 expression is downregulated in primary human breast cancer tissues and that it can bind directly to the promoter of Id-1, an important metastasis regulator in breast cancer, inhibiting its transcription.[274] KLF6, a ubiquitously expressed Krüppel-like transcription factor, has been thoroughly studied for its potential as a tumor suppressor since the advent of its discovery.[278] In prostate cancer, it was observed that this gene was a mutated in a subset of this type of cancer. 77% of the primary prostate tumor samples showed loss-of-heterozygosity through deletion of one of the *KLF6* alleles and in 71% of these tumors, the remaining allele was revealed to be mutated.[273] The wild-type form of KLF6 was shown to up-regulate p21 (WAF1/CIP1) in a p53-independent manner and inhibit cell proliferation, while the tumor-derived KLF6 mutants do not, suggesting that KLF6 plays a tumor suppressor role in human prostate cancer.[273]

A different example from the previous ones is KLF4, which can play both roles of either oncogene or tumor suppressor gene in different contexts. In colon cancer, it acts as a tumor suppressor, being essential for the induction of cell cycle arrest upon DNA damage, at different stages of the cell cycle.[279,280] It was shown to induce cell cycle arrest at G_1/S phase in a p53-dependent manner, through possible modulation of p21(WAF1/CIP1),[279] as well as at G_2/M by transcriptional repression of the cyclin B1 promoter and inhibiting its expression.[280] On the other hand, in skin cancer, it takes an oncogenic role, being reported that when its expression is induced in keratinocytes, their distinctive epithelial cell properties were lost, with the skin progressing through hyperplastic and dysplastic phases.[281] With time progression, the lesions would acquire a morphological and molecular resemblance to squamous cell carcinoma *in situ*.[281]

I.4.3. KLF15 – Molecular characterization

KLF15, initially designated Kidney-Krüppel-like Factor (KKLF), due to the organ where it was first identified, is a member of the KLF family of transcription factors[282,283] mainly expressed in the kidney, liver, skeletal and cardiac muscles and adipose tissue, with the

strongest expression occurring in the liver and kidney.[229,282,284] It is implicated in various metabolic processes. Among its roles in the liver, it has been show to regulate gluconeogenesis by controlling gluconeogenic substrate availability and transcriptionally regulating amino acid-degrading enzymes,[284,285] as well as by inducing lipogenic enzyme expression during early and euglycemic periods of fasting before reaching hypoglycemia and prior to PKA activation.[286]

Cardiac function and metabolism have also been reported as part of its roles. It was observed that KLF15 regulates a transcriptional program necessary for a correct myocardial lipid flux, doing so through a mechanism that involved the recruitment and interaction with the chromatin remodeling enzyme p300.[287] It was also shown that KLF15 is necessary to control the circadian rhythmicity associated with a correct myocardial repolarization, as aberrant expression of *KLF15* can cause a loss of the necessary rhythmicity, abnormal repolarization and increase susceptibility to ventricular arrhythmias.[288] It is also necessary for the correct maintenance of the blood vessels, as it was shown that KLF15 is strongly downregulated in failing human heart tissue and in human aortic aneurysms and that mice deficient in *Klf15* develop heart failure and aortic aneurysms through a p53- and p300-dependent process.[289] It was also observed that KLF15 negatively regulates the acetylation of p53 by p300 acetyltransferase, and in the absence of KLF15, an hyperacetylation of p53 occurs in both the heart and aorta, with the pathological phenotype being rescued through *TP53 deletion* or p300 inhibition.[289]

In the adipose tissue, it has been associated with adipogenesis, being necessary for adipocyte differentiation. Inhibition of its function led to an arrest in the adipogenesis process in preadipocytes *in vitro* that were exposed to adipocyte differentiation inducers. Ectopic expression of KLF15 induced lipid accumulation and expression of PPARγ in the presence of adipocyte differentiation inducers.[290] In addition, ectopic expression of C/EBPβ, C/EBPδ, or C/EBPα in NIH 3T3 cells (mouse fibroblast cell line), which induces their differentiation into adipocytes also caused the expression of KLF15. Lastly, KLF15 was shown to act synergistically with C/EBPα to increase the activity of the PPARγ2 gene promoter in the adipocytes.[290]

KLF15 also has a role in bile acid (BA) synthesis. With a deficiency in *KLF15*, the circadian expression of important enzymes in the bile acid production pathways is disrupted, along with tissue BA levels and triglyceride/cholesterol absorption.[291] It develops this effect through negative regulation of circadian expression of ileal *Fgf15*, not dependent of BA stimulation nor in a hepatic-based regulatory process.[291]

In the kidney, where it is also highly expressed, KLF15 has been associated with podocyte differentiation, being observed an induction in expression of differentiation markers.[292] In *Klf15*-null mice administered lipopolysaccharide or adriamycin, there was an increase in proteinuria and podocyte foot process effacement with a decrease in expression of podocyte differentiation markers in comparison to wild-type treated mice. It was also shown that KLF15 expression was decreased in glomeruli isolated from HIV transgenic mice as well as in kidney tissue biopsies from patients with HIV-associated nephropathy and idiopathic focal segmental glomerulosclerosis, indicating a potential podocyte protective role against injury.[292]

Apart from these, KLF15 is also implicated in lipid homeostasis, regulating hepatic steatosis through direct transcriptional regulation of *Twist2* by binding to its gene promoter,[293] as well as mediating ER stress-induced insulin resistance in the liver through regulation of mTORC1 activity.[294] In this last case, it was shown that deletion of *Klf15* in mice protected them against hepatic insulin resistance and fatty liver under high-fat dietary conditions and in response to ER-stress induction, presenting with decreased mTORC1 activity, augmented AMPK phosphorylation and PGC-1α expression and activation of autophagy, an intracellular degradation process known to enhance hepatic insulin sensitivity. In addition, in primary hepatocytes, *KLF15* deficiency replicated the inhibitory effect on the activation of mTORC1 by amino acids and insulin.[294]

Finally, another of its roles in the liver is to participate in hepatocyte maturation. Its expression profile in the liver is seen to increase starting from the embryonic stage throughout the developmental process, inducing the expression of several genes necessary for liver function, such as *Tat, Cps1, Cyp* and *Krt19*.[295] It was also shown it could replicate this effect, inducing the expression of these liver function genes in hepatoblasts derived from human induced pluripotent stem cells (iPSCs). Furthermore, KLF15 was able to suppress hepatoblast proliferation.[295]

I.4.3.1. KLF15 in carcinogenesis

With little over 20 years since it was initially described, the first accounts of an association between KLF15 and cancer only appeared in the beginning of the last decade.[296,297] Still, to this date, when compared to other members of the KLF family, data on KLF15 in cancer is somewhat limited and at times contradictory. In some types of tumors, it is suggested to play a tumor suppressor role. Namely, in breast cancer, it was observed that KLF15 was significantly downregulated, with patients with high KLF15 levels having higher OS, RFS and distant-metastasis free survival (DMFS) rates, being its prognostic

value independent of the expression of any other KLF.[298] Overexpression of KLF15 *in vitro* in breast cancer cell lines reduced cell proliferation and migration, also leading to cell cycle arrest at G_0/G_1 phase with consequent induction of apoptosis.[298] The same pattern was seen in gastric cancer, showing reduced expression levels of KLF15 in tumor tissue samples compared to normal adjacent tissue, as well as an association with improved clinical parameters, with the transcription factor expression levels inversely correlating with tumor staging, lymph node invasion and distant metastasis. Patients with higher expression levels of KLF15 also showed significantly higher DFS rates after surgery, clearly indicating its prognostic potential.[299] In gastric cell lines *in vitro*, experimental overexpression of KLF15 lead to the inhibition of cell proliferation, inducing cell cycle arrest at G_0/G_1 phase, in part through regulation of CDKN1A/p21 and CDKN1C/p57 expression.[299]

KLF15 was shown to be downregulated both in ovarian cancer tissues and cell lines, with its inhibitory effect on ovarian cancer progression being dependent on a regulatory axis between circular RNA CircMTO1, miR-182-5p and KLF15.[300] The circular RNA CircMTO1 serves as a sponge for the miR-182-5p, while the latter represses the anti-oncogenic activity of KLF15 through direct binding to its gene.[300] Furthermore, it was also reported that in papillary thyroid cancer (PTC), KLF15 expression was downregulated, with higher expression of the transcription factor being associated with better OS rates.[301] It was shown to be to a target of miR-181a, a miRNA which enhanced PTC cell growth, migration and induced EMT *in vitro*. Upon KLF15 overexpression in the PTC cell lines, the transcription factor partially rescued the tumorigenic effect of the miRNA on cell proliferation and migration.[301]

Nonetheless, KLF15 does not seem to develop the same kind of role in all types of cancer, as in glioma it seems to be upregulated in tumor tissue in comparison to its normal counterpart. It was also shown to be inversely correlated with miR-376a-3p, a miRNA that is downregulated in glioma cancer tissue and is capable of reducing the cell viability and the migratory and invasive capabilities of glioma cell lines *in vitro*.[302] A miR-376a-3p binding site on the KLF15 gene promoter was found and validated, and rescue experiments proved that miR-376a-3p exerted its tumor suppressive effect by targeting KLF15, while KLF15 overexpression was able to abolish this regulatory effect of the miRNA and impose its oncogene role.[302] In a similar way, in colorectal cancer, KLF15 was found upregulated in tumor tissue. An inverse correlation with miR-376a-3p was observed, with KLF15 being described as a target of this miRNA, very much alike the previous study.[303] It was found that the lncRNA TTN-AS1, which was also found upregulated in colorectal cancer and was validated as targeting miR-376a-3p, positively

regulated KLF15 by sponging miR-376a-3p. This way, KLF15 develops its oncogene role in colorectal cancer through a TTN-AS1/miR-376a-3p/KLF15 regulatory axis.[303]

As was the case with other members of this family of transcription factors, KLF15 may have this dual role depending on a specific cellular context. An exception is warranted, as in lung adenocarcinoma (LUAD) one group first described KLF15 as markedly upregulated, and associating it with worse clinical markers of prognosis such as tumor stage, tumor differentiation and worse OS rates.[304] Knockdown of KLF15 *in vitro* decreased cell proliferation rates, colony formation capability, migratory capacity and EMT marker expression, as well as inducing apoptosis and hindering their growth in mouse xenograft models.[304]

However, they were afterwards refuted on this account by another group that found KLF15 to be downregulated, with opposite molecular evidences to the ones previously given.[305] KLF15 expression was found to be associated with better OS in patients with LUAD patients. In LUAD cell lines, KLF15 was found equally downregulated, with its overexpression leading to a decrease in cell viability and colony formation, as well as induction of cell cycle arrest at G_0/G_1 phase through up-regulation of CDKN1A/p21 and CDKN1C/p57 expression.[305]

Regarding any type of biliary cancer or even liver cancer, no information is available so far in connection with KLF15.

Hypothesis and Objectives

The KLF transcription factor family regulates important physiological and pathological processes, by modulating the expression of genes involved in distinct signaling pathways. Numerous studies have demonstrated the critical role of some members of this family in the pathogenesis of various cancers, with some being considered as potential diagnostic/prognostic tools and therapeutic targets. Yet, the role of KLFs in CCA remains an unexplored subject. Particularly, KLF15, is tightly connected with liver metabolic function and differentiation and its dysregulation was previously reported in distinct types of cancer, yet the role of KLF15 in CCA remains an unexplored subject. For this reason, this dissertation aims to explore the role of KLF15 in cholangiocarcinogenesis and evaluate its potential as a diagnostic, prognostic and therapeutic tool.

Thus, the following objectives were proposed to be accomplished:

I. Analysis of the expression levels of KLF15 in human CCA tissues compared to controls.

II. Analysis of the expression levels of KLF15 in human CCA cell lines compared to normal controls.

III. Assessment of the impact of epigenetic modifications in modulating KLF15 expression.

IV. Evaluation of the role of KLF15 in the progression of CCA *in vitro*.

V. Evaluation of the role of KLF15 in the progression of CCA *in vivo*.

Materials and Methods

M.1. Human samples

CCA and surrounding normal human tissues from 8 independent cohorts of patients [Montal (Spain), Copenhagen (Denmark), The Cancer Genome Atlas (TCGA), The Thailand Initiative in Genomics and Expression Research (TIGER), Job (France), Nakamura (Japan), Jusakul (Singapore) and San Sebastián (Spain)] were studied.

M.1.1. Montal cohort

Affymetrix Human Genome U219 Array Plate was used to perform genome-wide expression profiling of 182 CCA tumor samples and 38 non-neoplastic bile ducts (GSE132305).[306]

M.1.2. Copenhagen cohort

Whole transcriptome profiling [humanRef-8v2 BeadChips (Illumina Inc)] was performed in the samples of the Copenhagen cohort, which included a total of 104 CCA surgical specimens (68 intrahepatic and 36 perihilar CCAs), 60 normal surrounding liver samples, and 6 normal intrahepatic bile ducts (GEO: GSE26566).[122,307]

M.1.3. The Cancer Genome Atlas (TCGA) cohort

The results shown for this cohort are based on data generated by the TCGA Research Network: https://www.cancer.gov/tcga. RNA-seq data from the TCGA cohort (36 CCAs and 9 surrounding liver samples)[179] were obtained through the FireBrowse portal [BROAD Institute of MIT & Harvard, MA, USA (https://gdac.broadinstitute.org/)].

M.1.4. The Thailand Initiative in Genomics and Expression Research (TIGER) cohort

Affymetrix Human Transcriptome Array 2.0 was employed to perform genome-wide transcriptome profiling of 91 CCA surgical samples and 92 normal surrounding liver tissue samples (GSE76311).[308]

M.1.5. Job cohort

Transcriptome profiling of the samples was performed using Affymetrix Human Transcriptome Array 2.0, for 78 CCA tumor tissue samples and 31 normal surrounding liver tissue samples (ArrayExpress accession number: E-MTAB-6389).[309]

M.1.6. Nakamura cohort

Samples from 111 CCA tumor tissue samples with respective surrounding normal liver tissue were analyzed, with their transcriptomic sequencing being achieved through the use of the Illumina HiSeq 2000 platform.[119]

M.1.7. Jusakul cohort

Whole-genome sequencing was carried out using Illumina Hiseq X10, Illumina Hiseq2500 and Illumina Hiseq2000 instruments on 71 CCA tumor tissue samples and paired non-malignant surrounding liver tissue samples (EGAS00001001653).[127]

M.1.8. San Sebastian cohort

KLF15 mRNA expression was determined by real-time quantitative polymerase chain reaction (qPCR) in CCA human biopsies (n=17) and surrounding normal human liver tissues (n=16) obtained from the Basque Biobank of the Donostia University Hospital (San Sebastián, Spain). The clinical information of patients included in the study is summarized in Table M.1.

Table M.1. Clinical information of patients from the San Sebastian cohort.

Patient ID	CCA subtype	Sex	Age	Disease Stage	Tumor Size (cm)	CA19-9	CEA
1	iCCA	Male	85	T1N0M0	3.8	n/a	n/a
2	iCCA	Female	78	T1N0M0	6	35.8	0.9
3	iCCA	Female	82	T2aN0M0	5.5	3528	307
4	iCCA (with liver mtx: T2b)	Male	79	T2bN0M0	0.4	0.6	5.6
5	iCCA	Male	61	T1N0M0	4	1	2.4
6	iCCA	Female	63	T3N0M0	5	n/a	n/a
7	iCCA (with liver mtx: T2b)	Male	68	T2bN1M1	2.5	27.1	3
8	iCCA	Male	60	T1N0M0	5.2	19	2.9
9	dCCA	Male	73	T3N1M0	n/a	606.6	13.3
10	pCCA	Male	64	T2aN1M0	3	21.3	2.8
11	dCCA	Male	78	T3N0M0	2.3	135.4	4
12	iCCA	Male	70	T1N0M0	4	9.8	1.9
13	iCCA	Female	63	T1N1M0	5.5	30.8	0.8
14	iCCA	Male	76	T1N0M0	3.5	1490	6.8
15	iCCA	Male	74	T1N0M0	3.5	37.3	2.2
16	iCCA	Female	74	T1N0M0	1.1	10.2	3.5
17	iCCA	Male	65	T3N0M0	5.3	27.2	2.7

n/a: not available. Abbreviations: CA19-9, carbohydrate antigen 19-9; CCA, cholangiocarcinoma; CEA, carcinoembryonic antigen; dCCA, distal CCA; iCCA, intrahepatic CCA; mtx, metastasis; pCCA, perihilar CCA.

Research protocols were approved by the Clinical Research Ethics Committees from each corresponding participating Institution and all patients signed written consents to allow the use of their samples for biomedical research.

M.2. Survival analysis

The potential association of KLF15 expression with the OS and RFS of patients with CCA regardless disease etiology (pan-CCA) was evaluated by univariable log rank (Mantel-Cox) test. The categorical classification according to high or low abundance of KLF15 was conducted by dichotomizing patients based on the mean expression value. Log rank (Mantel-Cox) statistical test comparing survival Kaplan-Meier curves was used and a p-value <0.05 was used as a cut-off to detect significant differences.

M.3. Cell lines and culture conditions

M.3.1. Cell lines

Normal human cholangiocytes (NHC) and CCA human cell lines were used in this study.

M.3.1.1. Normal human cholangiocytes (NHC)

NHCs were isolated from liver tissue gathered from a female patient who underwent surgical resection at the Donostia University Hospital (San Sebastian, Spain) which was confirmed as normal tissue by an experienced pathologist. NHCs were isolated as previously described by our group.[310] Briefly, small pieces (~1 mm^3) of liver tissue were mechanically and enzymatically digested by incubating the samples at 37ºC in a bath shaker for 30 minutes in a solution containing Dulbecco's modified Eagle's medium/Ham's F-12 nutrient mixture (DMEM/F-12) + GlutaMAX medium (Thermo Fisher Scientific), 3% fetal bovine serum (FBS), 1% penicillin-streptomycin (P/S) (both from Gibco – Thermo Fisher Scientific), 0.1% bovine serum albumin (BSA), 17 mg pronase, 12.5 mg type IV collagenase and 3 mg DNase (all four from Sigma-Aldrich). Next, sequential filtrations were performed through 100 µm and 40 µm sterile nylon cell strainers (Falcon – Corning). The tissue fragments trapped between the two pore-sizes were incubated for another 30 minutes in the digesting solution but replacing pronase by 13 mg hyaluronidase (Sigma-Aldrich). Afterwards, consecutive filtrations of the tissue samples were repeated and intrahepatic bile duct units (IBDU) ranging from 40 µm to 100 µm were obtained. IBDUs were washed with fully supplemented DMEM/F-12 medium (**Table M.2**) to inactivate enzyme traces. Finally, cells were resuspended in the same growth medium and seeded in thin collagen-coated cell culture flasks (Corning). Extensive molecular characterization of isolated NHCs was carried out.[310] Liver tissue was obtained according to the guidelines approved by the Ethics Committees at Biodonostia Institute and prior signature of the pertinent written informed consent.

Table M.2. Composition of the fully supplemented DMEM/F-12 medium.

Reagent (Company)	**Concentration**
DMEM/F-12+GlutaMAX (Gibco – Thermo Fisher Scientific)	89% (v/v)
Fetal Bovine Serum (FBS) (Gibco – Thermo Fisher Scientific)	5% (v/v)
MEM non-essential aminoacids 100X (Gibco – Thermo Fisher Scientific)	1% (v/v)
Lipid mixture 1000X (Sigma-Aldrich)	0.1% (v/v)
MEM vitamins solution (Gibco – Thermo Fisher Scientific)	1% (v/v)
Penicillin/Streptomycin (Gibco – Thermo Fisher Scientific)	1% (v/v)
Soybean Trypsin Inhibitor (Gibco – Thermo Fisher Scientific)	0.05 mg/mL
Insulin Transferrin Selenium (Gibco – Thermo Fisher Scientific)	1% (v/v)
Bovine Pituitary Extract (Gibco – Thermo Fisher Scientific)	30 µg/mL
Dexamethasone (Sigma-Aldrich)	393 ng/mL
3, 3', 5-triiodo-L-thyronine (T3) (Sigma-Aldrich)	3.4 µg/mL
Epidermal Growth Factor (EGF) (Gibco – Thermo Fisher Scientific)	25 ng/mL
Forskolin (Ascent-Scientific)	4.11 mg/mL

M.3.1.2. CCA human cholangiocytes

Four CCA human cell lines were used: HUCCT1, EGI1, TFK1 and WITT. The origin and mutational pattern of these cell lines are described in **Table M.3.**

Table M.3. Characteristics (subtype and known mutations) of the CCA cell lines used throughout the study.

Cell line	CCA subtype	Mutations
HUCCT1	iCCA	*KRAS, TP53*
EGI1	eCCA	*KRAS, GNAS, CDKN2A*
TFK1	eCCA	*TP53, BAP1, CDKN2A*
WITT	eCCA	*CDKN2A*

Abbreviations: CCA, cholangiocarcinoma; eCCA, extrahepatic CCA; iCCA, intrahepatic CCA.

M.3.2. Cell culture conditions

All normal and tumor cholangiocytes were cultured in thin collagen-coated cell culture flasks or plates (Corning). To this end, a solution containing 0.1% of glacial acetic acid (Corning) and 50 mg/L of rat tail collagen type I (Corning) in ultrapure water was prepared. After filtering the collagen solution using a 0.22 µm pore size sterile filter system (Corning), the surface of cell culture flasks was covered with the collagen solution for 3 hours (1 hour for cell culture plates). Afterwards, the collagen was removed and DPBS 1X (Gibco - Thermo Fisher Scientific) was added.

All cells were cultured in monolayer in a controlled environment (i.e., 37ºC, 5% CO_2 and 85% relative humidity). NHC, EGI1 and WITT cells were grown in fully-supplemented DMEM/F-12 medium (**Table M.2**.), whereas TFK1 and HUCCT1 cells were cultured in DMEM/F-12 or RMPI-1640 medium, respectively, all supplemented with 10% FBS and 1% P/S. Once 80-90% of confluence was reached, the cells were passaged using 0.05% trypsin-EDTA (Gibco – Thermo Fisher Scientific), while the cellular surplus was frozen in FBS (Gibco – Thermo Fisher Scientific) containing 10% DMSO (Sigma-Aldrich).

M.4. Gene expression measurement

M.4.1. Total RNA isolation

Cultured cholangiocytes (~2-3x10^5 cells/well) were seeded in thin collagen-coated 6-well plates (Corning) with their corresponding culture media. The next day, cells were either incubated for 48 hours with 100µM Zebularine, or followed right away with the RNA isolation protocol, being washed twice with DPBS 1X (Gibco – Thermo Fisher Scientific) and lysed using 1 mL of cold Tri-Reagent® (Sigma-Aldrich) assisted by scraping. Then, samples were frozen at -80ºC, contributing to cell lysis. Once the samples were thawed, 200 µl of cold chloroform (Merck Millipore) were added to each tube, and vigorously vortexed for 20 seconds to mix the two phases. A 15 minutes incubation period at room temperature was carried out, followed by centrifugation at 12,000g and 4ºC for 15 minutes. The sample presented two phases, of which the aqueous phase (top) was collected into a new sterile clean tube to which 0.5 mL of cold 100% 2-propanol (PanReac AppliChem) were added. Both solutions were mixed by inversion and incubated for 10 minutes at room temperature. Later, the tubes were centrifuged at 12,000g for 10 minutes at 4ºC, discarding the supernatant afterwards. Next, 1 mL of 75% ethanol (VWR) was added to the RNA pellets, which were washed by gentle vortexing and centrifuged at 7500g for 5 minutes at 4ºC. Upon removal of the supernatant, the RNA pellets were air-dried at room temperature. The pellets were resuspended in 20 µL of UltraPure™ DNase/RNase-free distilled water (DNase/RNase-free dH_2O) (Invitrogen – Thermo Fisher Scientific). Finally, RNA concentration and purity were quantified by ultraviolet spectrophotometry using the *NanoDrop® ND-1000* apparatus (Thermo Fisher Scientific).

M.4.2. Reverse transcription (RT)

In general, 1 µg of total RNA was reversely transcribed to produce complementary DNA (cDNA). Different protocols were employed for human tissue samples and cells in culture.

M.4.2.1. Human tissue samples

The highly efficient SuperScript® VILO™ cDNA Synthesis Kit (Thermo Fisher Scientific) was used to synthesize first-strand cDNA from human tissue biopsies. A master mix containing 10X SuperScript® Enzyme Mix (2 µL/sample) and 5X VILO™ Reaction Mix (4 µL/sample) was combined with 1 µg of total RNA from human liver samples.

Subsequently, DNase/RNase-free dH_2O was added until reaching a final volume of 20 µL and a three-step protocol [*i*) 10 minutes at 25ºC, *ii*) 1 hour at 42ºC, and *iii*) 5 minutes at 85ºC] was performed in a *Veriti 96-Well* thermal cycler (Applied Biosystem). The resultant cDNA was diluted to a final concentration of 12.5 ng/µL.

M.4.2.2. Cells

A multistep RT was implemented for cultured cells. Briefly, total RNA (1 µg) underwent DNase treatment by adding 1 µL of DNase I Amplification Grade (Invitrogen – Thermo Fisher Scientific) and 1 µL of 10X DNase I Reaction Buffer (Invitrogen – Thermo Fisher Scientific) for 20 minutes at 37ºC, to remove gDNA contamination. Then, the DNase I reaction was stopped through magnesium chelation with 1 µL of 25 mM Ethylenediaminetetraacetic acid (EDTA) (Invitrogen – Thermo Fisher Scientific) for 10 minutes at 65ºC, 1 minute at 90ºC and cooled at 4ºC. Afterwards, cDNA was synthesized by adding 30 µL of RT-PCR master mix [consisting of 8 µL buffer 5X; 4 µL random primers (100 ng/µL); 4 µL deoxyribonucleotide triphosphate (dNTP) mix; 2 µL DTT; 1.2 µL RNase OUT; 1.2 µL moloney-murine leukemia virus reverse transcriptase (M-MLVRT) (all from Invitrogen –Thermo Fisher Scientific); 9.6 µL DNase/RNase-free dH_2O] to each tube. These were incubated under the following conditions: 37°C for 60 minutes, 95°C for 1 minute and then kept at 4°C. All steps were performed using the *Veriti 96-Well* thermal cycler (Applied Biosystem). Finally, a concentration of 12.5 ng/µL was achieved by diluting the cDNA in DNase/RNase-free dH_2O.

M.4.3. Quantitative polymerase chain reaction (qPCR)

The mRNA expression levels of genes of interest were determined by qPCR analysis. For this purpose, a master mix containing 10 µL of iQ™ SYBR® Green Supermix (Bio-Rad), 0.6 µL of a 10 µM stock solution of each forward and reverse primer (**Table M.4**) and DNase/RNase-free dH_2O until a final volume of 17 µL per sample was prepared and placed into a Hard-Shell® 96-well PCR plate (Bio-Rad). Thereafter, 3 µL (i.e., 37.5 ng) of the previously synthesized cDNA was loaded into the plate and, subsequently, the amplification products were detected in the *CFX96 Touch™* apparatus (Bio-Rad), following the iQ™ SYBR® Green Supermix standard protocol: *i*) cDNA denaturation and activation of the enzyme were induced by heating the plate at 95ºC for 10 minutes; *ii*) amplification of cDNA was carried out during 40 (or 50 for KLF15) cycles of 3 steps

consisting in 95°C for 15 seconds, 60°C for 30 seconds (annealing) and 72°C for 45 seconds (extension), *iii*) incubation of 15 seconds at 95ºC followed by *iv*) a gradual increase of the temperature from 60ºC to 93ºC (in 1ºC increments) to obtain the melting curve profile. Resultant data were collected and analyzed with CFX Maestro™ Software (Bio-Rad). Expression of *Glyceraldehyde-3-phosphate dehydrogenase (GAPDH)* and *Hypoxanthine Phosphoribosyltransferase 1 (HPRT1)* were used as housekeeping controls for data normalization and gene expression was determined using the ΔCT method. The mRNA expression levels are displayed as percentage relative to the vehicle-treated or control group (100% of expression).

Table M.4. Human primers sequences employed for qPCR (all from Sigma-Aldrich).

Gene	Sequence
BMP4	Forward 5'-CTCCAAGAATGGAGGCTGTAGGAA-3' Reverse 5'-CCTATGAGATGGAGCAGGCAAGA-3'
CCNB1	Forward 5'-AAGGCGAAGATCAACATGGC-3' Reverse 5'-GTTACCAATGTCCCCAAGAG-3'
EPCAM	Forward 5'-CCATGTGCTGGTGTGTGAAC-3' Reverse 5'-CCTTCTGAAGTGCAGTCCGC-3'
FN1	Forward 5'-GGGCAACTCTGTCAACGAAG-3' Reverse 5'-CACACCATTGTCATGGCACC-3'
HPRT1	Forward 5'-TATGGCGACCCGCAGCCCT-3' Reverse 5'-CATCTCGAGCAAGACGTTCA-3'
KI67	Forward 5'-CCACGCAAACTCTCCTTGTA-3' Reverse 5'-TTGTCAACTGCGGTTGCTCC-3'
KLF15	Forward 5'-GCTGCAGCAAGATGTACACC-3' Reverse 5'-CTTCACACCTGAGTGCGAGC-3'
PCNA	Forward 5'-ACACTAAGGGCCGAAGATAACG-3' Reverse 5'-ACAGCATCTCCAATATGGCTGA-3'

Abbreviations: BMP4, Bone Morphogenic Protein 4; CCNB1, Cyclin B1; EPCAM, Epithelial Cell Adhesion Molecule; FN1, Fibronectin 1; HPRT1, Hypoxanthine Phosphoribosyltransferase 1; KLF15, Krüppel-like Factor 15; PCNA, proliferating cell nuclear antigen.

M.5. Histological analyses

Tissue samples from mice were collected and fixed in 4% paraformaldehyde for 24 hours. Next, tissues were processed using the MTM tissue processor (Slee Medical GmbH), embedded in paraffin (Gibco – Thermo Fisher Scientific) and cut using the HM355S microtome (Gibco – Thermo Fisher Scientific) in sections at a thickness of 4-5 µm.

M.5.1. Hematoxylin and eosin (H&E) staining

H&E staining was performed to analyze tissue morphology as previously described.[311] Mouse paraffin-embedded tissue samples were cut and de-paraffined by a two-step 5 minute incubation in xylene (VWR) at room temperature. Thereafter, slides were hydrated with different solutions of decreasing ethanol concentration [100%, 70% and 50% ethanol (VWR)] for 2 minutes each and finally with DPBS 1X (Gibco – Thermo Fisher Scientific). Slides were then incubated in Harris hematoxylin (Merck Millipore) for 5 minutes. After washing the samples with tap water, slides were incubated with eosin (Merck Millipore) for 5 minutes at room temperature. Following a washing step with tap water, samples were dehydrated with increasing grade alcohol solutions (50%, 70% and 100% ethanol). Finally, slides were incubated in xylene for 5 minutes at room temperature twice and mounted with DPX (Sigma-Aldrich).

M.5.2. Immunohistochemistry (IHC)

IHC was performed in formalin-fixed and paraffin-embedded mouse and human liver tissue sections. In order to remove the paraffin, slides were incubated in xylene and rehydrated in graded series of ethanol as previously described. Next, sections were placed on a 0.6% H_2O_2 (Sigma-Aldrich) in methanol (Applichem Panreac) solution for 15 minutes to block endogenous peroxidases. Following antigen retrieval with antigen unmasking solution (Vector Laboratories), slides were blocked using first the Avidin/Biotin Blocking Kit (Vector Laboratories) and later, a 20% FBS in DPBS 1X blocking buffer. Primary antibodies (**Table M.5**) were incubated overnight at 4ºC. After washing the antibodies with DPBS 1X, slides were incubated with the appropriate biotinylated secondary antibodies. Vectastain ABC Reagent (Vector Laboratories) followed by 3,3 diaminobenzidine (DAB) peroxidase substrate Kit (Vector Laboratories) was used for antigen visualization. Slides were counterstained with Mayer's hematoxylin

(Sigma-Aldrich), dehydrated and mounted as previously described. Representative pictures were taken in an Eclipse 80i (Nikon) microscope using the Digital sight DS-U2 camera controller (Nikon) using NIS-Elements.

M.6. Determination of protein expression by Immunoblotting

M.6.1. Protein extraction from cells in culture

Cells (~2-3x10^5cells/well) were seeded in thin collagen-coated 6-well plates (Corning) and harvested in their corresponding culture media. After 24 hours, cells were washed twice with DPBS 1X (Gibco – Thermo Fisher Scientific) and lysed with 80 µL of cold 20 mM N-ethylmaleimide (NEM) in radio-immunoprecipitation assay (RIPA) lysis buffer assisted by scraping. RIPA buffer contains: 150 mM NaCl, 50 mM Tris pH 7.5, 0.1% SDS, 1% Triton X100, 0.5% sodium deoxycholate, protease inhibitors (1 tablet/50 mL, Complete; Roche) and phosphatase inhibitors (1 mM orthovanadate, 10 mM NaF, 100 mM β-glycerophosphate) (All from Sigma-Aldrich). Whole-cell lysates of cultured human cells were collected and frozen at -80ºC, which contributes to cell membrane disruption. Once thawed, the samples were centrifuged at 18,000g for 10 minutes at 4ºC. The supernatant was collected and the total amount of protein was quantified.

M.6.2. Protein quantification

Protein concentration was measured using the Pierce™ BCA Protein Assay Kit according to the manufacturer´s instructions (Thermo Fisher Scientific). Briefly, dH_2O was used to prepare a 1:5 dilution of each protein sample in a 96-well plate (Corning). Simultaneously, a calibration curve was prepared (ranging from 0 to 2 mg/mL of BSA). Additionally, the vehicle solution (i.e., 20 mM NEM in RIPA) was included in the plate as a blank sample. Afterwards, A and B reagents of the BCA Kit were mixed (in a 1:50 proportion) and 200 µL of the mixture were added to each well. Then, the plate was incubated for 30 minutes at 37ºC in darkness and the absorbance was measured at 570 nm in a Halo LED 96® microplate reader (Dynamica Scientific Ltd., UK).

M.6.3. Protein electrophoresis and immunoblotting

To detect changes in protein expression, an appropriate amount of protein (ranging from 30 to 100 µg) from whole-cell lysates was denaturalized by adding 5X Protein Loading Buffer [consisting of 250 mM Tris pH 6.8, 10% SDS, 50% glycerol (all three from Applichem Panreac), 0.05% bromophenol blue (Probus) and 500 mM 2-mercaptoethanol (Sigma-Aldrich)] and heating the samples at 95ºC for 5 minutes. Then, proteins were separated in a sodium dodecyl sulfate polyacrylamide gel electrophoresis (SDS-PAGE) at 10% and electro-transferred onto a 0.2 µm pore-size nitrocellulose membrane (Bio-Rad). After blocking with 5% skim milk powder (in tris-buffered saline with 0.1% Tween® 20 (TBS-T)) (Sigma-Aldrich) for 1 hour at room temperature, membranes were incubated with the relevant primary antibody (Rabbit polyclonal anti-KLF15 – SIGMA (AV32587)) (**Table M.5**) diluted in their corresponding blocking solution overnight at 4ºC. Membranes were washed 3 times with TBS-T and probed with an appropriate horseradish peroxidase-conjugated (HRP)-conjugated secondary antibody (Cell Signaling) at 1:5000 dilution for 1 hour at room temperature in blocking solution. Next, membranes were washed and the antigen was exposed using the Novex® ECL HRP Chemiluminescent Substrate Reagent Kit (Invitrogen – Thermo Fisher Scientific) and the emitted chemiluminescence was visualized and captured in the *iBright™ FL1000* imaging system (Thermo Fisher Scientific). When necessary, membranes were stripped using a two-step stripping method consisting of 10 minutes incubation at room temperature in stripping buffer I [0.2 M Glycine (Sigma-Aldrich), 0.5 M NaCl (Sigma-Aldrich), pH: 2.8], followed by another 10 minutes incubation at room temperature of the membranes in stripping buffer II [0.5 M NaCl (Sigma-Aldrich), 0.5 M glacial acetic acid (Corning), pH: 2.5]. Thereafter, the procedure was repeated including membrane blocking, incubation with primary and secondary antibodies and band visualization in the *iBright™ FL1000* imaging system (Thermo Fisher Scientific) after exposure with Novex® ECL HRP Chemiluminescent Substrate Reagent Kit (Invitrogen – Thermo Fisher Scientific). β-actin protein levels were used as loading controls. Finally, the protein signal was quantified with the iBright Analysis Software (Thermo Fisher Scientific). Results are displayed as percentage relative to the vehicle-treated or control group which is set as 100% of expression.

Table M.5. Antibodies employed for IHC, IF, IP and/or WB assays.

Antibody	Clone	Company	Reference	Application
Rabbit polyclonal anti-KLF15	n/a	Sigma-Aldrich	AV32587	IHC, WB
Goat polyclonal anti-KLF15	n/a	Abcam	ab2647	IHC, IP, WB
Rabbit polyclonal CK19	n/a	Abcam	ab84632	WB, IHC
Mouse monoclonal anti β-actin	AC-74	Sigma-Aldrich	A5316	WB
Anti-mouse IgG, HRP-linked Antibody	n/a	Cell Signaling Technology	#7076	WB
Anti-rabbit IgG, HRP-linked Antibody	n/a	Cell Signaling Technology	#7074	WB

n/a: not applicable. Abbreviations: KLF15, Krüppel-like Factor 15; HRP, horseradish peroxidase; IgG, immunoglobulin G; IHC, immunohistochemistry; IF, immunofluorescence; IP, immunoprecipitation; WB, Western Blot.

M.7. Immunofluorescence

CCA cells (i.e., HUCCT1 and EGI1) were seeded at a density of $4x10^4$ and cultured on collagen-coated Millicell® EZ slides (Merk Millipore) for 24 hours. After that period, cells were washed briefly with PBS 1X and fixed with methanol, previously chilled at -20ºC, for 10 minutes at room temperature. For cell membrane permeabilization, samples were washed 3 times with ice-cold PBS 1X and incubated with 0.5% Tween-20/PBS 1X (PBS-T) for 10 minutes at room temperature. After 3 successive washes of 5 minutes each with PBS 1X, cells were blocked with 1% BSA/0.5% Tween-20/PBS 1X (PBS-T+BSA) for 45 minutes at room temperature and incubated overnight at 4°C in a humidified chamber, with anti-KLF15 in PBS-T+BSA (1:100; Abcam). Afterwards, cells were again washed 3 times with PBS 1X, upon which were incubated for 1 hour at room temperature with Alexa Fluor 594 secondary antibody in PBST+BSA (1:1000; Life Technologies). Coverslips were mounted on slides using VECTASHIELD® mounting medium with DAPI (Vector laboratories). Images were obtained at 40X with Eclipse 80i (Nikon) microscope using NIS-Elements.

M.8. Lentiviral transduction

CCA cells were subjected to recombinant lentivirus infection to establish cell lines with stable overexpression of KLF15, following the manufacturer's protocol (ABM, Richmond, BC, Canada). Briefly, 24 hours prior to lentiviral transduction, cells ($5x10^4$ per well) were seeded in a 24-well plate overnight. On the day of the transduction, a mixture of culture medium with polybrene (at a concentration of 8 µg/mL) was prepared, to enhance infection efficiency. A multiplicity of infection (MOI) of 3 was chosen to transduce the cells, incubating them in medium+polybrene for 24 hours, leaving at least one well uninfected, as infection control. The next day, the medium was changed, to remove the lentivirus and polybrene, and the cells were left undisturbed overnight. The following day, the cells in each well were split into the desired dilution (1:3 to 1:5, depending on the confluency of the cells at the moment of splitting) and platted into a new 24-well plate for 48 hours in complete medium. After this period, the cells were ready for antibiotic selection with puromycin (concentration of 2 µg/mL). Upon successful selection, the newly generated KLF15-overexpressing CCA cell lines were further expanded and maintained with an antibiotic selective pressure of 0.2 µg/mL puromycin.

M.9. Cell viability

Cell viability was assessed using Cell Proliferation WST-1 Assay (Roche) according to the manufacturer's instructions. Cells ($2.5x10^4$) were seeded in thin collagen-coated 96-well plates in their corresponding culture media and incubated during the corresponding timepoint (up to 72 hours) at 37ºC. Upon that period, 10 µL of WST-1 were added to each well, incubated at 37ºC for 1 hour and the signal was measured at 450 nm in a Halo LED 96® multiplate reader (Dynamic Scientific Ltd., UK).

M.10. Cell proliferation

Cell proliferation rates were determined by flow cytometry using the eBioscience™ Cell Proliferation Dye eFluor™ 670 (Invitrogen – Thermo Fisher Scientific). The eFluor™ 670 dye diffuses into the cells and covalently binds cellular proteins that contain primary amines, emitting red fluorescence (Ex 647 nm/Em 670 nm). The label is stable and is progressively halved within daughter cells following each cell division, thus diminishing the fluorescence intensity in each generation (**Figure M.1A**). Every generation of cells will appear as a different peak on a flow cytometry histogram (**Figure M.1B**).

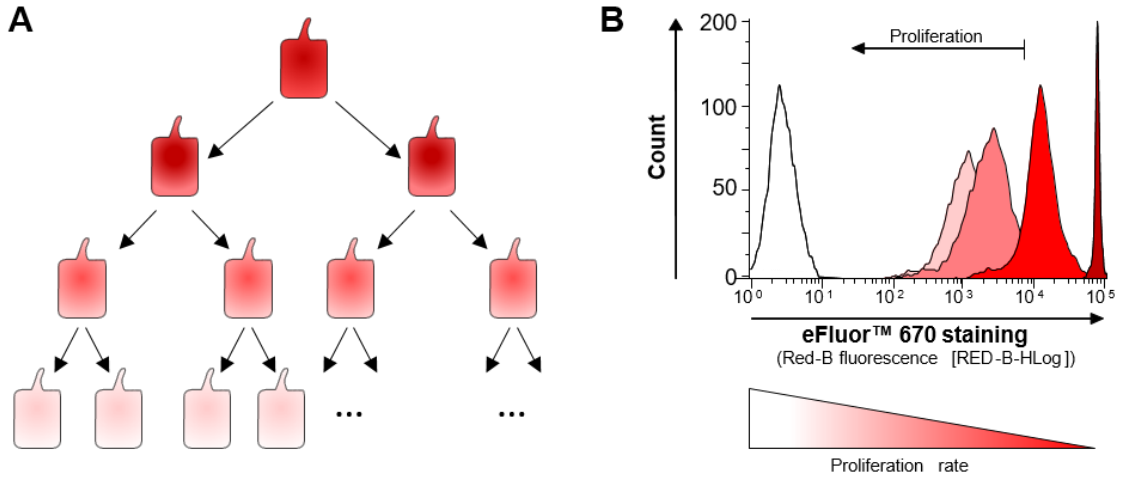

Figure M.1. Flow cytometry proliferation tracing with eFluor™ 670. (A) The basis of the assay consists of the progressive loss of the initial staining in each cell division as the dye is equally distributed among the daughter cells. **(B)** Representative histogram displaying stained and grown cells for different times: 24, 48 and 72 hours. Non-stained (white) and newly stained (dark red) cells are used as controls. As cells divide, lower staining intensity is detected in each cell division.

Briefly, cells were harvested and then counted using a Neubauer improved chamber (Marienfeld). Once the specific number of cells was separated, centrifugation was performed at 600g for 5 minutes at room temperature, followed by the removal of the supernatant. The cell pellet was resuspended in DPBS 1X (Gibco – Thermo Fisher Scientific) at a concentration of 10^6 cells/mL and labeled with a 10 µM stock eFluor™ 670, to a final concentration of 5 µM of the dye (1:2 dilution) for 10 minutes at 37ºC. The tube was mixed every 3 minutes during this incubation time. Then, 5 volumes of cold medium were added and the tubes were incubated for 5 minutes at 4ºC, to quench the staining. Next, cells were washed 3 times (centrifugation at 600g for 5 minutes) with medium, after which they were resuspended in their corresponding culture media and seeded in a thin collagen-coated 12-well plate (2 to 5x10^4 cells/well, depending on the cell line). Cells were left to attach overnight, and after 48 hours were harvested,

centrifuged and resuspended in DPBS 1X (Gibco – Thermo Fisher Scientific) according to flow cytometer manufacturer´s recommendations, and placed in a U-bottom 96-well plate (Falcon). The fluorescence signal was detected using the 661/15 nm filter of the *Guava Easycyte 8HT* flow cytometer (Merck Millipore) and analyzed with the Incyte™ 3.1 software (Merck Millipore). Of note, unstained cells and cells labeled just before launching the flow cytometer were used as negative and positive controls, respectively, to accurately adjust the flow cytometer settings. Results are represented as percentage relative to control cells (100% of proliferation).

M.11. Cell cycle

The cell cycle profile was analyzed by flow cytometry using TO-PRO™-3 iodide (Invitrogen – Thermo Fisher Scientific), which allows distinguishing G_0/G_1, S and G_2/M phases. Briefly, cells (~10^5) were harvested, washed with DPBS 1X (Gibco – Thermo Fisher Scientific) and then 70% ethanol chilled at -20ºC [in DPBS 1X (Gibco – Thermo Fisher Scientific), 1 mL/10^6 cells] was added dropwise while vortexing. Cells were incubated overnight at -20ºC. Next, the tubes were gently vortexed to ressuspend the pellets and 100 µL of their content was taken to new tubes. The samples were then centrifuged at 6000g for 5 minutes at room temperature, the supernatant was discarded and the cell pellets were subsequently stained with a DPBS 1X (Gibco – Thermo Fisher Scientific) solution (100 µL) containing TO-PRO™-3 iodide (Invitrogen – Thermo Fisher Scientific) (5 µL of a 10 µM stock) and RNAse A (1 µL of 10 mg/mL stock; Sigma). 50 µL from the previous sample mixtures were taken on to a U-bottom 96-well plate (Falcon) and incubated for 30 minutes at 37ºC in darkness. Afterwards, samples were diluted with DPBS 1X (Gibco – Thermo Fisher Scientific) at the recommended concentration, according to the flow cytometer manufacturer´s instructions. Finally, the fluorescent signal was detected using the 660/20 nm filter in the *Beckman Coulter CytoFLEX* flow cytometer (Life Sciences). The cell cycle was analyzed with the CytExpert software (Beckman Coulter, Life Sciences). Results are shown as the proportion of cells in G_0/G_1, S and G_2/M phases in the analyzed population (**Figure M.2**). Histograms were obtained using the flow cytometry analysis software Cytoflow (Massachusetts Institute of Technology, Cambridge, MA, USA).

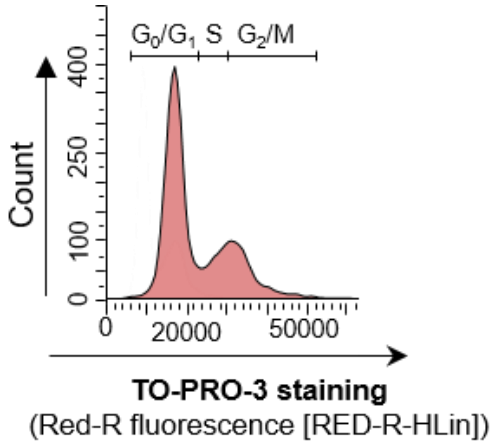

Figure M.2. Flow cytometry-based cell cycle analysis using TO-PRO™-3. The basis of the cell cycle assay consists of the quantitation of the DNA content of cells. As cells progress within the cell cycle, they duplicate their DNA content. In this way, cells in S phase will have more DNA than cells in G_1, taking up proportionally more dye and fluoresce more brightly until they double their DNA content. The cells in G_2 will be approximately twice as bright as cells in G_1.

M.12. Cell death

Cell death was determined by flow cytometry using a fluorescent staining method with TO-PRO™-3 iodide (Invitrogen, Thermo Fisher Scientific). TO-PRO™-3 iodide fluorescent dye (Ex 642 nm/Em 661 nm; red) has a very strong affinity for dsDNA upon loss of membrane and nuclear integrity, indicating late apoptosis.[312,313]

M.12.1. TO-PRO™-3 staining

Cells (1-3x10^4, depending on the cell line) were seeded in 24-well plates in their corresponding culture media and grown for 48 hours. A positive cell death control was included by adding 0.5% of hydrogen peroxide (H_2O_2) 24 hours prior to the cell harvesting. After 48 hours, supernatants and cells were collected and centrifuged at 600g for 5 minutes at room temperature. Cell pellets were then washed once with cold DPBS 1X (Gibco, Thermo Fisher Scientific), centrifuged again under the same conditions and then resuspended in 1:10 dH_2O-diluted Annexin V Binding Buffer (BioLegend) at a concentration of 10^6 cells/mL. Thereafter, cells were placed in a U-bottom 96-well plate (Falcon) and labeled with 1 µM TO-PRO™-3 iodide fluorescent dye (5 µL/well) in darkness for 15 minutes at 4ºC with and, subsequently, diluted with Annexin V Binding Buffer at the recommended concentration, according to the flow cytometer manufacturer´s instructions. Finally, the differentially labeled cell populations were distinguished setting up the appropriate filters (661/15 nm) in the *Guava Easycyte 8HT* flow cytometer (Merck Millipore). The death rate was analyzed with the Incyte™ 3.1

software (Merck Millipore). Single-stained samples were used to establish the levels of fluorescence compensation. Results are shown as relative to control cells.

M.13. Colony formation

The colony formation assay, also known as clonogenic assay, is a cell survival assay based on the ability of a single cell to grow into a colony. Briefly, a 1% agar (Ecogen) solution was prepared in dH_2O and heated for 2-3 minutes in a microwave to completely dissolve it. The melted agar solution and culture medium (the pertinent for each cell type) containing 10% FBS was placed and kept in a water bath at 40°C. For the bottom layer of agar, 1% agar solution was combined with 10% FBS culture medium in a 1:1 ratio, and 1.5 mL were added to each well of a 6-well plate. While the agar mixture was solidifying in the wells at room temperature, cells were harvested and counted using a Neubauer chamber (Marienfeld). For the upper layer of agar, 8000 CCA cells were taken in 1.5 mL of a solution of 0.3% agar in their corresponding culture media and subsequently seeded on top of the bottom agar layer. Once solidified, 500 µL of mediawere added to each well. The following day, and every 2-3 days for the next 3 weeks, appropriate culture medium was added. The colonies on the plate were fixed with crystal violet (Sigma-Aldrich). Finally, colonies were quantified with the ImageJ software 1.50 (NIH, Bethesda, MA, USA). Results are displayed as the number of colonies compared to the control group.

M.14. Cell migration

Cell migration was evaluated *in vitro* by a “wound-healing assay”. Cells ($3x10^5$) were seeded in 6-well plates in their corresponding culture media and incubated at 37ºC until they reached ~80% confluence as a monolayer. Thereafter, three longitudinal scratches were done in the cell monolayer using a 200 µL pipette tip. Next, cells were washed twice with PBS to remove floating cells, and “starvation” medium is added. This medium is low on FBS (1-3%, depending on the cells’ tolerance) to reduce any proliferative stimulants and guarantee that the cells that appear on the wound during the timecourse of the experiment are a result of migration. Cell migration was monitored every 12 hours. Pictures were taken at 0 and 24 h after the scratching using a Leica DM IL LED microscope equipped with a DFC 3000 G Leica digital. The wound healing area was quantified using Adobe Photoshop CS5 (Version 12.1) (Berkeley, CA, USA) and results are represented relative to the control group.

M.15. Mitochondrial energetic metabolism assessment by Seahorse Analyzer

Cell bioenergetics (respiratory capacity) of CCA cell lines were determined in an XF96 Extracellular Flux Analyzer (Seahorse Bioscience, North Billerica, MA, USA) using the *XF Cell Mito Stress Test Kit*, which evaluates the two main energy pathways, OXPHOS and glycolysis, following the manufacturer's instructions. This technology permits to measure key parameters of mitochondrial function by measuring the oxygen consumption rate (OCR) during sequential injections of reagents that modulate different components of the mitochondrial respiration. Indeed, the kit includes: i) oligomycin, an ATP synthase (the complex V) inhibitor, was used to measure ATP turnover and determine proton leak; ii) carbonyl cyanide-P-trifluoromethoxyphenylhydrazone (FCCP), an uncoupling agent that induces the collapse of the proton gradient and disrupts the mitochondrial membrane potential, allowing the determination of the maximum respiratory function; and iii) rotenone and antimycin A, which inhibit the electron transport chain by inhibiting complex I and III, respectively, leading to the shutdown of the mitochondrial respiration, being used to measure non-mitochondrial respiration.[314] Briefly, $5x10^3$ cells were seeded in each well of a collagen-coated 96-well Seahorse microplate (Seahorse) and cultured in fully-supplemented DMEM/F-12 media (**Table M.2**), for 48 hours. Next, cell culture medium was replaced by Assay medium containing minimum essential medium (MEM) (Gibco) supplemented with glucose, L-glutamine and sodium pyruvate (Sigma) at pH 7.4 and incubated for 1 hour at 37°C without CO_2. Baseline OCR measurements were performed as convenient in each assay, and sequential injections of mitochondrial inhibitors [i.e., 1 µM oligomycin, 1.2 µM FCCP and 0.5 µM both rotenone-antimycin A (all from Sigma-Aldrich)] were performed recording three measurements after each injection. Metabolic parameters were calculated as indicated by Seahorse Bioscience and as described in **Figure M.3**.

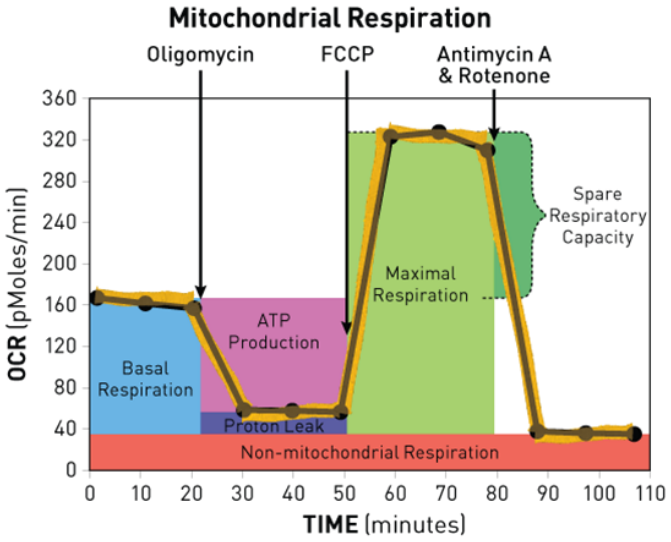

Figure M.3. Mitochondrial metabolic functions. Oxygen consumption rate (OCR) is measured along the expirement during the sequential injection of different mitochondrial inhibitors, providing the different metabolic values (Adapted from Seahorse Bioscience).

M.16. Mass spectrometry and proteomic analyses

Comparisons of the cellular proteomic profiles of control (WT and Lenti-Cont) and *KLF15* overexpressing CCA (EGI1) cells were performed.

All samples were extracted or eluted using 7 M urea, 2 M thiourea, 4% CHAPS. Samples were incubated for 30 minutes at room temperature under agitation and digested following the Filter-Aided Sample Preparation protocol[315] with minor modifications. Trypsin was added to a trypsin:protein ratio of 1:10, and the mixture was incubated overnight at 37ºC, dried out in a RVC2 25 speedvac concentrator (Christ), and resuspended in 0.1% formic acid (FA).

Samples were analyzed in a novel hybrid trapped ion mobility spectrometry – quadrupole time of flight mass spectrometer parallel accumulation serial fragmentation (tims TOF Pro with PASEF, Bruker Daltonics) coupled online to a nanoElute liquid chromatograph (Bruker). This mass spectrometer takes advantage of a novel scan mode termed parallel accumulation – serial fragmentation (PASEF), which multiplies the sequencing speed without any loss in sensitivity[316] and has been proven to provide outstanding analytical speed and sensibility for proteomics analyses.[317] Sample (200 ng) was directly loaded in a 15 cm nanoElute FIFTEEN C18 analytical column (Bruker) and resolved at 400 nL/minute with a 30 minute gradient. The column was heated to 50ºC using an oven.

M.16.1 Proteomic analysis

Spectral counts for each protein (the number of identified spectra matching to peptides from that protein, also named SpC or PSMs) were used for the differential analysis. Data was loaded onto the Perseus platform and further processed (log_2 transformation, imputation). A *t*-test was applied in order to determine the statistical significance of the differences detected. Functional analyses of proteins were performed in the STRING database,[318] and by gene ontology (GO) enrichment using DAVID Bioinformatics Resources.[319] In addition, heatmaps were generated using Heatmapper for data visualization.[320]

M.17. *In vivo* CCA models

The role of *KLF15* was studied *in vivo* using subcutaneous xenograft CCA mouse models. All experimental procedures were approved by the *Ethical Committee for Animal Experimentation* of the supporting Institutions and were used in conformity with the Institution's guidelines for the use of laboratory animals. [CEEA20/014 and CEEA21/009 (Biodonostia, San Sebastian)]

M.17.1 Sleeping Beauty model of CCA

This study was performed in collaboration with Dr. Diego Calvisi (University Clinic of Regensburg, Germany), aiming to determine the role of KLF15 in CCA development. For this purpose, the sleeping beauty model of CCA was generated by the administration of plasmids encoding for NCID1 and AKT together with the "sleeping beauty" transposase through hydrodynamic tail vein injection (10% of the total mouse weight) to 10 FVB mice. After 4.5 weeks, mice were sacrificed and livers were extracted, weighed and measured. Liver tissue samples were formalin-fixed and paraffin-embedded. 5 µm-thick sections were cut and stained with hematoxylin & eosin for morphological assessment as previously described.

M.17.2 Subcutaneous mouse model of CCA

M.17.2.1 Subcutaneous model of CCA with KLF15 overexpressing cells

CCA (EGI1) WT, Lenti-Cont or Lenti-KLF15 cells ($2x10^6$) were subcutaneously injected in both flanks of 10 immunodeficient CD1 nude mice (Crl:CD1-Foxn1^{nu}, strain 086, homozygous) (Charles River), for each condition. Tumor volumes were monitored by

measuring the tumor size with a caliper twice a week for 2 months. Tumor volume (V) was calculated using the following formula: $V = (D \times d^2)/2$ (where “D” represents the largest diameter measured and “d” the shortest).

M.17.2.2 Subcutaneous model of CCA with intratumoral injection of lentivirus with KLF15

CCA (EGI1) cells ($2x10^6$) were subcutaneously injected in both flanks of 30 immunodeficient CD1 nude mice (Crl:CD1-Foxn1^{nu}, strain 086, homozygous) (Charles River). Once the average tumor size was 95 mm3, mice were homogeneously distributed into 3 study groups. Two intratumor lentiviral injections ($1x10^7$ lentivirus/tumor) were administered to each tumor, with either control or *KLF15* lentivirus or saline for the *sham* group, and spaced 2 weeks in between them. Tumor volumes were monitored by measuring the tumor size with a caliper twice a week for 32 days. Tumor volume (V) was calculated using the following formula: $V = (D \times d^2)/2$ (where “D” represents the largest diameter measured and “d” the shortest).

M.18. Statistical analysis

Statistical analyses were performed using the GraphPad Prism 8.01 software (GraphPad Software). Once the normal distribution of the data was assessed with Shapiro-Wilk test, the statistical difference between two data sets was determined using the parametric paired or unpaired Student´s t-test or the non-parametric Mann-Whitney test, depending on the result of the normality test. For comparison between more than two data sets, one-way analysis of variance (ANOVA) with Tukey´s *post hoc* test or Kruskal-Wallis with Dunn´s *post hoc* test were implemented for the analysis of normally and non-normally distributed data, respectively. For correlations, Spearman’s rank correlation coefficient was employed. Data are indicated as mean ± standard error of the mean (SEM), and differences of $p < 0.05$ were considered statistically significant.

Results

R.1. Characterization of KLF15 expression in human liver and CCA tumors

R.1.1. KLF15 *is mainly expressed in epithelial cells within the liver*

In order to test the adequacy of studying KLF15 in the context of CCA, we firstly decided to assess which cell types express KLF15 in human healthy livers. To achieve this, we analyzed a single-cell RNA-sequencing (scRNA-seq) dataset accessible through the Human Protein Atlas database (https://www.proteinatlas.org).[321] The expression of this transcription factor was predominantly detected in the epithelial cell types of the liver, namely hepatocytes and cholangiocytes, followed by HSCs, while being barely found in immune cells (**Figure R.1**).

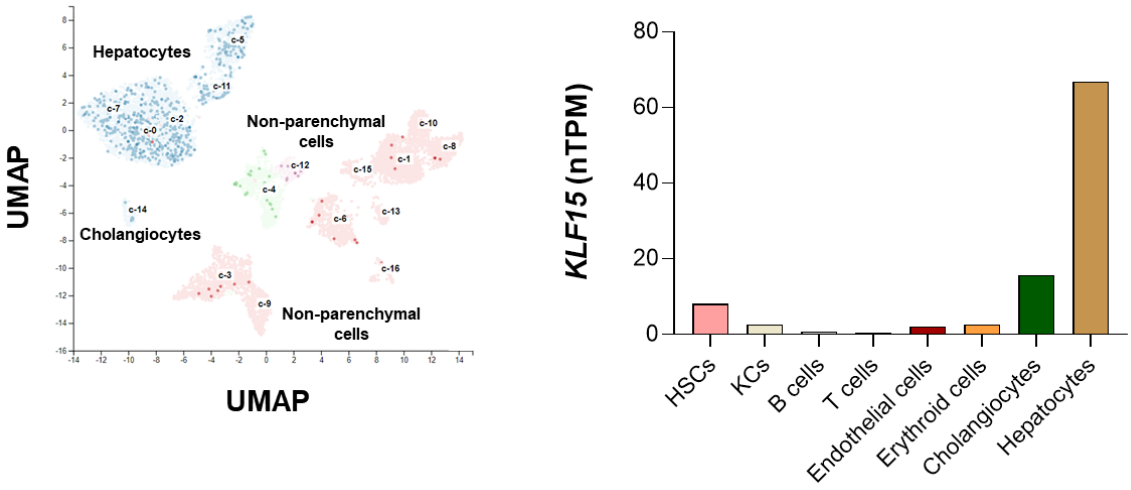

Figure R.1. KLF15 is predominantly expressed in epithelial cells within human healthy liver. (A) tSNE plots and proportion of cell types in human healthy livers from a scRNA-seq dataset available in the Human Protein Atlas; **(B)** normalized expression (normalized transcripts per million, nTPM) of *KLF15* in different liver cell types.

R.1.2. The expression of KLF15 *is downregulated in human CCA biopsies compared to normal human liver tissue*

After confirming that *KLF15* is expressed in healthy cholangiocytes, we intended to evaluate if this transcription factor could be dysregulated in CCA. For this purpose, the mRNA levels of *KLF15* were analyzed in CCA human biopsies, surrounding normal (SN) human liver tissues and normal bile ducts (NBD) analyzed through 3 different approaches (i.e. mRNA microarray, RNA-seq and qPCR) and in 6 distinct cohorts of patients [i.e. Montal (CCA, n=182; NBD, n=38), Copenhagen (CCA, n=210; SN, n=143; NBD, n=9), TCGA (CCA, n=36; SL, n=9), TIGER (CCA, n=91; SL, n=91), Job (CCA, n=78; SL, n=31) and San Sebastian (CCA, n=21; SL, n=18)]. The expression (mRNA) levels of *KLF15* were found to be decreased in the mRNA microarray and RNA-seq

datasets among all the cohorts of patients with CCA, when compared to a given type of control (surrounding human liver tissue or normal bile duct) (**Figure R.2A-E**). Importantly, in the San Sebastian cohort, decreased levels of *KLF15* measured by qPCR were detected in human CCA samples, compared to non-tumor surrounding liver samples, validating the findings obtained in the other cohorts (**Figure R.2F**).

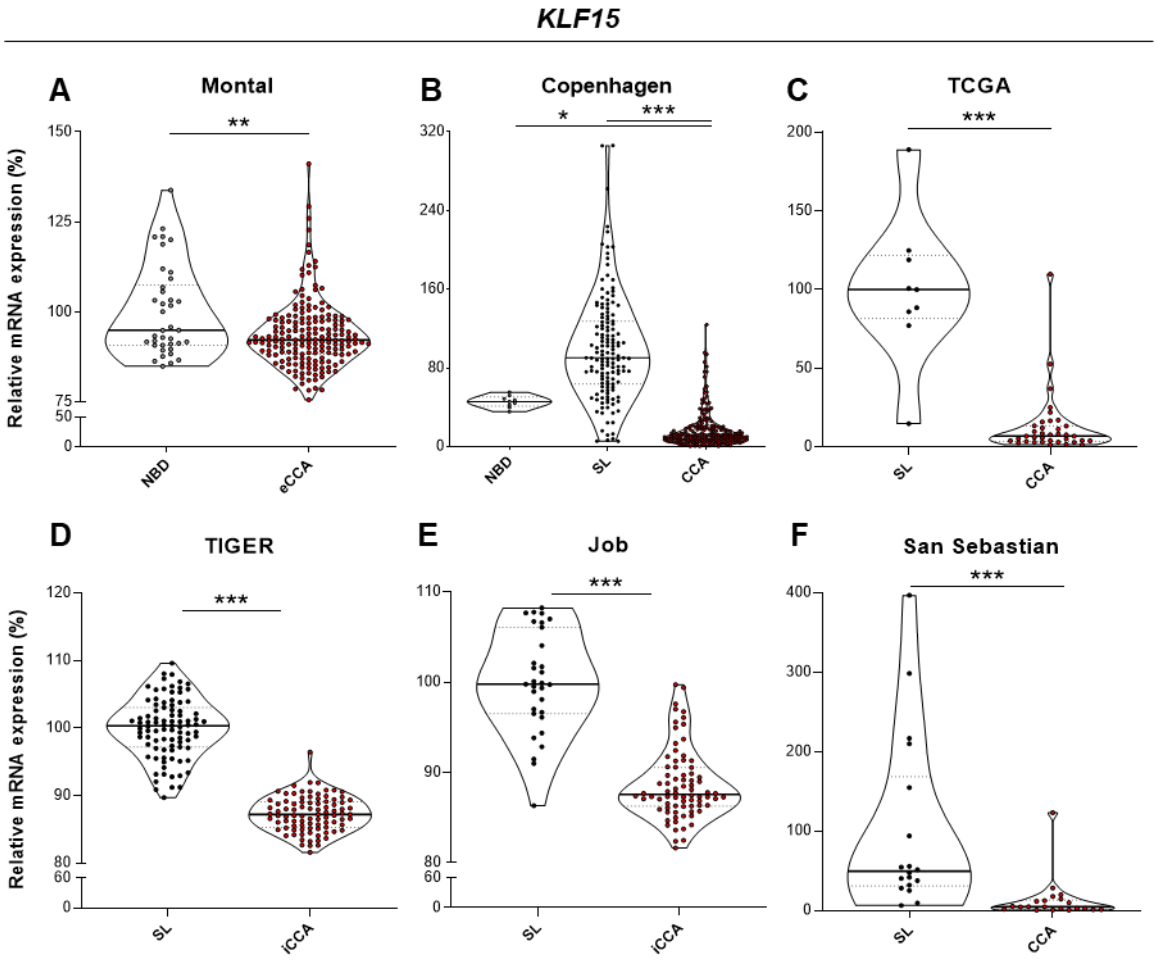

Figure R.2. KLF15 is downregulated in human CCA tumors. (A) *KLF15* mRNA (microarray) expression in eCCA tumors (n=182) compared to normal bile ducts (NBD n=38) from the Montal cohort. **(B)** *KLF15* mRNA (microarray) expression in CCA tumors (n=210) compared to surrounding normal human tissue (n=143) and to NBD (n=9) from the Copenhagen cohort. **(C)** *KLF15* mRNA (RNA-seq) expression in CCA tumors (n=36) compared to surrounding normal human tissue (n=9) from the TCGA cohort. **(D)** *KLF15* mRNA (microarray) expression in iCCA tumors (n=91) compared to surrounding normal human tissue (n=91) from the TIGER cohort. **(E)** *KLF15* mRNA (microarray) expression in iCCA tumors (n=78) compared to surrounding normal human tissue (n=31) from the Job cohort. **(F)** *KLF15* mRNA expression measured by qPCR in CCA tumors (n=21) compared to surrounding normal human tissue (n=18) from the San Sebastian cohort. Data are shown as mean ± SEM. Mann-Whitney **(A** and **C-F)** and Kruskal-Wallis (**B**) tests were used. *, ** and *** represent *p*-values of <0.05, 0.01 and 0.001, respectively in comparison to surrounding normal liver tissue or to NBDs. Abbreviations: CCA, cholangiocarcinoma; KLF15, Krüppel-like factor 15; NBD, normal bile duct; SL, surrounding liver.

In addition, the expression of *KLF15* was found downregulated in human CCA tumors regardless of the tumor's mutational profile, when compared to both NBD and SL (**Figure R.3**). In fact, no significant differences between patients stratified according to the presence of the most common genetic alterations in CCA (i.e., *IDH1*, *KRAS* or *TP53*), and the ones without these genetic mutations (Udt mut), consequently suggesting that *KLF15* downregulation may be considered a general event during cholangiocarcinogenesis.

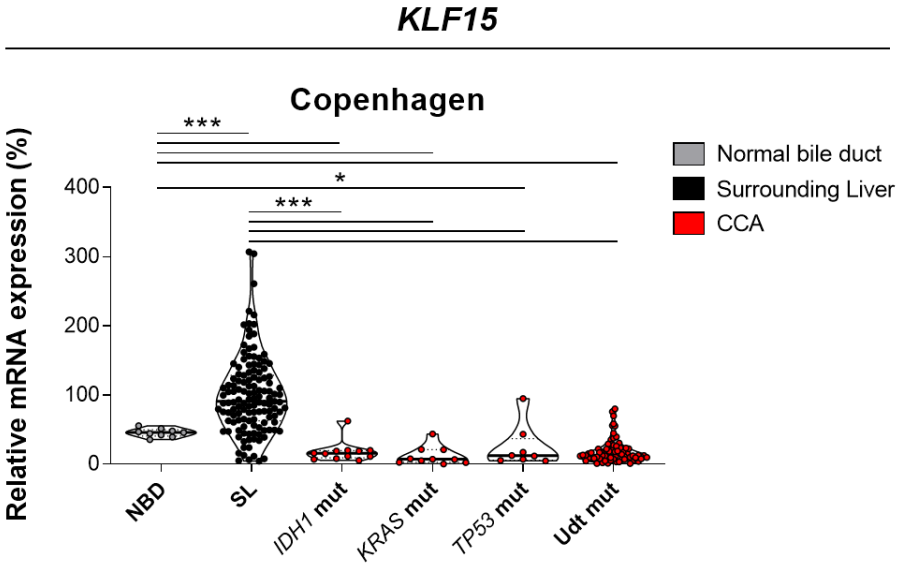

Figure R.3. KLF15 downregulation in CCA occurs independently of the underlying tumor driving mutations. *KLF15* mRNA (microarray) expression in *IDH1*-, *KRAS*- or *TP53*-mutant CCA tumors or in tumor without any of these genetic mutations (Udt group) (n=104) compared to surrounding normal human tissue (n=132) and to NBD (n=9) (Copenhagen cohort). Data are shown as mean ± SEM. Kruskal-Wallis test was used. * and *** represent *p*-values of <0.05 and 0.001, respectively in comparison to surrounding normal liver tissue or to NBDs. Abbreviations: CCA, cholangiocarcinoma; KLF15, Krüppel-like factor 15; NBD, normal bile duct; SL, surrounding liver; Udt mut, undetermined mutations.

R.1.3. The expression of KLF15 *is downregulated in human CCA cells compared to normal human cholangiocytes (NHCs)* in vitro

The expression levels of the transcription factor KLF15 were then assessed through qPCR in four human CCA cell lines (i.e., HUCCT1, EGI1, Witt and TFK1) compared to NHCs. The data gathered showed a considerably reduced *KLF15* expression in all of the human CCA cell lines analyzed when compared to NHCs in culture (**Figure R.4A**), further corroborating the pattern observed in the human samples. Since the *KLF15* gene codes for the KLF15 transcription factor, its proteins levels were also analyzed, both through immunoblotting and immunofluorescence. A marked reduction in KLF15 protein

levels was observed in all CCA cell lines when compared to NHCs, measured by both immunoblotting and immunofluorescence (**Figure R.4B-C**). This reduction in protein expression parallels the alterations verified at the transcriptional level, providing a robust confirmation of the downregulation of KLF15 in CCA.

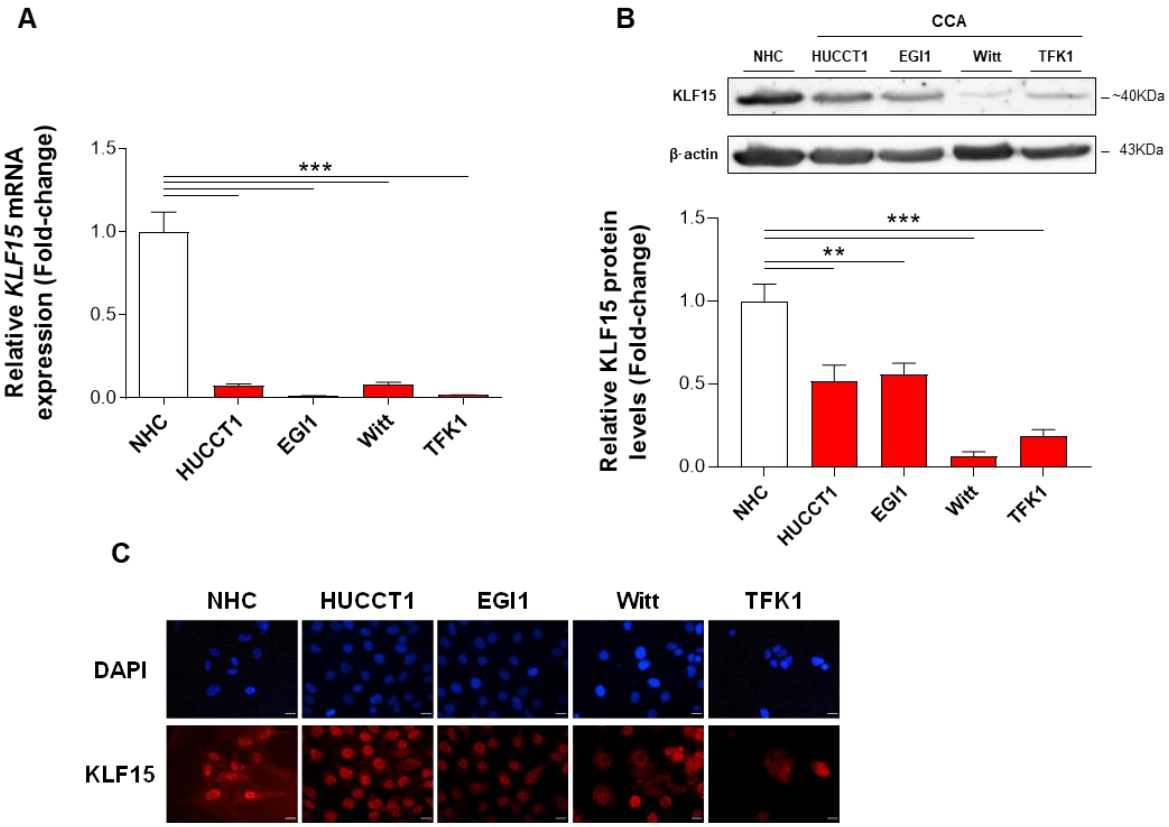

Figure R.4. KLF15 is markedly reduced at the protein level in human CCA cell lines compared to NHC in culture. (A) Relative mRNA expression of *KLF15* measured by qPCR in 4 different CCA cell lines (red bars) and NHC (white bar) (n=3). **(B)** Representative immunoblot and quantification of KLF15 protein in 4 CCA cell lines (red bars) compared to NHC (white bar). β-actin was used as a loading control (n=7). **(C)** Immunofluorescence images of KLF15 in 4 CCA cell lines (HUCCT1, EGI1, Witt and TFK1) compared to NHC (scale bars: 10 μm). Data are shown as mean ± SEM. Mann-Whitney test was used. ** and *** represent *p*-values of <0.01 and 0.001, respectively in comparison to NHCs. Abbreviations: CCA, cholangiocarcinoma; NHC, normal human cholangiocytes.

R.1.4. Klf15 is downregulated in mouse CCA tumors

We next evaluated the expression levels of *Klf15* in mouse CCA tumors. By hydrodynamic tail vein injection, plasmids encoding the oncogenes NICD/AKT and the sleeping beauty transposase were administered to mice to induce the development of CCA (**Figure R.5A-B**). The expression levels of *Klf15* were once again evaluated through qPCR and, in resemblance with human data, *Klf15* was found sharply reduced when compared to the expression levels detected in control mouse liver (**Figure R.5B**).

Overall, we herein confirm that the downregulation of *KLF15* in CCA is a common event occurring during human and murine cholangiocarcinogenesis.

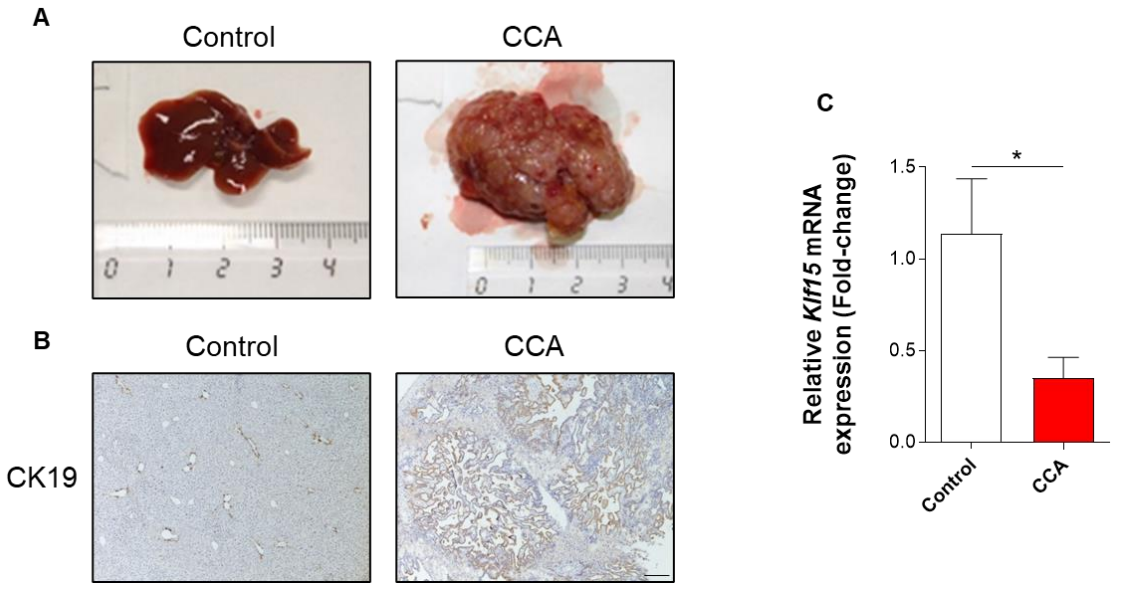

Figure R.5. *Klf15* expression levels are reduced in mouse CCA tumors. (A) Representative images of livers from control mice (n=5) and mice with CCA (n=8) at sacrifice. **(B)** Representative immunohistochemistry images of CCA lesions staining for CK19 in livers from control mice and mice with CCA. **(C)** Relative *Klf15* mRNA expression (qPCR) expression in liver tissue samples from mice with CCA (n=8) compared to control mice (n=5). Data are shown as mean ± SEM. Mann-Whitney test was used. * represents p-values of <0.05 in comparison to control mice.

R.1.5. Reduced KLF15 levels *are associated with worse clinicopathological findings in patients with CCA*

Upon confirming the dysregulation of KLF15 in CCA, its correlation with clinicopathological parameters in human patients with CCA was further investigated. Our data showed that *KLF15* levels progressively decreased with the differentiation status of human CCA tumors, with patients with poorer tumor differentiation showcasing the more pronounced decrease in *KLF15* expression. In addition, patients with lymph node invasion and more advanced tumor stages displayed decreased *KLF15* expression levels, when compared to patients without lymphatic affection or early-stage disease, respectively (**Figure R.6.A-C**).

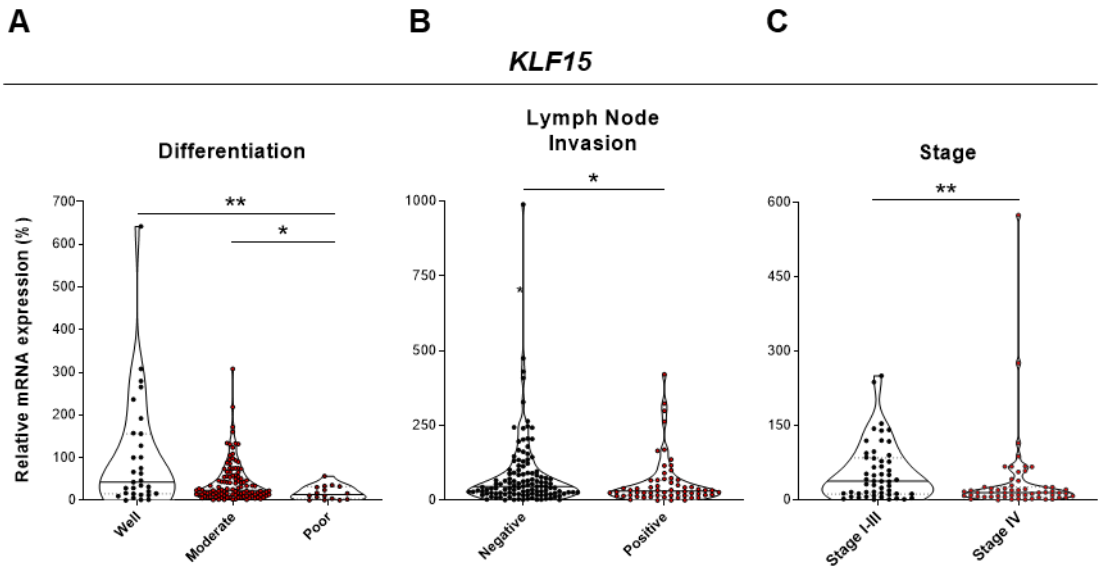

Figure R.6. Low *KLF15* expression in CCA tumors correlates with worse tumor features and more advanced disease in patients with CCA. (A) *KLF15* mRNA (microarray) expression in CCA tumors stratified by the tumor differentiation grade: well- (n=31), moderately- (n=114) or poorly- (n=16) differentiated (pooled data from Copenhagen and Nakamura cohorts). **(B)** *KLF15* mRNA (microarray) expression in CCA tumors from patients stratified according to the presence/absence of lymph node invasion [negative (n=122), positive (n=60)] (pooled data from Copenhagen and Nakamura cohorts). **(C)** *KLF15* mRNA (microarray) expression in patients with CCAs grouped by tumor stage, according to AJCC guidelines in the Nakamura cohort: early- [stage I-III (n=53)] or late- [stage IV (n=57)] stage. Data are shown as mean ± SEM. Mann-Whitney test was used. * and ** represent *p*-values of <0.05 and 0.01, respectively.

We next correlated the expression of *KLF15* with makers of tumor differentiation and progression in patients with CCA. To do so, we combined the normalized expression data of the Copenhagen, Nakamura and TIGER cohorts and observed that the expression of *KLF15* negatively correlated with the expression of several different tumor-progression related genes, such as oncogenic biliary markers (i.e., *SOX9*, *KRT19* and *KRT17*), stemness markers (i.e., *CD44*, *EPCAM*, *KLF4*, *MYC*, *PROM1* and *THY1*) and EMT markers (i.e., *VIM*, *TCF3*, *TCF4*, *TWIST1* and *MUC1*) (**Table R.1**).

Table R.1. KLF15 expression negatively correlates with different oncogenic markers in human CCA tumors. Correlation values between KLF15 expression levels and expression levels of the gene of interest in human CCAs (n=579) (pooled data from Copenhagen, Nakamura and TIGER cohorts). Spearman's rank correlation coefficient was used. Abbreviations: EPCAM, epithelial cell adhesion molecule; KLF4, Krüppel-like factor 4; KRT17, cytokeratin 17; KRT19, cytokeratin 19; MUC1, mucin 1; MYC, c-myc; PROM1, prominin-1 (CD133); SOX9, SRY-Box transcription factor 9; TCF3, transcription factor 3; TCF4, transcription factor 4; THY1, thymocyte differentiation antigen 1 (CD90); TWIST1, twist-related protein 1; VIM, vimentin.

Categories	Gene	r	95% Confidence Interval	*p*-value
Oncogenic Biliary Markers	*SOX9*	-0,3576	-0,5045 to -0,1905	< 0,0001
	KRT19	-0,3768	-0,5209 to -0,2119	< 0,0001
	KRT7	-0,2578	-0,4178 to -0,08233	0,0034
Stemness	*CD44*	-0,3765	-0,4662 to -0,2790	< 0,0001
	EPCAM	-0,2891	-0,4453 to -0,1158	0,001
	KLF4	-0,3121	-0,4071 to -0,2103	< 0,0001
	MYC	-0,2221	-0,3861 to -0,04462	0,0121
	PROM1	-0,2505	-0,3500 to -0,1454	< 0,0001
	THY1	-0,3452	-0,4376 to -0,2456	< 0,0001
EMT	*VIM*	-0,3391	-0,4320 to -0,2390	< 0,0001
	TCF3	-0,3728	-0,4629 to -0,2751	< 0,0001
	TCF4	-0,184	-0,2872 to -0,07672	0,0006
	TWIST1	-0,2638	-0,3623 to -0,1595	< 0,0001
	MUC1	-0,4103	-0,4969 to -0,3155	< 0.0001

To undoubtedly evaluate the value of KLF15 as a prognostic marker in CCA, we measured the potential association of KLF15 with the OS and RFS of patients with CCA through the log rank (Mantel-Cox) test. Kaplan-Meyer analysis revealed that patients from the Nakamura, Jusakul and Job cohorts with higher *KLF15* expression levels have an improved OS, when compared to patients with lower *KLF15* expression levels (**Figure R.7.A-C**). In addition, patients with decreased *KLF15* levels display shorter RFS rates than those with higher *KLF15* expression levels (**Figure R.7.D**), thus confirming the prognostic value of KLF15 for CCA.

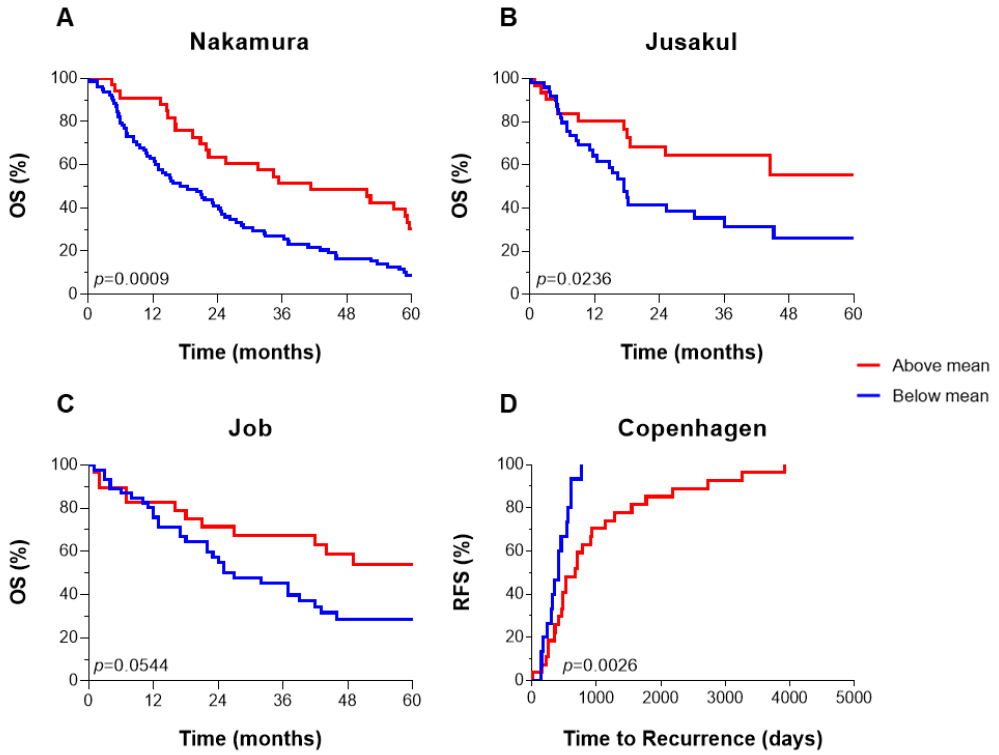

Figure R.7. Low KLF15 expression in CCA tumors correlates with worse overall and recurrence-free patient survival rates. Overall survival (OS) of patients stratified by low and high *KLF15* mRNA expression according to the mean value in the **(A)** Nakamura (n=111). **(B)** Jusakul (n=81) and **(C)** Job (n=76) cohorts. **(D)** Recurrence-free survival (RFS) of patients grouped by low and high *KLF15* mRNA expression according to the mean value in the Copenhagen cohort (n=42). Log-rank (Mantel-Cox) test was used.

R.1.6. KLF15 *downregulation correlates with hypermethylation of promoter enhancing regions of the gene in human CCA tumors*

In order to understand a possible mechanism through which the expression of KLF15 is downregulated in CCA, we next evaluated if alterations in the DNA methylation of the *KLF15* gene were evident in human CCA tumors, when compared to surrounding tissue. The regions starting from 200-1500 base pairs upstream of the transcription starting site, designated TSS1500, the 5' untranslated (5'-UTR) region of the *KLF15* gene as well as the gene body were assessed (**Figure R.8A**). The TSS1500 region is considered a proximal promotor region, while the 5'-UTR and the gene body, although not being part of the promoter, can also be methylated and consequently affect gene expression.[322,323] Noteworthy, the promotor region TSS1500, as well as the 5'-UTR and the gene body were found hypermethylated in CCA tumors, in comparison with surrounding normal tissue (**Figure R.8B**). Additionally, *KLF15* expression levels negatively correlated with

the hypermethylation of all the previously identified regions (**Figure R.8C**), providing a stronger argument for a methylation-induced silencing of *KLF15* expression in CCA.

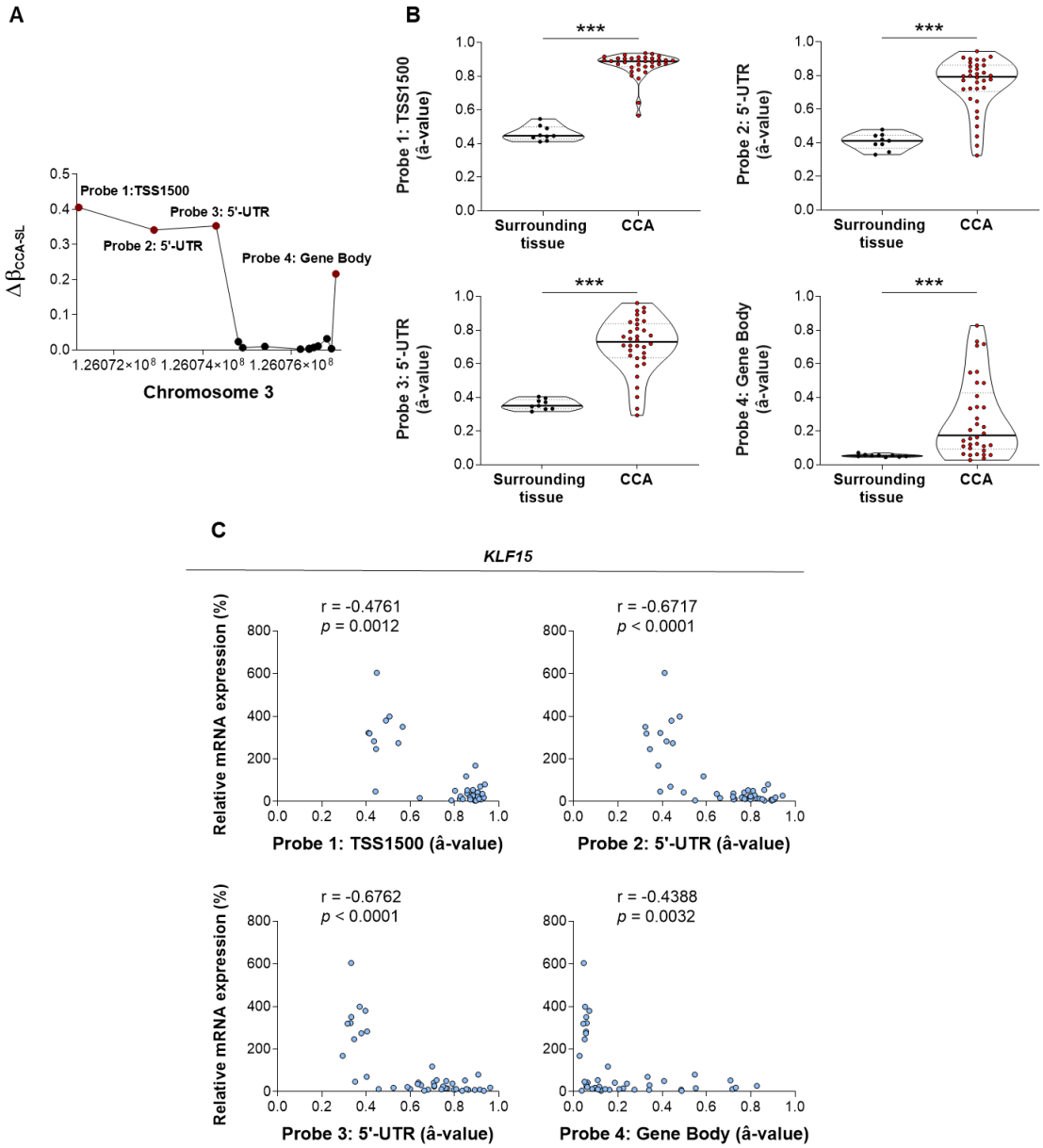

Figure R.8. *KLF15* downregulation correlates with DNA hypermethylation in enhancer regions near gene promotor. (A) Change in DNA methylation and location of hypermethylated probes in the *KLF15* gene from patients with CCA from the TCGA cohort. **(B)** Levels of DNA methylation in CCA samples (n=34) compared to surrounding normal tissue (n=9) from patients with CCA from the TCGA cohort. **(C)** Correlation between *KLF15* expression levels and DNA methylation levels among both CCA and surrounding normal tissue (n=43). Data are shown as mean ± SEM. Mann-Whitney test **(B)** and Spearman's rank correlation coefficient **(C)** were used. *** represent *p*-values of 0.001.

To confirm if KLF15 gene hypermethylation is actually related with the reduction in the expression of this transcription factor, four human CCA cell lines (i.e. HUCCT1, EGI1, Witt and TFK1) were treated with an hypomethylating agent – Zebularine (100 μM) – for 48 hours. Notably, incubation of human CCA cells with Zebularine increased the expression of *KLF15* by up to 200% in all tested cell lines (**Figure R.9**), confirming the relevance of DNA hypermethylation in the regulation of *KLF15* expression in CCA.

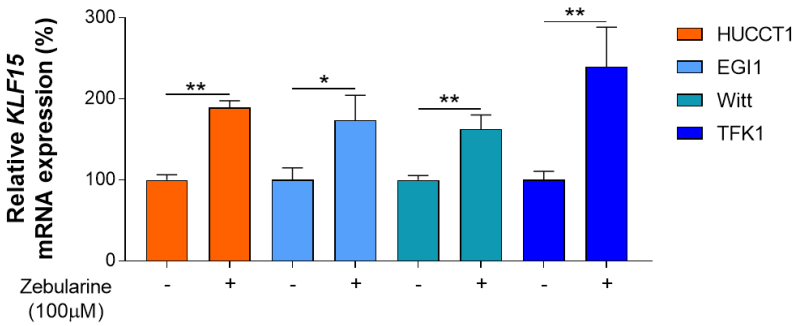

Figure R.9. Zebularine-induced hypomethylation increases KLF15 expression in human CCA cell lines *in vitro*. Relative mRNA expression (qPCR) of KLF15 in 4 different CCA cell lines (i.e., HUCCT1, EGI1, Witt and TFK1) upon 48 hours of incubation with hypomethylating agent Zebularine (100μM) compared to vehicle-treated cells (n=4). Mann-Whitney test was used. Data are shown as mean ± SEM. * and ** represent p-values of <0.05 and 0.01, respectively.

Although promising, the changes induced by Zebularine represented only a partial rescue in *KLF15* expression, not reaching the same expression found in NHC in culture (data not shown). Consequently, other mechanisms might be additionally involved in the regulation of the expression of this transcription factor. Other regulatory mechanisms of DNA transcription are often dysregulated in the context of cancer and can account for the differential expression of distinct genes, including histone acetylation. For this purpose, an inhibitor of HDACs – Trichostatin A (TSA) – was used at different concentrations, to assess if this epigenetic process might also alter *KLF15* expression in human CCA cell lines and NHCs in culture. We found no differences in *KLF15* expression after incubating cells with increasing doses of TSA (**Figure R.10**). Therefore, histone acetylation seems to have no discernible effect on *KLF15* expression, setting aside this mechanism for the regulation of this transcription factor, which suggest additional (epi)genetic mechanisms responsible for the reduction of KLF15 in CCA.

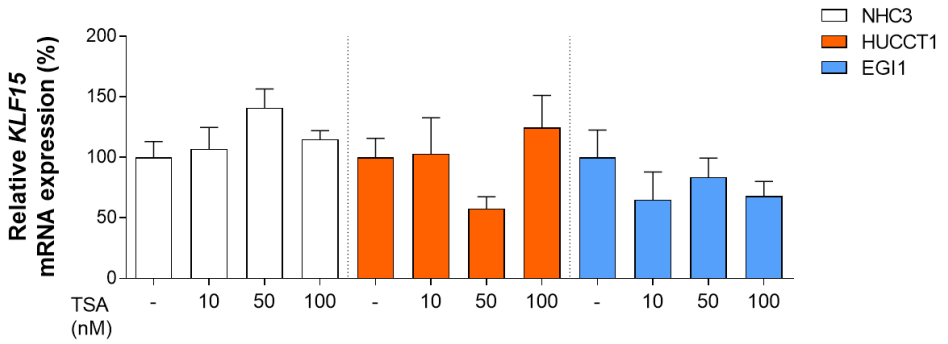

Figure R.10. Histone acetylation have no effect on the regulation of *KLF15* expression *in vitro*. Relative mRNA expression (qPCR) of KLF15 in 2 different CCA cell lines (i.e., HUCCT1 and EGI1) upon 48 hours of incubation with an inhibitor of Histone deacetylases (HDACs) – TSA (10, 50, 100nM) – compared to vehicle-treated cells (n=3). Mann-Whitney test was used. Data are shown as mean ± SEM. Abbreviations: TSA – Trichostatin A.

R.2 Modulation of KLF15 in CCA

R.2.1. Establishment of KLF15-overexpressing CCA cells

After confirming that KLF15 is downregulated in human CCA tumors, being an important prognostic factor, we next evaluated whether restauration of KLF15 expression levels in CCA cells may affect the behavior and phenotype of these cells and have a therapeutic effect on CCA. For this purpose, a human CCA cell line (EGI1) was successfully transduced with lentivirus for the stable overexpression of *KLF15* (EGI1 Lenti-KLF15). In parallel, adequate control lentiviral and non-transduced cell lines (EGI1 Lenti-Cont and EGI1 WT, respectively) were also generated and used for the following experiments. After infecting EGI1 cells, we observed that EGI Lenti-KLF15 cells displayed increased KLF15 expression, both at the mRNA (qPCR) and protein (immunofluorescence) levels, when compared to both EGI1 Lenti-Cont and EGI1 WT cells, reaching the expression levels detected in NHCs (**Figure R.11**).

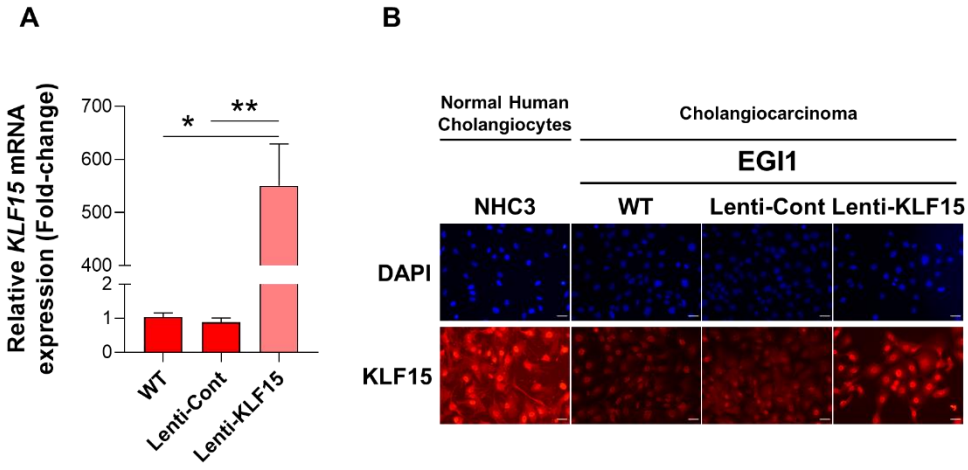

Figure R.11. Establishment of KLF15-overexpressing CCA cells (EGI1 Lenti-KLF15). (A) Relative mRNA expression (qPCR) (n=3) and **(B)** immunofluorescence images of non-transduced (WT), control lentivirus (Lenti-Cont) and KLF15 lentivirus (Lenti-KLF15) transduced EGI1 CCA cells, as well as NHC in culture (scale bars: 10 μm). Data are shown as mean ± SEM. Mann-Whitney test was used * and ** represent *p*-values of <0.05 and 0.01, respectively.

R.2.2. Functional evaluation of the effect of KLF15 overexpression in vitro

To understand the functional effects of the experimental upregulation KLF15 in human CCA cell lines, we next characterized the phenotype of these cells in terms of proliferation, survival, tumorigenicity, invasiveness and overall aggressiveness, which can give us some insights into the role and involvement of KLF15 in the development and progression of CCA. Therefore, several different aspects were first evaluated *in vitro*.

R.2.2.1. KLF15 overexpression reduces CCA cell viability and proliferation, inducing cell cycle arrest in S and G_2/M phases

The viability of these cells and their control counterparts was evaluated using the WST-1 assay, during a 72-hour time-course. The data obtained showed a decrease in cell viability of the EGI1 Lenti-KLF15 cells in all the time-points evaluated, when compared to both control cell lines (**Figure R.12A**) that showed a similar and overlapping growth curve. As a result, the growth rate of EGI1 Lenti-KLF15 cells was slower, when compared to controls, which may be due to alterations in the cell proliferation and/or cell death. Therefore, we next evaluated cell proliferation by flow cytometry (eFluor™ 670 dye) and observed that KLF15-overexpressing CCA cells showed a marked reduction of their proliferation rate, in comparison to both control conditions (**Figure R.12B**). In parallel, a decrease in the mRNA levels of the marker of proliferation *KI67*, as well as the DNA

polymerase δ cofactor *PCNA* was observed (**Figure R.12C**), further corroborating the evidence that previous data showed.

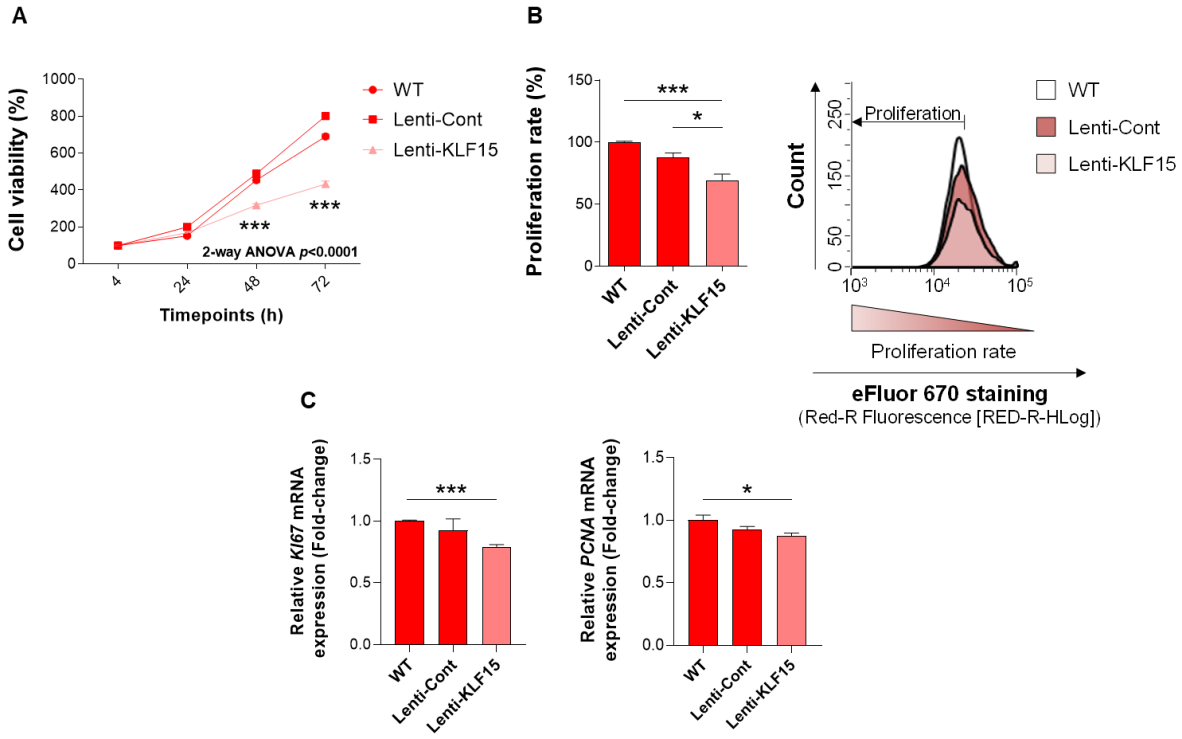

Figure R.12. KLF15-overexpressing CCA cells have reduced cell viability and lower proliferation rate *in vitro*. (A) Cell viability was assessed in EGI1 WT, EGI1 Lenti-Cont and EGI1 Lenti-KLF15 by the WST-1 assay for up to 72 hours (n=3). **(B)** Quantification of eFluor™ 670 signal intensity measured by flow cytometry in EGI1 WT, EGI1 Lenti-Cont and EGI1 Lenti-KLF15 upon 48 hours of growth (n=4). **(C)** Relative mRNA expression (qPCR) of *KI67* and *PCNA* in EGI1 WT, Lenti-Cont and Lenti-KLF15 (n=4). Data are shown as mean ± SEM. One-way ANOVA and Mann-Whitney tests were used. *, ** and *** represent p-values of <0.05, 0.01 and 0.001, respectively.

In order to validate the results of the proliferations assays, the cell cycle progression of these cells was evaluated by flow cytometry through TO-PRO™-3 staining. Upon 48 hours of cell growth, an increase in the proportions of EGI1 Lenti-KLF15 cells in the S and G_2/M phases was observed, when compared to control cells, along with a reduction in the proportion of cells in G_0/G_1 phase. (**Figure R. 13A**). In addition, there was also a decrease in the mRNA and protein levels of cyclin B1 (**FigureR.13B-C**), which is a protein mastering the transition from G2 to mitosis, therefore pinpointing an arrest in the G_2/M phase in KLF15-overexpressing cells.

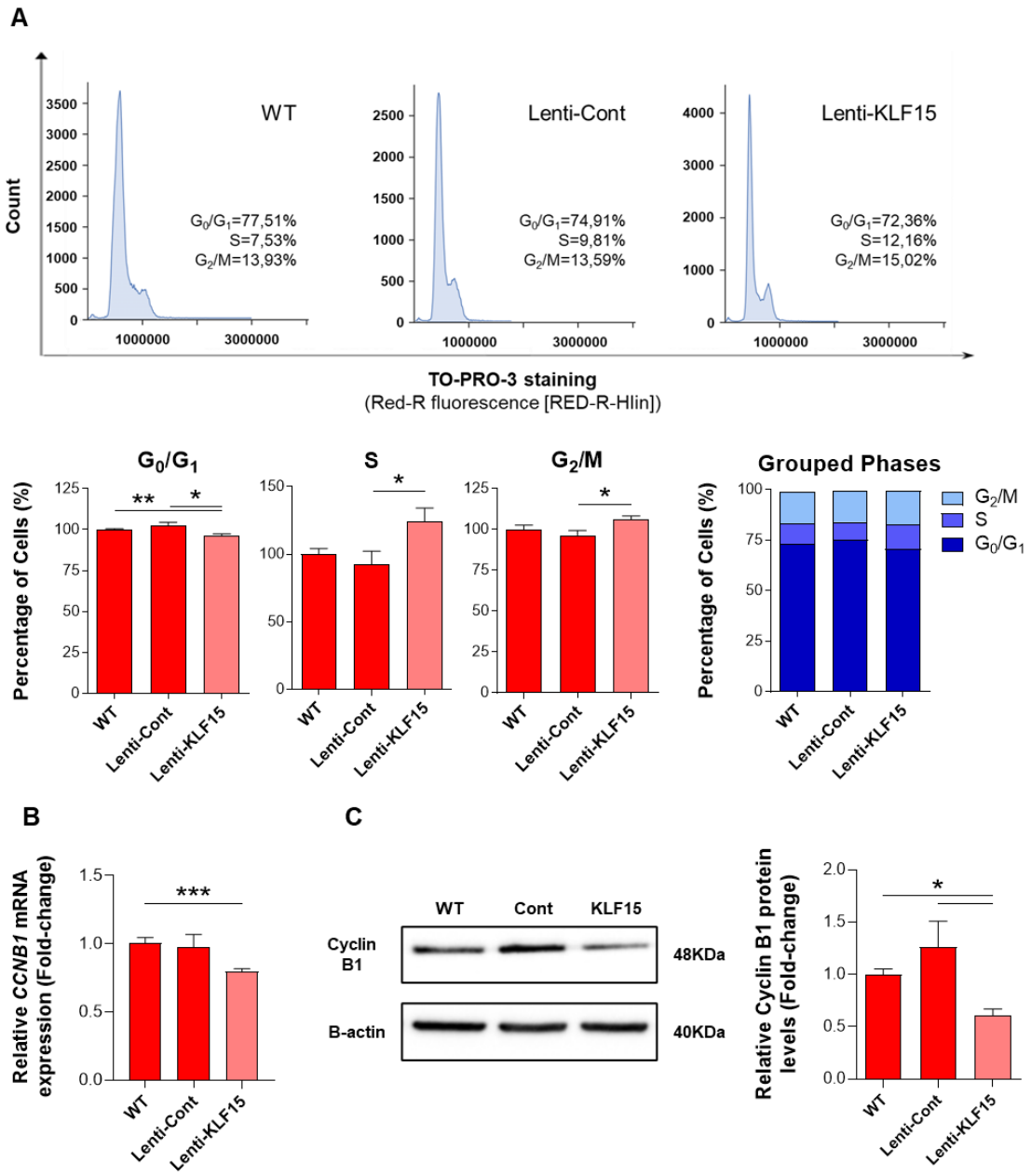

Figure R.13. KLF15 overexpression induces cell cycle arrest in G2/M phase. (A) Representative cell distribution histograms and quantification of the signal of TO-PRO™-3 in EGI1 WT, Lenti-Cont and Lenti-KLF15 (n=5). **(B)** Relative mRNA expression (qPCR) of *CCNB1* in EGI1 WT, Lenti-Cont and Lenti-KLF15 (n=3) **(C)** Representative immunoblot and quantification of CyclinB1 in EGI1 WT, Lenti-Cont and Lenti-KLF15 (n=3). Data are shown as mean ± SEM. Mann-Whitney test was used. * and ** represent *p*-values of <0.05 and 0.01, respectively. Abbreviations: CCNB1, Cyclin B1.

R.2.2.2. Baseline cell death levels remain unchanged upon KLF15 experimental upregulation

We next evaluated if cell cycle arrest and the consequent decrease in cell proliferation was complemented by a dysregulation in cellular death rates, which would all account

for the overall reduction in cell viability after KLF15 upregulation. For this purpose, the cell death rates of KLF15 overexpressing cells and their corresponding controls were determined by flow cytometry with by TO-PRO™-3 nuclear staining. Baseline cell death levels of EGI1 Lenti-KLF15 were not significantly altered, when compared to both WT and Lenti-Cont (**Figure R.14**), thus indicating that the decrease in viability observed after KLF15 experimental overexpression occurs more likely due to a more anti-proliferative mechanism, rather than a pro-cell death one.

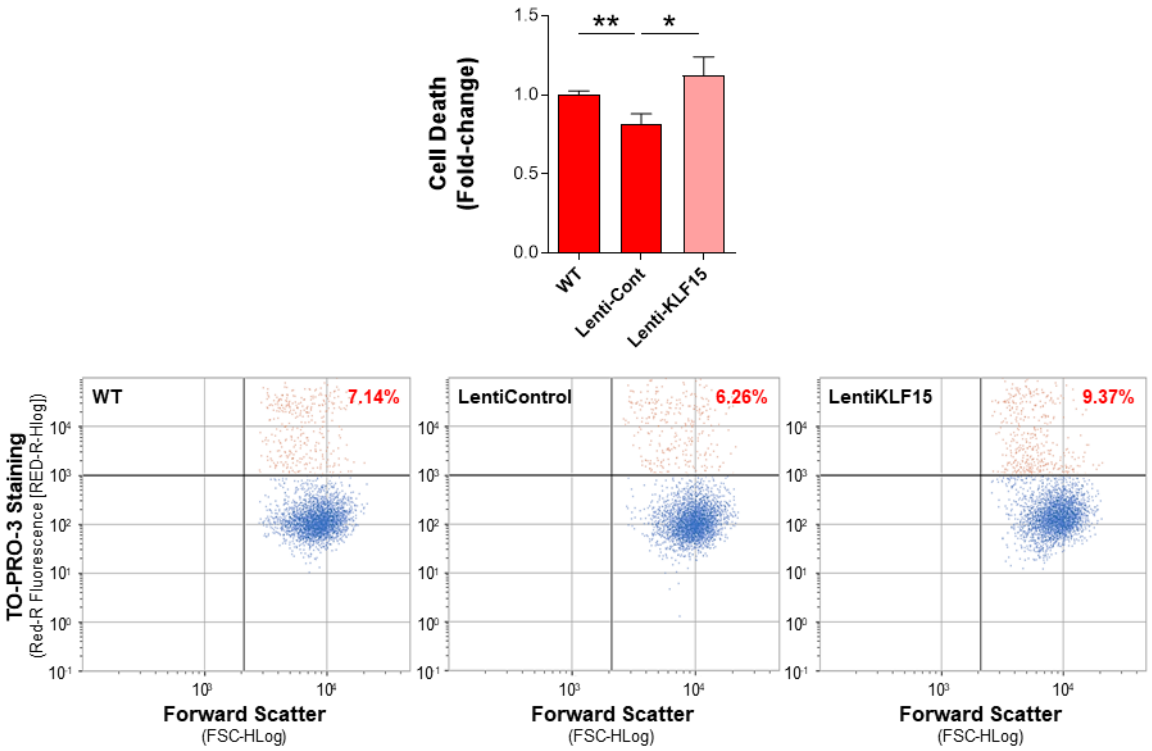

Figure R.14. Baseline cell death levels in KLF15-overexpressing CCA cells. Quantification and representative flow cytometry dot plots depicting KLF15-overexpressing CCA cells (EGI1 Lenti-KLF15) and corresponding transduced (EGI1 Lenti-Cont) and non-transduced (EGI1 WT) controls, stained with TO-PRO™-3 (orange dots), upon 48 hours of growth. Blue dots correspond to live non-stained cells (n=5). Data are shown as mean ± SEM. Mann-Whitney test was used. ** represent *p*-values of <0.01.

R.2.2.3. KLF15 overexpression reduces CCA colony formation ability

Anchorage-independent growth capability is a strong indicator of aggressiveness in cancer,[324] since normal or more benign cells lack this trait, following anoikis-related apoptosis. Therefore, we next evaluated the colony formation ability of these cells by growing these cells in soft agar. As shown in **Figure R.15**, there was a clear decrease in the number of colonies formed by KLF15-overexpressing CCA cells in comparison to

both respective controls. These observations suggest a possible role of KLF15 on the tumorigenic capacity of CCA cells.

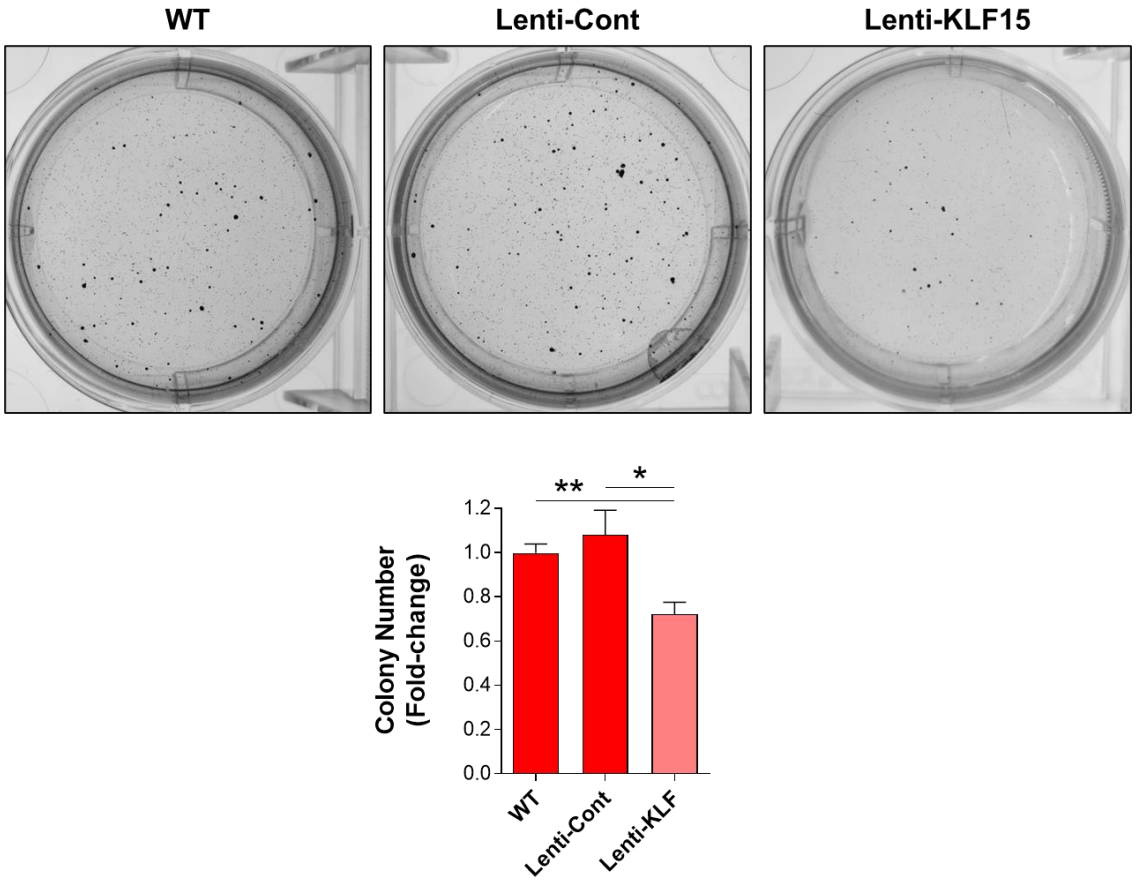

Figure R.15. KLF15 overexpression reduces CCA cells colony formation capacity. Representative images and quantification of soft agar colony formation assays in EGI1 WT, EGI1 Lenti-Cont and EGI1 Lenti-KLF15 cells (n=3). Data are shown as mean ± SEM. Student's t-test was used. * and ** represent *p*-values of <0.05 and 0.01, respectively.

R.2.2.4. KLF15 experimental overexpression reduces the migration capability and mesenchymal potential of CCA cells

Not only cell proliferation and survival indicate an increased malignancy of cancer cells, but also their invasiveness and migration capability. To this matter, migration of EGI1 Lenti-KLF15 and respective controls (WT and Lenti-Cont) was evaluated through wound healing assay. A marked reduction in the migratory ability of KLF15-overexpressing CCA cells was observed, when compared to both control conditions (**Figure R.16**).

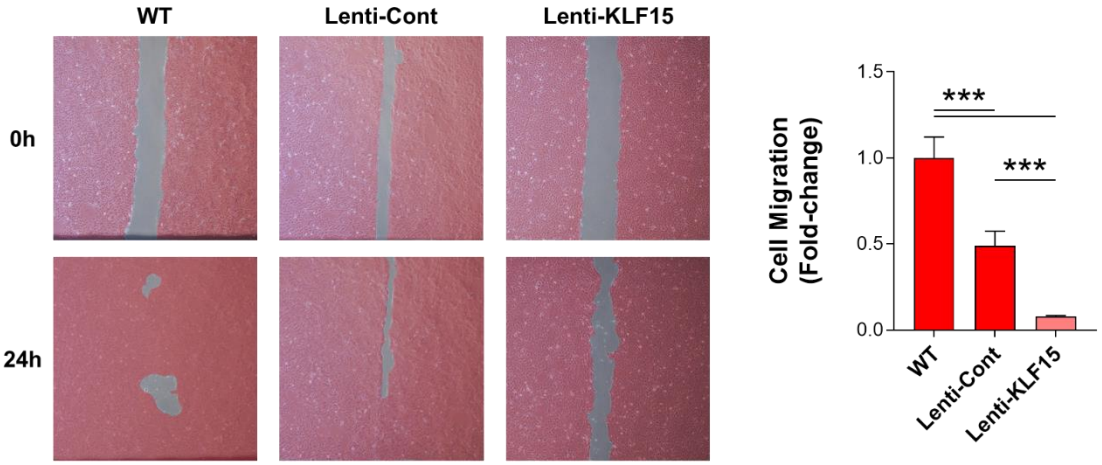

Figure R.16. KLF15 overexpression leads to decreased cell migration in CCA cells. Representative images of the wound-healing assay in EGI1 WT, EGI1 Lenti-Cont and EGI1 Lenti-KLF15 cells (n=5). Data are shown as mean ± SEM. Mann-Whitney test was used. *** represent *p*-values of <0.001.

With EMT being seen as a common path for the development of a more aggressive and invasive phenotype in cancer, several known markers involved in pathways related to EMT were evaluated in CCA cells, upon KLF15 overexpression. Experimental overexpression of KLF15 increased the mRNA expression of the ligand of the TGF-β superfamily of proteins *BMP4*, the epithelial cell marker *EPCAM* and the cell adhesion and migration related glycoprotein *FN1* (**Figure R.17**), which pinpoints a decrease in the mesenchymal potential of these cells.

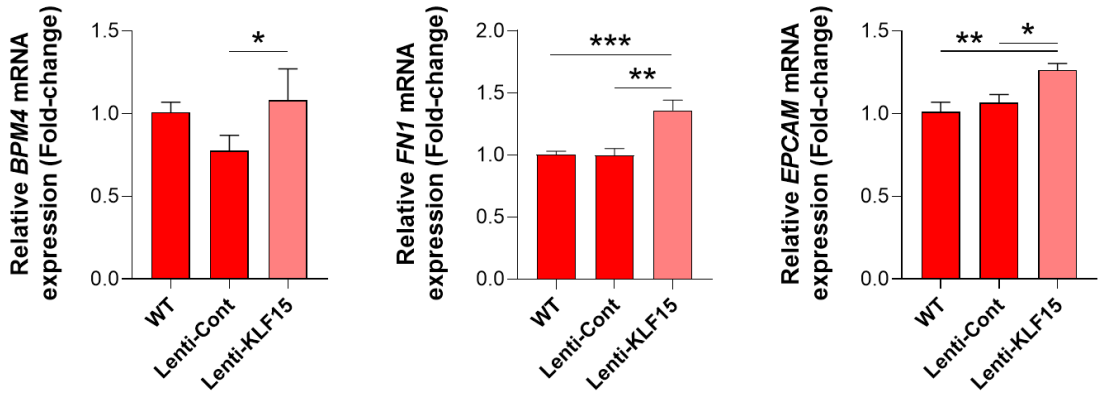

Figure R.17. Experimental overexpression of KLF15 induces the expression of markers of mesenchymal to epithelial transition in CCA cells. Relative mRNA expression (qPCR) of *BMP4*, *EPCAM* and *FN1* in EGI1 WT, EGI1 Lenti-Cont and EGI1 Lenti-KLF15 cells (n=4). Data are shown as mean ± SEM. Mann-Whitney test was used. * and ** represent *p*-values of <0.05 and 0.01, respectively.

R.2.2.5. KLF15 overexpression hinders the mitochondrial energetic output of CCA cells

Since KLF15 is highly involved in cellular energetic metabolism,[285,286,325] we aimed to evaluate the mitochondrial metabolism of KLF15-overexpressing cells, by measuring their oxygen consumption rate (OCR) (**Figure R.18B**). In fact, increased mitochondrial respiration and ATP production is a common hallmark of cancer cells, fueling uncontrolled cell growth and invasiveness.[326] Importantly, a significant reduction in baseline respiration, maximal respiration, ATP-linked respiration, and non-mitochondrial respiration was observed, when compared to both control conditions (**Figure R.18B**). This indicates a possible decrease in the energetic output of the cells that can account for the decreased viability, proliferation and migration caused by KLF15 overexpression. Of note, the proton leak-linked OCR was also shown to be reduced, even if to a lesser extent than the other parameters (**Figure R.18B**).

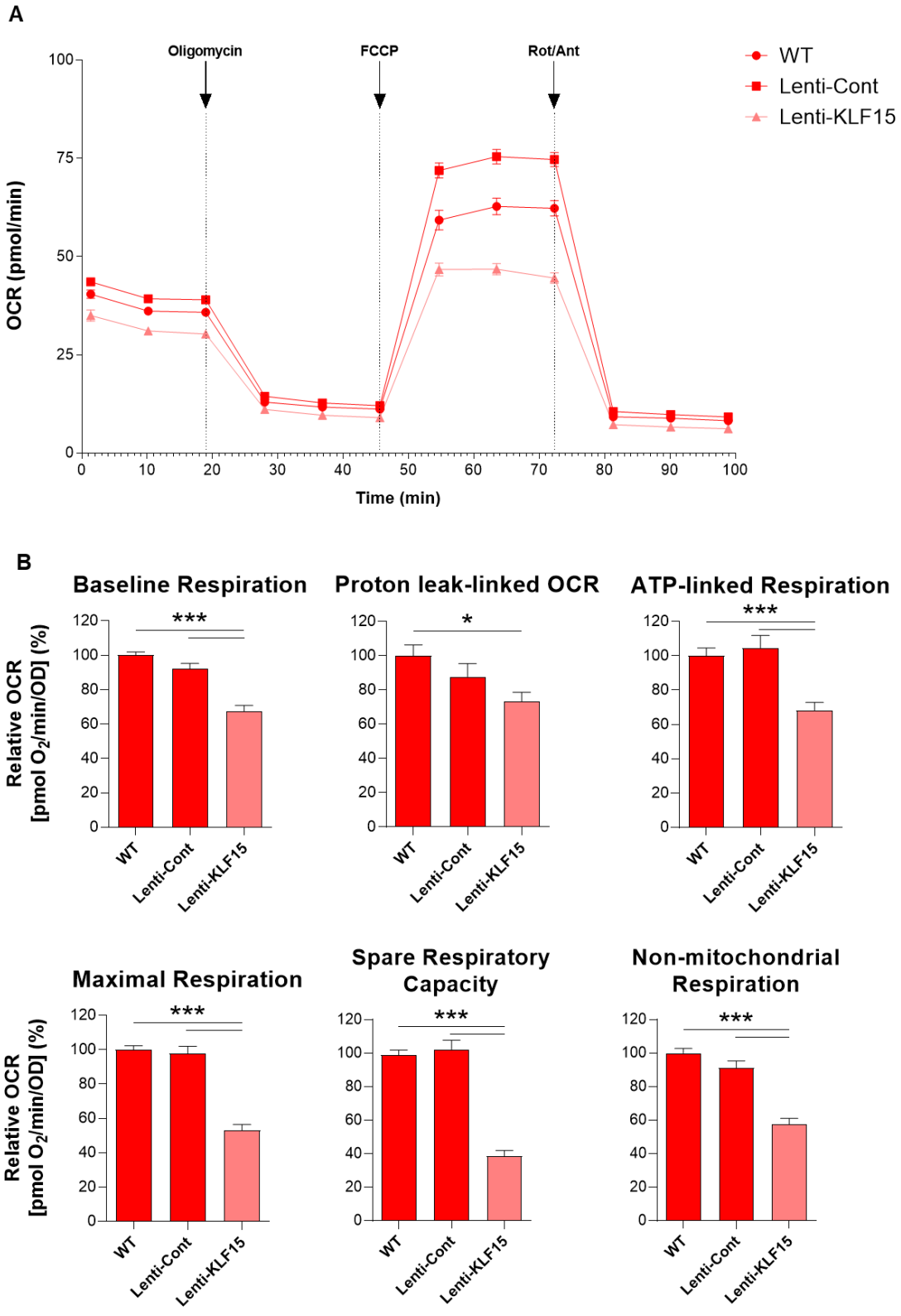

Figure R.18. KLF15-overexpressing cells show reduced mitochondrial energetic metabolism. (A) Graphical representation of oxygen consumption rate (OCR) along time in EGI1 WT, Lenti-Cont and Lenti-KLF15. **(B)** Relative OCR levels for baseline respiration, proton leakage, ATP respiration, maximal respiration, spare respiratory capacity and non-mitochondrial respiration in EGI1 WT, Lenti-Cont and Lenti-KLF15 (n=3). Data are shown as mean ± SEM. Mann-Whitney test was used. * and *** represent *p*-values of <0.05 and 0.001, respectively.

R.2.3. KLF15 overexpression leads to altered proteomic profiles in CCA cells

Since KLF15 was herein shown to play a role in the pathophysiology of CCA cells, we next aimed to evaluate the pathways that might be associated with these alterations. For this reason, a proteomic analysis by MS was performed in KLF15-overexpressing and control CCA cells, as well as in non-tumor cholangiocytes (i.e., NHCs). Proteomic analysis by MS identified 274 significantly altered proteins between EGI1 Lenti-KLF15 and both controls (EGI1 WT and Lenti-Cont), among which the levels of 114 proteins (42%) were decreased, while the levels of 160 proteins (58%) were increased (**Figure R.19A-B**). GO analysis of the proteins found upregulated in the overexpression context identified a pattern of enrichment in proteins participating in biological processes related to oxidation-reduction (i.e., G3PD, LDH-A, IMPDH1/2), glycolysis (i.e., PGAM1, PGM1), response to drug (i.e., MRP1, ABCD3, XRCC5), cell cycle (i.e., Nup43, KIF11) and cell division (i.e., Nup107-160, PKNγ) (**Figure R.19C**). On the other hand, GO analysis of downregulated proteins in KLF15 overexpressing cells compared to respective controls revealed their involvement in metabolic processes, such as mitochondrial electron transport and pentose biosynthetic process (i.e., 6PGD and G6PD), as well as in EMT (i.e., ITGα-V, PTPN11, TGM2) and in cell proliferation pathways, such as MAPK (i.e., EGFR) and Wnt signaling (i.e., CAV-1) (**Figure R.19D**).

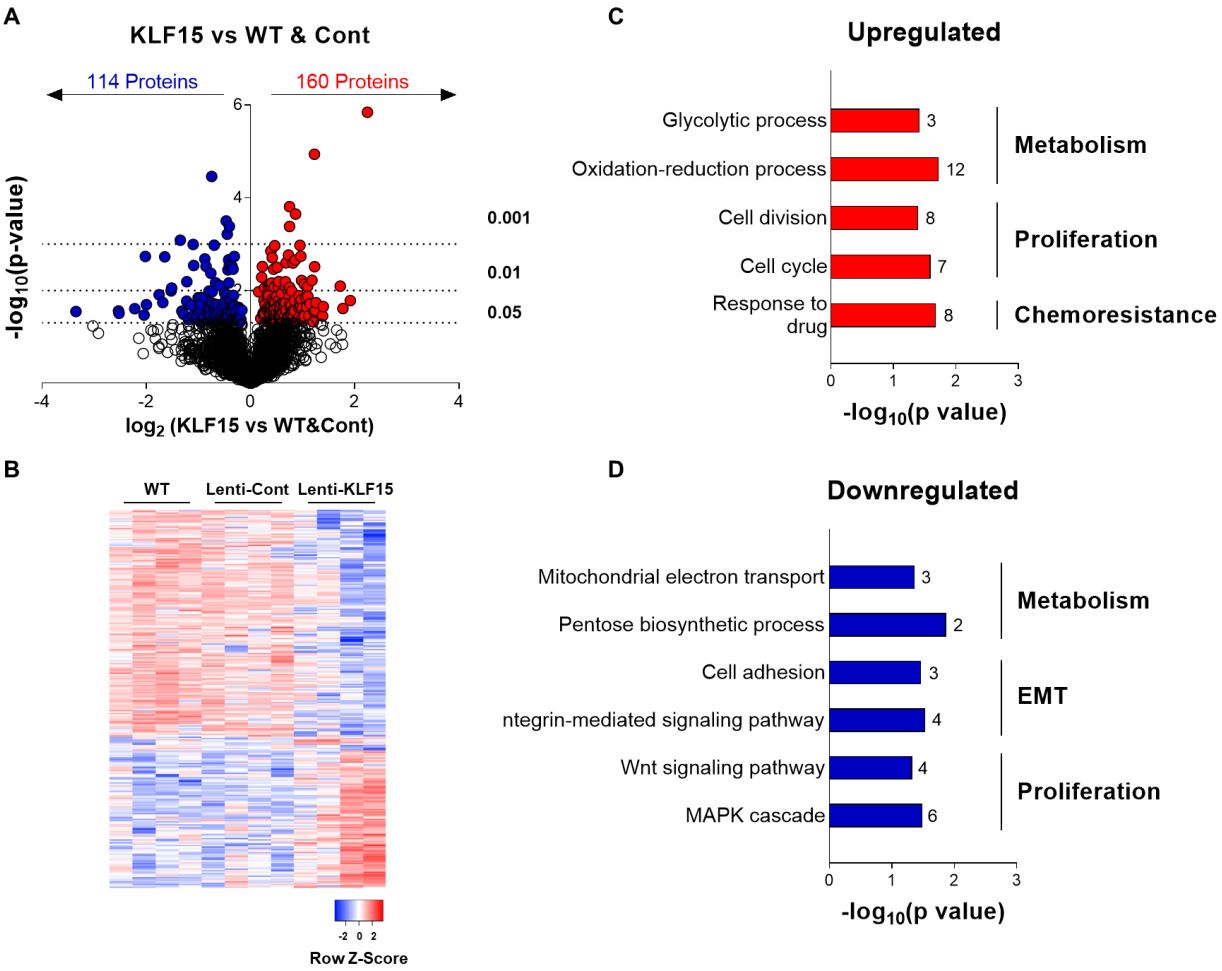

Figure R.19. Comparative proteomic profile between EGI1 Lenti-KLF15 and control cells. **(A)** Volcano plot of all identified differentially expressed proteins (n=274) by MS comparing fold enrichment in EGI1 Lenti-KLF15 to EGI1 WT and EGI1 Lenti-Cont. **(B)** Heatmap representation of all differentially expressed proteins (n=274) in EGI1 Lenti-KLF15, EGI1 Lenti-Cont and EGI1 WT. **(C-D)** GO of differentially expressed proteins (n=274) in the previously mentioned CCA groups, with distinct representations for the upregulated (n=160) **(C)** and downregulated (n=114) **(D)** biological processes.

Equally as important as finding the proteins that could be distinctly altered in CCA due to KLF15 overexpression, is identifying the ones which become normalized to the levels detected in a non-tumor cell context as it would be for NHCs. In this sense, we firstly identified the proteins significantly altered in CCA controls cells (EGI1 WT and Lenti-Cont), when compared to NHCs. Among these proteins, the levels of 34 proteins in KLF15-overexpressing cells were normalized to the levels detected in non-tumor cells (**Figure R.20A**). GO analysis of the aforementioned proteins found them to be involved in biological processes such as regulation of growth (i.e., EGFR, RUVB1), proteolysis (i.e., ERAP1, VCIP1) and response to stress (i.e., ENOA, 14-3-3ε) (**Figure R.20B**). Among these proteins, a few were selected, namely EGFR, RUVB1 and 14-3-3E, and

their relative protein abundance was determined among the different experimental groups (**Figure R.20C**), to confirm the previous assessment. As expected, the levels of these proteins were significantly altered in controls CCA cells and reverted to non-tumor levels in KLF15-overexpressing cells.

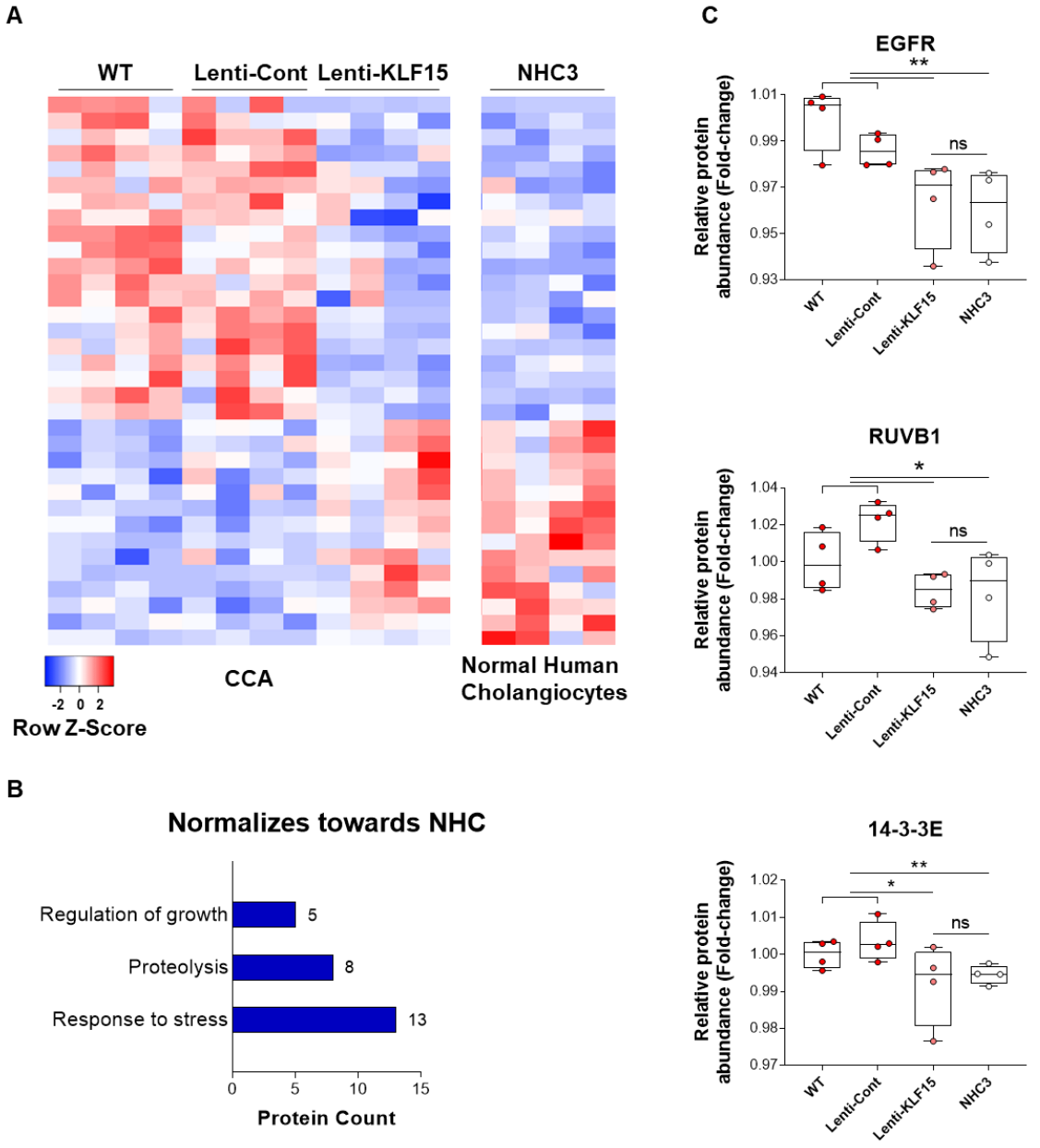

Figure R.20. Comparative proteomic profile between EGI1 Lenti-KLF15 and control cells. **(A)** Heatmap representation of proteins identified as differentially expressed upon KLF15 overexpression in CCA that shift towards levels similar to NHC (n=34) in EGI1 Lenti-KLF15, EGI1 Lenti-Cont, EGI1 WT and NHC. **(B)** GO of proteins identified as differentially expressed upon KLF15 overexpression in CCA that shift towards levels similar to NHC **(C)** Relative protein abundance levels of proteins of interest identified through proteomic analysis by GO. Abbreviations: NHC, normal human cholangiocytes. Data are shown as mean ± SEM. Mann-Whitney test was used. * and ** represent p-values of <0.05 and 0.01, respectively.

R.2.4 Effect of KLF15 overexpression in CCA development and progression in vivo

To further confirm whether KLF15 overexpression also impacts on CCA tumor growth *in vivo*, its effect was tested on a subcutaneous mouse model of CCA. First, EGI1 Lenti-KLF15 cells, as well as both control cells (EGI WT and EGI Lenti-Cont) were subcutaneously injected in back flanks of immunodeficient mice and tumor growth was monitored by measuring the tumor size using a caliper. While tumors generated from EGI WT and EGI Lenti-Cont grew exponentially overtime, a marked reduction in tumor growth of KLF15-overexpressing EGI1 cells was observed (**Figure R.21A**). In agreement, at sacrifice, the weight of tumors generated from EGI1 Lenti-KLF15 cells was significantly lower when compared with both control cells, thus confirming the relevance of this transcription factor in CCA growth *in vivo*. (**Figure R.21B-D**).

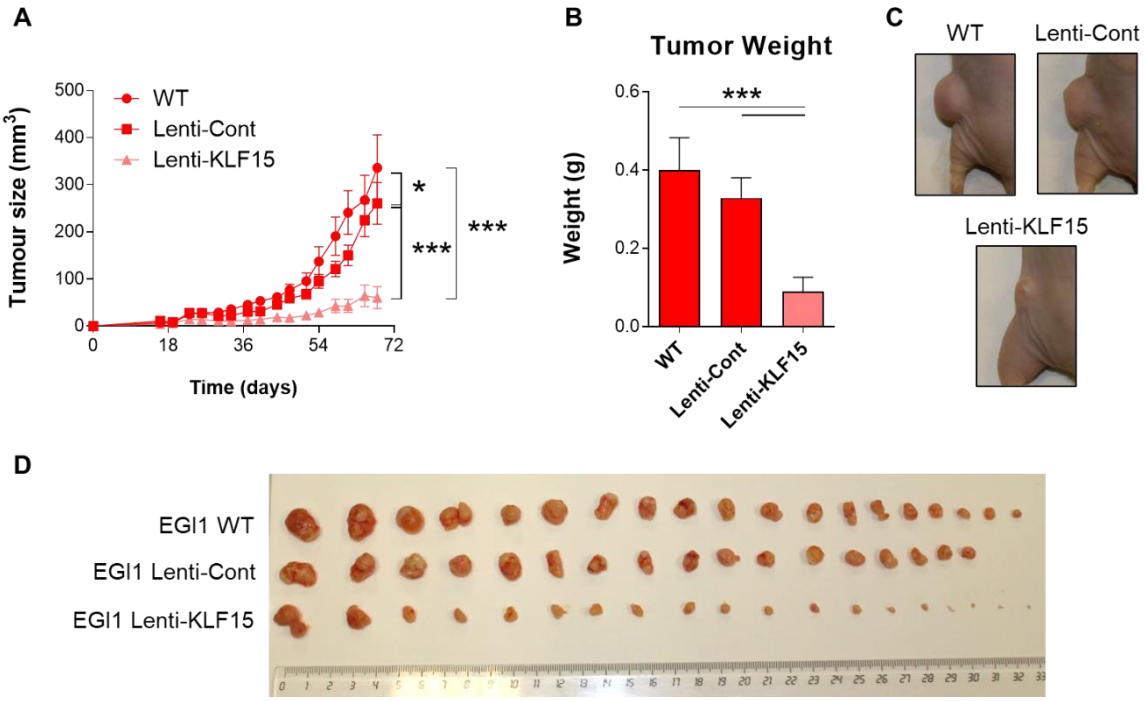

Figure R.21. KLF15 overexpression halts tumor growth in a subcutaneous model of CCA. **(A)** Tumor volume growth of EGI1 WT (n=19), EGI1 Lenti-Cont (n=17) and EGI1 Lenti-KLF15 (n=19) human CCA cells subcutaneously injected in immunodeficient mice. **(B)** Tumor weight of tumors at sacrifice **(C)** Representative images of EGI1 WT, EGI1 Lenti-Cont or EGI1 Lenti-KLF15 CCA tumors grown in immunodeficient mice and **(D)** extracted at the end of the experiment. Data are shown as mean ± SEM. 2-way ANOVA **(A)** and Mann-Whitney **(B)** t-test were used. * and *** represent *p*-values of <0.05 and 0.001, respectively.

Finally, in a more therapeutic perspective, we decided to evaluate whether KLF15 overexpression may counteract CCA tumor growth *in vivo* once the tumors are already generated. To do so, CCA tumors were generated by subcutaneous injection of EGI1 CCA cells in immunodeficient nude mice. Once the tumors reached approximately

90mm^3, 2 intratumor injections of Lenti-KLF15 or control lentivirus (blank lentivirus – Lenti-Cont) were administered, spaced 2 weeks between the first and second injections. In parallel, a group of mice was injected with saline as a procedure control, to assure growth levels in non-transduced tumors were comparable to tumors injected with control lentivirus (data not shown). Noteworthy, in already established subcutaneous CCA tumors, exogenous KLF15 overexpression was able to halt tumor growth, when compared to control tumors, thus confirming the therapeutic value of KLF15 restoration in human CCAs (**Figure R.22A-B**).

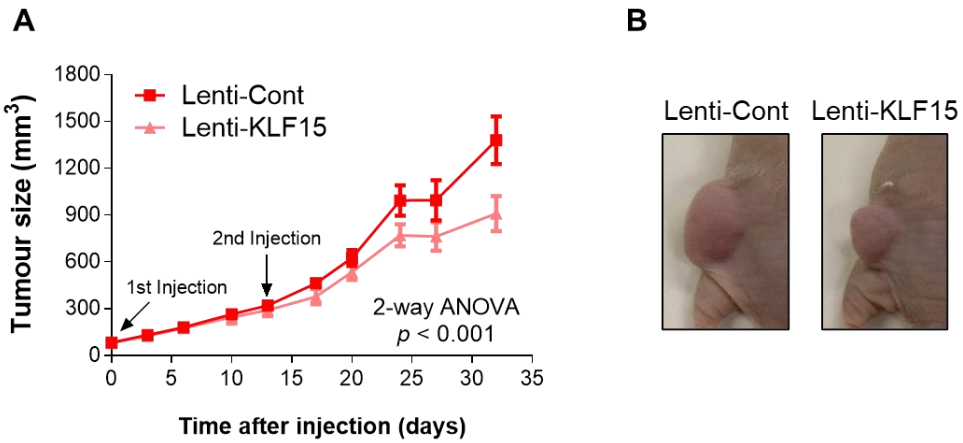

Figure R.22. Intratumor injection of Lenti-KLF15 halts tumor growth in a subcutaneous model of CCA. (A) Tumor volume of subcutaneously injected CCA cells (EGI1) in immunodeficient mice injected intratumorally with blank lentivirus (Lenti-Cont) (n=17) or lentivirus with KLF15 gene insert (Lenti-KLF15) (n=16) **(B)** Representative images of Lenti-Cont or Lenti-KLF15 intratumorally injected CCA tumors in immunodeficient mice. Data are shown as mean ± SEM. 2-way ANOVA was used.

Discussion

Despite not being among the most frequent cancer types, CCAs are aggressive tumors with increasing incidence, thus being a major social, health and economic problem worldwide. So far, no effective therapeutic strategies have been found for the care of patients with CCA, with surgical resection presenting itself as the only potential curative alternative, although high chances of disease recurrence after surgery are evident.[36,58,78,327] Due to their high heterogeneity, the need to uncover the molecular mechanisms governing cholangiocarcinogenesis is of paramount importance, paving the path for precise targeted therapies in these highly chemoresistant tumors. Several known signaling pathways related to proliferation, survival and chemoresistance have been found to be dysregulated in CCA, triggered through different cellular and biological cues, sometimes through an override of their canonical routes and other times by the induction of compensatory mechanisms turned into oncogenic stimuli.[117,328–330] In this regard, transcription factors are key players, that can be downstream effectors, as well as target several components of important pathways.[331–334] Depending on their targets, they can potentially play very distinctive roles in cancer development and progression, as they can either act as oncogenes or tumor suppressors.[335–337] This makes them specially enticing potential therapeutic targets worthy of further study.[338,339] In parallel, their alteration in an oncogenic context can also make them subjects of interest as diagnostic and even prognostic markers,[340,341] making the research of such subjects a worthwhile endeavor.

The KLF family of transcription factors plays an important role in human physiology, being involved in processes such as cell proliferation and differentiation[281] or organogenesis.[237,248,249] In addition, these family of transcription factors is highly implicated in the pathogenesis of human disorders extending from cardiac problems,[257] metabolic dysfunctions[263] to even cancer.[274,275] Among the members of the family, KLF15 has gain attention in the last years, due to its strong association to cardiac,[288] renal,[292] hepatic,[295] and metabolic functions.[286] In the field of cancer, information regarding the role KLF15 might play is limited,[298–305] with no information at all when it comes to hepatobiliary cancers. Consequently, with this work, we intended to explore the role that KLF15 has in the development and progression of CCA and assess its diagnostic, prognostic, and therapeutic potential.

Before addressing the role of KLF15 in cholangiocarcinogenesis, we firstly decided to identify the cells mostly expressing this transcription factor in a healthy liver. In fact, a more pronounced expression of *KLF15* in liver epithelial cells, namely hepatocytes and cholangiocytes, was observed. KLF15 was shown to be abundantly expressed in the liver[283] and the data herein obtained adds an extra layer of information to what was

already known about KLF15 in the liver, identifying the cell types majorly accounting for the hepatic expression of this transcription factor. Since cholangiocytes were among the cells expressing KLF15 in the liver, we hypothesized its potential involvement during cholangiocarcinogenesis. Following this, we provided evidence of a differential expression of KLF15 in CCA, showing a significant downregulation of this transcription factor in clinical biopsies from six independent international CCA patient cohorts at the mRNA level. Noteworthy, this downregulation was shown to occur independently of the mutational profile of the tumors, suggesting that this phenomenon is a general event during cholangiocarcinogenesis. Additionally, this downregulation was confirmed both at the mRNA and protein levels in CCA cells *in vitro* when compared to their normal control counterparts and observed in tumor samples from mice with CCA compared to liver. We were also able to associate KLF15 expression with clinical parameters and prognosis in human patients, since decreased KLF15 levels were particularly found in patients with late-stage and poorly-differentiated CCAs, being associated with lymph node affection and with worse OS and RFS in different cohorts of patients, Overall, considering all these evidences, a potential role of KLF15 as a tumor suppressor in this type of cancer was hypothesized. To date, little to nothing was previously known about the expression levels of KLF15 in liver cancer. On the other hand, in other forms of tumors, different functions for KLF15 may be evident based on tissue-specificity. For example, in lung adenocarcinoma, there is contradicting evidence in this matte since KLF15 was first described as being substantially upregulated,[304] while a posterior study by another group found the exact opposite trend and evidences.[305] In breast,[298] gastric,[299] papillary thyroid[301] and ovarian[300] cancers, KLF15 was shown to be downregulated, acting as a tumor suppressor. Nevertheless, in glioma[302] and colorectal cancer,[303] this transcription factor was shown to be highly expressed when compared to non-malignant control samples, suggesting an oncogenic role. Consequently, it is crystal clear that the role of KLF15 in cancer is tissue-specific, thus highlighting the existence of other mechanisms that are organ-dependent that cooperate with KLF15 to promote carcinogenesis.

To try to understand the regulatory mechanisms involved in the downregulation of KLF15 in the context of CCA, we turned our focus into epigenetic mechanisms. DNA hypermethylation of CpG-enriched enhancing regions near the promoter of the *KLF15* gene was evident, which could indicate this epigenetic process as one of the forms of silencing this gene during cholangiocarcinogenesis. In fact, similar findings were observed in other non-oncological disorders. In the context of ischemic heart failure, DNA hypermethylation of the CpG islands of the promoter of *KLF15* had been identified as one of the main regulatory mechanisms responsible for the disturbed expression of this

transcription factor, as a way of modifying the cardiac metabolism so the tissue could better adapt to the pathological conditions it suffered from.[342] By performing further experiments with hypomethylating agents *in vitro*, we were able to show a partial recovery in *KLF15* expression, counteracting this regulation. Nevertheless, the levels of mRNA reached when treating the CCA cell lines with hypomethylating compound were not comparable to the "physiological" levels obtained in normal human cholangiocytes in culture suggesting additional mechanisms controlling KLF15 expression. In the cardiac muscle of patients with hypertrophic cardiomyopathy, *KLF15* gene was identified as being located in a hyperacetylated region, showing higher mRNA levels in the pathological samples, when compared to healthy controls.[343] Therefore, we also decided to evaluate histone acetylation as another potential player in the regulation of *KLF15* expression in CCA. For this purpose, by treating CCA cells with TSA, a class I and II HDAC chemical inhibitor, *in vitro*, we observed no changes in *KLF15* mRNA levels, suggesting other layers of (epi)genetic regulation. Therefore, contrarily to what happen in other diseases, these results suggest that histone acetylation is not involved in the regulation of KLF15 levels during cholangiocarcinogenesis. Still, this mechanism cannot be totally ruled out since TSA only acts on class I and II HDACs and the histone acetylation regulation of KLF15 may be governed by class III HDACs. Nevertheless, another hypothesis is that this type of genetic regulation of KLF15 can be a tissue-specific phenomenon and so the acetylation status in cholangiocytes may be different than in cardiomyocytes, for example, and not suffer alterations upon oncogenic transformation towards CCA.

Other forms of regulation could be at play in this case. Post-transcriptional regulation of KLF15 through non-coding RNA (ncRNA), such as microRNAs (miRNAs), has been documented in several different situations. In ovarian cancer, miR-376a was shown to promote proliferation, migration and invasive capabilities which, mechanistically, was in part due to the targeting of KLF15.[344] On the other hand, in glioma, the targeting of KLF15 by miR-376a-3p was related to a tumor suppressive role, reducing proliferation and metastatic capacity.[302] In a similar fashion, in colorectal cancer, miR-376a-3p also develops a tumor suppressive role through negative regulation of KLF15, although a pro-oncogenic compensatory mechanism was observed where the long non-coding RNA (lncRNA) TTN-AS1 acts as a sponge for miR-376a-3p, counteracting its KLF15 silencing effect and promoting tumor progression.[303] In papillary thyroid cancer, miR-181a was shown to target KLF15, leading to increased cell growth and invasiveness, acting as an oncogene.[301] Furthermore, in the context of ischemia/reperfusion injuries, miR-137-3p leads to increased cardiomyocyte apoptosis by targeting KLF15.[345] Interestingly, in CCA,

miR-137 has already been described has a potential tumor suppressor, with a characteristic downregulation being observed in tumor tissues as well as cancer cell lines.[346] It was shown that increasing its expression suppressed cell proliferation, invasiveness and tumorigenicity, as well as induced cell cycle arrest and hindered tumor growth *in vivo*. Further analysis revealed that miR-137 achieved its tumor suppressive effect through direct regulation of the *WNT2B* gene.[346] Since both miR-137 and KLF15 are downregulated in CCA, that makes it unlikely that miR-137 could directly regulate *KLF15* in this context. Nevertheless, any of these miRNAs might play a role in the modulation of KLF15 in CCA and deserve further studies in the future.

In order to study the role of KLF15 and its mechanisms of action in CCA, we generated a new *in vitro* model by overexpressing KLF15 in human CCA cells through recombinant lentivirus infection. In parallel, a cell line transduced with a control blank lentivirus (EGI1 Lenti-Cont), lacking the gene of interest was generated and used concomitantly with a second control non-transduced cell line from the batch used in the transductions (EGI1 WT). By using these 2 types of controls both the effect of the KLF15-overexpression and any possible off-target effect resulting from the transduction process could be considered in every experiment. KLF15 overexpression in CCA cells decreased cell viability and proliferation rate, in parallel with a decrease in some proliferation markers. In addition to that, we observed that this effect happens in part due to cell cycle arrest, mainly at the G_2/M phases. This effect is supported by a decrease in Cyclin B1, both at the mRNA and protein levels, which is involved in the transition between the G_2 and M phases,[347,348]. It is relevant to point out that KLF15 overexpression has been previously shown to decrease mesangial cell proliferation through inhibition of high glucose-induced ERK1/2 MAPK signaling activation in a context of diabetic nephropaty.[349] Interestingly, it is also worthy of note that KLF15 overexpression was observed both in breast and gastric cancers, resulting in cell cycle arrest at the G_0/G_1 phase by modulating p21.[299,350] Differences in the participants involved on the growth arrest in different types of cells and diseases could indicate once again the existence of tissue-specific mechanisms, though the commonalities in the processes used to inhibit cell growth and proliferation point towards the possibility of a common central role played by this transcription factor.

Proteomic analysis of KLF15-overexpressing cells revealed that one of the main altered processes on this cell line was related to proliferation. Of note, KLF15 had been found to regulate the Wnt/β-Catenin pathway in cardiac cells by interacting and inhibiting the transcription of β-Catenin and TCF4, effectively regulating cardiac progenitor cell fate and differentiation.[351] Wnt signaling pathway was one of the processes downregulated

in our proteomic analysis, giving rise to the possibility of KLF15 modulating this route in different types of tissues and pathophysiological conditions. As previously stated, this transcription factor was shown to modulate ERK1/2 signaling in a context of diabetic nephropaty,[349] but it has also been identified as a regulator of the p38/MAPK signaling pathway in cardiac tissue, with its overexpression being able to have an inhibitory effect on the pathway.[352] Being the MAPK cascade the other main proliferation-related process found downregulated through our proteomic analysis, this is yet another evidence suggesting the importance of KLF15 in the regulation of the transcriptional machinery of the cell. When comparing KLF15-overexpressing cells with non-tumoral human cholangiocytes to identify which of the previously significantly altered proteins had recovered closer to healthy levels, several proteins involved in processes related to response to stress, regulation of growth and proteolysis were identified. Interestingly, EGFR was one common "hit" between both comparisons, leading us to speculate the importance of the oncogenic transformation of the MAPK signaling pathway in CCA, as well as the key role KLF15 might play in regulating this route. It is important to also highlight RUVB1[353,354] and ENOA,[355,356] both linked to proto-oncogene c-Myc pathway. Their normalization to levels close to those of the ones detected in NHC can give indication to the decrease in aggressiveness and tumorigenicity of the Lenti-KLF15 cells. Finally, the other relevant "hit", 14-3-3ε, seems to play an important role in cell cycle progression in different tissues,[357–359] as well as significant interaction with the Hippo/YAP signaling pathway.[360,361] The Hippo/YAP signaling pathway, while important for its role during developmental stages,[173] has also been implicated in cholangiocarcinogenesis, with increased nuclear levels of YAP being observed in CCA tumors and correlating with poor prognosis.[176] YAP has been shown to be activated in CCA through mutations in *ARID1A*, a gene encoding for a subunit of SWI/SNF chromatin-remodeling complex that inhibits YAP transcriptional activity,[180] although mutations in genes of the Hippo/YAP pathway are not observed frequently. Additionally, YAP was also shown to be activated in CCA through Hippo-independent signals, such as inflammatory cytokines (IL-6), extracellular matrix (ECM) composition and growth factors (PDGF and FGF).[362]

In recent studies, there has been interest to understand the mechanisms underlying mechanosensitive-related signaling pathways in cholangiocytes. Desplat and colleagues showed how mechanosensors, in this case Piezo1, respond to the mechanical stress and activate the signaling pathways necessary for cholangiocytes to adapt to those conditions.[363] KLF15 was identified as a downstream effector of Piezo1, in skeletal muscle, in the context of muscle atrophy.[364] Interestingly, Piezo1 is not only upregulated

in CCA and associated with worse prognosis, but also might be involved in the increase of CCA cell motility via YAP activation.[365] This supports the possibility of another layer of regulatory mechanisms of KLF15 expression in response to mechanical stress cues in CCA, due to build-up of biliary tract pressure caused by bile duct obstruction, which has been reported to happen,[366,367] and can act as a tumor growth stimulant. This adds on to the collection of evidence that KLF15 might exert a marked influence on multiple levels of cellular growth and proliferation in human pathophysiology, and specifically in CCA.

Klotho, first identified for its function as an aging-suppressor gene, has been identified as possible downstream target of KLF15.[368] Also referred to as α-Klotho and encoded by the *KL* gene, this protein's function seems to go beyond anti-ageing, as it has been reported as a tumor suppressor in different types of cancer, such as lung, gastric, and pancreatic adenocarcinoma,[369] as well as being an antagonist and modulator of the Wnt signaling pathway.[370,371] In CCA, Klotho has been reported to be upregulated.[372] As KLF transcription factors can act by promoting or inhibiting gene transcription,[229,230] in the case that KLF15 acted upon *KL* gene expression through a negative regulatory mechanism, it would explain that upregulation of Klotho in CCA can be a result of KLF15 downregulation. β-Klotho is the main isoform expressed in the liver and, although different than α-Klotho, it still maintains a high resemblance to the alpha isoform.[373] In the case that β-Klotho conserved the same binding motif as α-Klotho, KLF15 could possibly directly regulate its expression. If that is not the case and it was an indirect regulation, KLF15 can still modulate β-Klotho if this protein is dependent on the same pathways and downstream effectors that allowed for KLF15 to regulate α-Klotho. If this proved to be true, another potential regulatory mechanism could be attributed to KLF15.

In addition, considering that the rate of cell growth depends on a balance of cell proliferation and cell death, we verified that KLF15 overexpression had little to no impact on the cell death rate of CCA cells, although there is evidence of an anti-apoptotic and pro-autophagic effect of KLF15 overexpression in the context of cardiovascular diseases, in conjunction with inhibition of the Akt/mTOR signaling pathway.[374] In this regard, we cannot exclude a potential survival adaptation of KLF15-overexpressing CCA clones. Despite the lack of differences in cell death between the different cell lines at baseline levels and our data suggesting that this balance is shifted towards an inhibition of proliferation, the effect that KLF15 could have on apoptotic and cellular death processes could not be evident basally, but only by makings the cells more susceptible to chemotherapy or targeted therapies. The proteomic analysis identified chemoresistance as one of the main altered processes in these cells, with alterations in

members of the ATP-binding cassette transporter superfamily, such as MRP1 and ABCD3. Interestingly, several types of transporters known to be involved in mechanisms of chemoresistance (MOC) have already been associated with KLF15, either through direct regulation or modulation of upstream signaling pathways.[375–381] Among those are transporters such as human proton-coupled folate transporter (hPCFT)[375], solute carrier transporter SLC21A6 and ATP-binding cassette transporters MRP2 and MDR1.[381]

Lenti-KLF15 cells also showed reduced tumorigenicity, evidenced by a decrease in colony formation capabilities *in vitro*, as well as an impaired migration ability. To further reinforce this idea of reduced aggressiveness and higher epithelial phenotype upon KLF15 overexpression, the levels of several markers related to EMT and epithelial differentiation showed a shift towards a less mesenchymal and more epithelial phenotype. In line with these results, the proteomic analysis data we obtained identified EMT as one of the main processes altered in these cells. Accordingly, previous studies on papillary thyroid carcinoma had proposed that KLF15 was a target gene of miR-181a, being its expression regulated through direct binding to the 3'-UTR of KLF15 mRNA. This miRNA promoted growth both *in vitro* and *in vivo*, as well as improving the migratory capabilities of the cells and their ability to undergo EMT. The study also showed that KLF15 overexpression was able to counteract in part the effect miR-181a had in promoting the viability and migration of these cells *in vitro*.[301]

The mitochondrial energy output of the KLF15-overexpressing cells when compared to the respective controls revealed a marked decrease across all the parameters measured during the metabolic assessment, suggesting alterations in mitochondrial energetic metabolism and ATP production. This is in accordance with the decrease in cell viability observed, as the assay used to evaluate viability assesses mitochondrial function, and can explain the decrease in proliferation. Another one of the main processes that the proteomic analysis performed on these cell lines identified as significantly altered was metabolism. One of the few known target genes of KLF15 is the insulin-sensitive glucose transporter GLUT4,[282] identified shortly upon the discovery of the transcription factor itself. Since then, some associations have been made with lipid transporters in metabolically active tissues, like the muscle.[382] To date, the major focus of study of KLF15 in pathophysiology of human disorders is in relation to its role in the metabolic processes of cells. KLF15 has been linked to adipogenesis and adipocyte differentiation through regulation and coordination of circadian rhythmicity.[383] It has also been shown to regulate lipid metabolism in different tissues through regulation and cooperation with PPARδ,[290,384] as well as PPARα.[385] In response to changes in energy status or nutritional

adaptations to the environment, it was observed that KLF15 was able to induce switches in hepatic metabolic programs between lipogenesis and gluconeogenesis during fasting. This occurred through the formation of a complex with LXR/RXR to inhibit *Srebf1* expression and, consequently, downstream lipogenic enzymes expression, promoting the shift towards gluconeogenesis in the liver.[286] In similar fashion, in brown adipocytes, it has the ability to regulate a "fuel" switch between glucose and fatty acids, by increasing the expression of genes related to fatty acid oxidation concomitantly suppressing glucose oxidation by inhibiting the activity of the pyruvate dehydrogenase complex (PDC).[386] Lastly, KLF15 was also identified as a key participant in nitrogen metabolism. The maintenance of nitrogen homeostasis in mammals was shown to follow a circadian rhythmicity orchestrated by KLF15.[387] It has also been shown to modulate hepatic gluconeogenesis through transcriptional regulation of amino-acid degrading enzymes.[284,285] Still, the modulation of metabolism by KLF15 in the context of cancer remains a totally unexplored field and deserves attention. The proteomic analysis performed brought us some "hits" related to processes regarding metabolism, namely an upregulation of LDH-A, responsible for the interconversion of lactate in pyruvate,[388] and of PGAM1, that catalyzes the intercoversion between 3-phosphoglycerate (3-PG) and 2-phosphoglycerate (2-PG) in glycolysis and gluconeogenesis.[389–391] PGAM1 was reported to control of intracellular levels of 3-PG and 2-PG, promoting tumor cell proliferation and growth, by steering the balance between glycolysis and anabolic biosynthesis. To this effect, PGAM1 knockdown resulted in an increase of 3-PG, which in turn binds to and inhibits 6PGD, effectively disrupting the pentose phosphate pathway.[391] In fact, 6PGD was found downregulated in our proteomic analysis, being in agreement with has been described and showing a potential mechanism through which the role of KLF15 in oncometabolism can affect tumor progression and development. Further experiments into the metabolic pathways involved would be necessary before coming into any definite conclusion.

After evaluating the therapeutic effect of KLF15 overexpression in CCA *in vitro*, we finally evaluated its therapeutic potential in distinct animal models. A first *in vivo* subcutaneous CCA xenograft model revealed that KLF15-overexpressing cells generate tumors with markedly reduced growth rates when compared to their respective controls. Using an approach more similar to the one that could be translated into clinics, we proceeded to treat mice with subcutaneous CCA tumors by injecting KLF15 lentivirus intratumorally. The lentiviral injection and consequent KLF15 overexpression halted tumor growth when compared to the control group. These results validated our previous *in vitro* data and despite promising, they only represent a beginning. Now, an orthotopic *in vivo* model

would be the next step, as CCA is a type of cancer that requires a rich surrounding ECM and subcutaneous models are artificial models that do not adequately mimic those conditions. In addition, since KLF15 downregulation was also observed in mice with CCA generated through the overexpression of the AKT/NICD1 oncogenes, in combination with the sleeping beauty transposase, it would be also imperative to evaluate the effect of KLF15 overexpression in the development and progression of CCA in this (and other sleeping beauty-based) mouse models. In fact, our group has been optimizing the conditions for some hydrodynamic injection-based CCA models using plasmids encoding for different oncogenes, allowing us to validate the effect of KLF15 overexpression in different CCA models with different mutational backgrounds in the future, which increases its clinical relevance as a potential therapeutic tool.

For the translation of our findings onto a clinical setting, there is need to find agonists/activators for it, as the approach followed in this work of lentiviral transduction to acquire stable overexpression is far from becoming a standard medical practice. In this matter, since KLF15 was found to be hypermethylated in patients with CCA we explored the use of hypomethylating agents, as a way to induce an increase in *KLF15* expression. Hypomethylating agents are cytidine analogs that incorporate during DNA synthesis, causing a modification in the DNA strand that blocks the methylation of the base the DNMTs.[392] Currently, two hypomethylating agents are seeing use in the clinic, decitabine (5-aza-2'-deoxycitidine) and azacitidine (5-azacitidine), for the treatment of patients with myelodysplastic syndromes[393] and acute myeloid leukemia (AML).[394] Although DNA methylation of tumor suppressor genes is a common event in solid tumors and not only in hematologic malignancies,[395] the use of hypomethylating agents in a clinical setting to treat solid tumors still seems illusive. While both azacitidine and decitabine have been used in several trials for solid tumors including ovarian, prostate, gastrointestinal, lung, breast, and head and neck cancers, and melanoma, results between the different trials have differed widely, with some groups showing strong responses and larger cohorts having little to no response.[393] Still, with the success seen in the treatment of hematologic cancers, further study in solid tumors is warranted. Nevertheless, these compounds are safe, but they are known to have a high degree of hematologic toxicity, mostly in the form of myelosuppression.[396,397] In addition to that, due to their lack of specificity, they are prone to off-target undesirable effects, such as expression of oncogenic loci[398] and activation of transposable elements[399] caused by global demethylation. Therefore, although these drugs might have beneficial effects for patients with CCA, partially by increasing KLF15 expression, novel and safer strategies aiming to specifically activate this transcription factor should be studied in the future.

To summarize, this study provides the first insights into the potential roles and functions of the transcription factor KLF15 in cholangiocarcinogenesis. KLF15 showed a preferential expression profile for epithelial cells in the liver, while being markedly downregulated in CCA tumors from 6 independent cohorts of patients and CCA cell lines *in vitro*, thus suggesting its role as a tumor suppressor. It is important to point out that the decreased expression of the transcription factor in CCA human tumors was independent of the tumor's underlying driver mutations, as no significant differences in KLF15 expression were observed between patients stratified according to their *IDH1*, *KRAS* or *TP53* mutational status. This suggests that aberrant KLF15 downregulation might be a common phenomenon in CCA. Further, decreased *KLF15* expression in patients correlated with worse prognosis, including more advanced disease and shorter OS and RFS survival rates. Epigenetic regulation of KLF15 seemed to play a key role, as several promoter enhancing regions of the gene were found to be hypermethylated, with a strong correlation with its decreased expression. A KLF15-overexpressing human CCA cell line was generated as our *in vitro* working model, being validated both at the mRNA and protein levels. Functional evaluation showed that KLF15 overexpression resulted in decreased cell viability, tumorigenicity, migration and proliferation and induced cell cycle arrest, while cell death remaining seemingly unaffected. *In vivo*, a subcutaneous tumor model showed decreased tumor growth rates in KLF15-overexpressing cells, while a more clinically relevant model of subcutaneous tumors with intratumoral injection of lentivirus was able to halt tumor growth with the injection of KLF15 lentivirus. Some of the next steps to better understand this transcription factor include evaluating sensitization of these cells to chemotherapy or to different types of targeted therapy. Chromatin immunoprecipitation assays or CUT&RUN assays, to identify transcriptional targets of KLF15 could also offer some information about its mechanistic functions and might be of great value in order to understand the network modulated by KLF15 in CCA. Furthermore, taking into consideration the close relationship between KLF15 and metabolism, a detailed study of the impact of KLF15 overexpression in cholangiocyte metabolism might be of value. Performing further *in vivo* models, such as an orthotopic model or the *sleeping beauty* CCA model with plasmids for different oncogenes, would not only validate the role of KLF15 in CCA, but also increase its clinical relevance. Upon confirmation of the therapeutic potential of KLF15 in CCA, it will be possible to assess its practical use in a clinical setting as a therapeutic tool and assess its utility as a diagnostic and prognostic biomarker.

Conclusions

1- The transcription factor KLF15 showed preferential expression in epithelial cells in healthy liver, namely hepatocytes and cholangiocytes.

2- The mRNA expression levels of KLF15 are downregulated in human CCA tissues compared to surrounding non-tumor liver tissue and/or normal bile ducts in 6 international cohorts of patients.

3- KLF15 expression levels in human CCA tissues do not change according to tumor's mutational profile but are equally reduced in tumors with TP53, KRAS, IDH1/2 or none of these mutations, when compared to non-tumor liver tissue and/or normal bile ducts, implying that KLF15 downregulation is a common event during cholangiocarcinogenesis.

4- The mRNA and protein levels of KLF15 are decreased in human CCA cell lines compared to normal human cholangiocytes *in vitro*.

5- Decreased KLF15 expression in human CCA tumors is particularly evident in patients with poorly-differentiated tumors, lymph node invasion and advanced tumor stages, correlating with reduced overall and recurrence-free survival.

6- The expression of KLF15 is, at least in part, epigenetically regulated by mechanisms of DNA methylation but is not affected by modulation of histone acetylation.

7- Experimental overexpression of KLF15 in CCA cell lines *in vitro* showed reduced cell viability and proliferation, inducing cell cycle arrest at G_2/M phases.

8- KLF15 overexpressing CCA cells presented decreased colony formation and migratory capacities, and reduced expression of EMT-related markers.

9- Experimental overexpression of KLF15 in CCA cells reduces mitochondrial energetic activity, potentially inducing a metabolic rewiring in CCA.

10- Proteomic analysis of KLF15-overexpressing CCA cells revealed alterations in proteins involved in processes related to proliferation, EMT and metabolism.

11- Overexpression of KLF15 in CCA cells leads to the normalization of proteins associated to the regulation of growth to levels similar to those detected in normal human cholangiocytes.

12- KLF15-overexpressing CCA cells display impaired subcutaneous tumor growth when implanted in immunodeficient mice, when compared to control CCA cells.

13- Exogenous overexpression of KLF15 through lentivirus intratumor injection in a subcutaneous xenograft model of CCA in immunodeficient mice halted CCA tumor growth.

Our data are consistent with the idea that KLF15 act as a tumor suppressor in CCA. In this way, KLF15 holds promise as a possible diagnostic and prognostic biomarker in a clinical setting as well as an important therapeutic target. Further research into mechanisms regulating the expression of KLF15 in CCA, its precise mechanisms of action and also the development of novel strategies and/or molecules capable of restoring KLF15 expression in CCA may clearly impact on disease pathogenesis. Consequently, if efficiently translated into clinics, these findings may improve patient's welfare and outcome, reducing CCA social and health burden.

Summary in Spanish

(Resumen en español)

Introducción

El cáncer biliar o colangiocarcinoma (CCA) es un proceso tumoral de carácter maligno que afecta principalmente a las células de los conductos biliares llamadas colangiocitos.[36,58,78] Se trata del segundo tipo de cáncer primario de hígado más frecuente, tras el carcinoma hepatocelular (en inglés *hepatocellular carcinoma*, HCC), representando el ~3% de todos los tumores gastrointestinales. Pese a ser considerado un cáncer poco frecuente, su incidencia (0.3-6:100.000)[54–56] y mortalidad asociada (1-6:100.000) están aumentando en todo el mundo.[36,57–59] Sin embargo, la distribución geográfica del CCA es heterogénea, siendo su incidencia mayor en regiones del sudeste asiático (China, Corea del Sur, Tailandia y Japón),[36,58,60] debido a las infecciones producidas por parásitos hepáticos endémicos que predisponen a su desarrollo (tales como *Opisthorchis viverrini* o *Clonorchis sinensis*) o por la alta prevalencia de infecciones por los virus de la hepatitis B (HBV) o C (HCV).[55,70–72] El CCA se presenta generalmente asintomático en estadios iniciales, lo cual conlleva en general a un diagnóstico tardío y a una alta probabilidad de diseminación a otros tejidos y órganos. Este hecho, junto con la elevada quimiorresistencia que presentan este tipo de tumores, limita las opciones terapéuticas y hace que los pacientes con CCA tengan muy mal pronóstico.[36] Por ello, es importante esclarecer los mecanismos moleculares involucrados en el desarrollo y progresión de estos tumores para desarrollar nuevas estrategias terapéuticas.

Los factores de transcripción *Krüppel-like factors* (KLFs) constituyen una familia de proteínas altamente conservada que desarrollan múltiples funciones a nivel fisiopatológico en humanos. Con 18 miembros identificados hasta el momento, la familia KLF se caracteriza por la presencia de tres *zinc finger motifs* del tipo C_2H_2 que les permiten desarrollar su función de regulación de la transcripción del ADN.[229,230] Su actividad es diversa, desde la regulación de la organogénesis[237,248,249] al correcto funcionamiento de distintos órganos.[233,236,239] También tienen un papel importante en enfermedades, derivado de su desregulación.[256,258,260,263]

Teniendo la capacidad de coordinar y regular distintos procesos celulares, como el crecimiento celular, proliferación y/o diferenciación,[270,271] alteraciones en sus niveles o actividad pueden provocar la transformación neoplásica en distintos tejidos. Los KLFs tienen la capacidad de actuar como reguladores negativos o positivos de la expresión de distintos genes, pudiendo desarrollar el papel de supresores tumorales u oncogenes en diferentes tejidos.[273–275,400,401]

Uno de los miembros de esta familia, KLF15, inicialmente designado *Kidney-Krüppel-like Factor* (KKLF),[282,283] se expresa principalmente en riñón, hígado, músculo cardíaco y esquelético y tejido adiposo, siendo el hígado y riñón los órganos con mayor abundancia.[229,282,284] KLF15 tiene un papel importante en la regulación de la homeostasia metabólica[284–286,325] y cardíaca,[233,287,288] entre otros,[290,292] y su función está asociada al ritmo circadiano.[291,383,387] En el hígado es un regulador del metabolismo lipídico[293,294] y de la diferenciación de hepatocitos.[295]

En comparación con el resto de los miembros de la familia KLF, todavía se sabe muy poco sobre el papel de KLF15 en cáncer. Además, existen estudios con información contradictoria,[304,305] proponiendo a KLF15 como supresor tumoral[298–301] u oncogén,[302,303] evidenciando que, tal como es el caso de otros KLFs, su papel en el proceso neoplásico puede ser específico de cada tejido. Sin embargo, se desconoce el papel de KLF15 en cáncer hepático o biliar.

Hipótesis y objetivos

La familia de los factores de transcripción KLF tiene un papel esencial en la regulación de diversos procesos fisiológicos y patológicos, a través de la modulación de la expresión de genes involucrados en distintas vías de señalización. Diversos estudios han demostrado la importancia de los KLFs en la patogenia de múltiples tipos de cáncer, siendo considerados potenciales herramientas diagnósticas/pronósticas y posibles dianas terapéuticas. No obstante, se desconoce el papel de los KLFs en CCA. Debido a la alta expresión de KLF15 en el hígado, y su asociación con el metabolismo energético, diferenciación hepática y participación en otros tipos de cáncer, en este estudio nos planteamos la hipótesis de que KLF15 podría tener un papel importante en el proceso de colangiocarcinogenesis. Así, nos propusimos explorar el papel de KLF15 en CCA y evaluar su potencial como herramienta diagnostica, pronóstica y terapéutica.

Para ello, se han planteado los siguientes objetivos:

I. Analizar los niveles de expresión de KLF15 en tejidos de CCA humano en comparación con tejidos control.

II. Analizar los niveles de expresión de KLF15 en líneas celulares de CCA de humano en comparación con colangiocitos humanos normales.

III. Determinar el papel de las modificaciones epigenéticas sobre la expresión de KLF15 en células de CCA humano

IV. Evaluar el impacto de la sobreexpresión de KLF15 en la progresión del CCA *in vitro*

V. Evaluar el impacto de la sobreexpresión de KLF15 en la progresión del CCA *in vivo*

Material y métodos

Expresión génica de KLF15 en biopsias hepáticas de pacientes con CCA y en líneas celulares de CCA

Lo niveles de transcripción (ARNm) de *KLF15* fueron analizados en tumores de CCA humano e hígado sano adyacente al tumor en 8 cohortes diferentes de pacientes ("Montal","Copenhagen", "TCGA", "TIGER", "Job", "Nakamura", "Jusakul" y "San Sebastian").[119,122,127,179,306–309] Las muestras de tejido humano fueron recogidas en cumplimiento con la normativa de los respectivos Comités de Ética para la Investigación Clínica. Asimismo, la expresión de este gen fue determinada mediante PCR cuantitativa (qPCR) en líneas celulares de CCA humano (i.e., HUCCT1, EGI1, TFK1 y WITT) y en cultivos primarios de colangiocitos humanos normales (NHC).[402–404] Además, se analizó la expresión proteica de KLF15 en colangiocitos humanos normales y tumorales mediante *inmunobloting*.

Estudios de los mecanismos de regulación transcripcional de KLF15 en tumores de CCA y células en cultivo

Lo niveles de metilación del ADN en regiones promotoras del gen *KLF15* fueron analizados en tejido de CCA de pacientes e hígado sano adyacente al tumor por *microarray* en la cohorte de "Copenhagen". Además, la expresión génica de *KLF15* fue determinada mediante qPCR en líneas celulares de CCA humano (i.e., HUCCT1, EGI1, TFK1 y WITT) tras 48 horas de tratamiento con un agente hipometilante Zebularina o con un inhibidor de enzimas deacetilasas de histonas (HDAC) de clase I y II (Tricostatina A-TSA).

Estudios funcionales del efecto de la sobreexpresión de KLF15 en células de CCA en cultivo

La tasa de proliferación de las líneas de CCA (i.e., EGI1 WT, EGI1 Lenti-Cont y EGI1 Lenti-KLF15) fue determinada utilizando un marcaje con la sonda fluorescente *eBioscience™ Cell Proliferation Dye eFluor™ 670* (Invitrogen – Thermo Fisher Scientific) durante 48 horas y empleando el citómetro de flujo *Guava Easycyte 8HT* (Merck Millipore). Además, se evaluó el ciclo celular de las células de CCA por citometría de flujo utilizando *TO-PRO™-3 iodide* (Thermo Fisher Scientific).

En el caso del ensayo de muerte celular, los colangiocitos tumorales fueron marcados con la sonda fluorescente *TO-PRO™-3 iodide* (Thermo Fisher Scientific), cuya intensidad fue detectada tras 48 horas, en el citómetro de flujo *Guava Easycyte 8HT* (Merck Millipore).

Por otro lado, se estudió la capacidad de formación de colonias de las células de CCA y su crecimiento independiente de anclaje a sustrato, así como su capacidad migratoria mediante ensayos *wound-healing*. Asimismo, se determinó la expresión génica (qPCR) de marcadores de transición epitelio-mesénquima (EMT; i.e., *BMP4*, *EPCAM*, *FN1*) en las líneas de CCA. Por último, se evaluó el metabolismo energético mitocondrial de las líneas celulares tumorales analizando el consumo de oxígeno (OCR) en el aparato *XF96 Extracellular Flux Analyzer* (Seahorse Bioscience, North Billerica, MA, USA).

Identificación de proteínas diferencialmente expresadas en líneas celulares de CCA con sobreexpresión de KLF15 en comparación a líneas tumorales control y colangiocitos normales

Extractos celulares de colangiocitos humanos sanos (i.e., NHC) y de líneas tumorales de CCA (i.e., EGI1 WT, EGI1 Lenti-Cont y EGI1 Lenti-KLF15) fueron recogidos y analizados por espectrometría de masas. La identificación y cuantificación de los péptidos fue realizada utilizando el programa informático Mascot search engine (Matrix Science Ltd.) Los espectros peptídicos se compararon con la base de datos Uniprot/Swissprot. Sólo se consideraron péptidos con una tasa de descubrimientos falsos (en inglés *false discovery rate*, FDR) menor del 1% y que no estuviesen presentes en el control negativo. Para determinar los procesos biológicos relacionados con las proteínas diferencialmente expresadas, se llevó a cabo un análisis de enriquecimiento *gene ontology* (GO) usando el programa DAVID, un estudio de interacciones proteína-

proteína con la base de datos STRING y los *heatmaps* se generaron mediante el programa Heatmapper.[318–320]

Efecto de la sobreexpresión de KLF15 en modelos animales de CCA humano

Se estableció un modelo subcutáneo de CCA humano en ratones inmunodeficentes, implantando células de CCA humanas con sobrexpresión de KLF15 (EGI1 Lenti-KLF15) y los respectivos controles (EGI1 WT y EGI1 Lenti-Cont). El crecimiento tumoral se monitorizó utilizando un calibre 2 veces a la semana durante 2 meses.

Además, se estableció otro modelo subcutáneo de CCA humano implantando células de CCA humanas (EGI1) y se formaron 3 grupos homogéneos de ratones. Los ratones recibieron 2 inyecciones intratumorales, separadas 2 semanas entre ellas, conteniendo lentivirus para sobreexpresión de KLF15, lentivirus control (vacío), o solución salina, para cada grupo correspondiente. El crecimiento tumoral en el hígado fue monitorizado utilizando un calibre 2 veces a la semana durante 32 días.

Análisis estadístico

El análisis estadístico se llevó a cabo con el programa “GraphPad Prism” versión 8.01 (GraphPad Software). Una vez determinada la distribución normal de los datos mediante el test de Shapiro-Wilk, se emplearon para las comparaciones entre dos grupos los tests estadísticos *Student’s t-test* en el caso paramétrico o *Mann-Whitney test* en el caso no paramétrico. Para comparaciones entre más de dos grupos se utilizó el test paramétrico de análisis de varianza unidireccional (ANOVA) con *Tukey’s post hoc test* o el test no paramétrico *Kruskal-Wallis* seguido de *Dunn’s post hoc test*. Para correlaciones, el *Spearman’s rank correlation coefficient* fue utilizado. Los datos están representados como la media ± error estándar de la media (SEM). Las diferencias fueron consideradas significativas cuando el valor de $p<0.05$.

Resultados y discusión

Caracterización molecular de KLF15 en tejido de CCA humano y en líneas celulares de CCA en comparación con sus respectivos controles sanos

Se analizó el perfil de expresión de KLF15 en hígado, observándose una expresión preferencial en células epiteliales, tanto hepatocitos como colangiocitos. Del mismo

modo, se determinó la expresión de KLF15 en tejido de CCA de 6 cohortes independientes de pacientes y se observó una disminución significativa en comparación con tejido hepático adyacente no tumoral. Esta reducción resultó ser independiente del perfil mutacional del tumor. Además, en líneas celulares de colangiocitos humanos tumorales se observó igualmente una bajada significativa en los niveles de expresión de KLF15 en comparación con colangiocitos normales en cultivo, sugiriendo que esta desregulación de la expresión de KLF15 es un evento generalizado en la colangiocarcinogénesis.

El análisis del perfil de metilación del gen *KLF15* en tejido de pacientes de CCA verificó la existencia de regiones promotoras del gen ricas en secuencias CpG que se encuentran hipermetiladas, mostrando correlación inversa con los niveles de expresión génica de *KLF15*. *In vitro*, la incubación de líneas celulares de CCA con un agente hipometilante (Zebularina) provocó una recuperación parcial de la expresión de KLF15. Estos datos demuestran que el gen *KLF15* se regula epigenéticamente mediante metilación. Por otro lado, la tricostatina A (TSA), un inhibidor de HDACs, no modificó la expresión de KLF15 en las células de CCA en cultivo, indicando que la acetilación de histonas no un gran impacto sobre la regulación de la expresión de KLF15.

Efecto funcional de la sobreexpresión de KLF15 en células de CCA *in vitro*

Para estudiar el efecto funcional de la modulación de KLF15 en células de CCA se generó una línea celular que sobreexpresa KLF15 mediante transducción lentiviral (EGI1 Lenti-KLF15), utilizando en paralelo sus respectivos controles – una línea transducida con un lentivirus control vacío (EGI1 Lenti-Cont) y una línea no transducida (EGI1 WT). La sobreexpresión del factor de transcripción resultó en una reducción significativa de la viabilidad y proliferación celular, induciendo un arresto del ciclo celular en fase G_2/M. Este hecho fue corroborado por una disminución en los niveles de expresión de Ciclina B1, proteína involucrada en la transición entre G_2 y M.[347,348] Sin embargo, este fenómeno no se vio asociado con muerte celular.

A continuación, se analizó la capacidad de formación de colonias independiente de anclaje, observándose un menor número de colonias formadas por las células con sobreexpresión de KLF15. Del mismo modo, también se analizó la capacidad migratoria e invasiva de estas células mediante ensayos *wound-healing*, mostrando que la sobrexpresión de esta proteína induce un descenso en su capacidad migratoria.

Posteriormente, se determinaron los niveles de expresión de distintos marcadores asociados a EMT y diferenciación epitelial (i.e., *BMP4*, *EPCAM*, *FN1*), observándose un fenotipo menos mesenquimal y más epitelial tras la sobreexpresión de KLF15.

Por último, el estudio del metabolismo energético mitocondrial mostró un marcado descenso de su actividad tras la sobreexpresión de KLF15 en células de CCA, sugiriendo alteraciones en el metabolismo mitocondrial y producción de ATP.

Identificación de proteínas diferencialmente expresadas en líneas celulares de CCA con sobreexpresión de KLF15 en comparación a células tumorales control y colangiocitos normales

Se analizó el perfil proteómico de extractos celulares de colangiocitos tumorales (i.e., EGI1 WT, EGI1 Lenti-Cont y EGI1 Lenti-KLF15) y colangiocitos normales. Se identificaron cambios en los niveles de proteínas involucradas en metabolismo, uno de los principales procesos celulares asociados a KLF15,[285,286] más específicamente un aumento de LDH-A y PGAM1, y una disminución de 6PGD. Como ejemplo, PGAM1 ha sido descrito previamente como promotor de la proliferación celular y crecimiento tumoral.[391] PGAM1 además tiene la capacidad de alterar la vía de las pentosas fosfato inhibiendo 6PGD,[391] lo cual está en consonancia con nuestros datos proteómicos.

Por otro lado, también fueron identificados cambios de expresión en proteínas transportadoras de fármacos, específicamente MRP1 y ABCD3. En este sentido, KLF15 se ha asociado previamente con la regulación de distintos tipos de transportadores,[282,375] entre los que destacan MRP2 y MDR1,[381] pertenecientes también a la misma familia de transportadores ABC e involucrados en mecanismos de quimoresistencia.[376–379] Asimismo, se identificaron descensos de expresión de proteínas relacionadas con la vía de señalización Wnt y la cascada MAPK. Estos datos están en consonancia con estudios previos que indican que KLF15 es un regulador de la vía Wnt/β-Catenina en células cardiacas,[351] y de la vía MAPK, en el contexto de nefropatía diabética,[349] y tejido cardiaco.[352]

Mediante la comparación de los datos proteómicos de las células de CCA que sobreexpresan KLF15 y los colangiocitos normales identificamos algunas proteínas que recuperan su expresión a niveles similares a los de células sanas. Las proteínas identificadas fueron EGFR (el cual regula la vía de señalización de las MAPK), RUVB1[353,354] y ENOA[355,356] (ambas relacionadas con el proto-oncogén c-Myc), y 14-3-3ε, involucrado en la progresión del ciclo celular en distintos tejidos[357–359] y con la vía de

señalización Hippo/YAP.[360,361] Estos datos refuerzan la idea del papel de KLF15 regulando el crecimiento y proliferación celular, y su contribución a la colangiocarcinogénesis.

Impacto de la modulación de KLF15 *in vivo*

Los estudios realizados en ratones inmunodeficientes con inyección subcutánea de células de CCA mostraron que las células con sobreexpresión de KLF15 presentan menor crecimiento tumoral en comparación con las células control. Asimismo, en otro modelo de de CCA subcutáneo en ratones inmunodeficientes en el que se sobreexpresó KLF15 mediante la inyección intratumoral de lentivirus recombinantes, se verificó dicha disminución del crecimiento tumoral en comparación con el grupo control.

Conclusiones

1- El factor de transcripción KLF15 se expresa principalmente en las células epiteliales del hígado, en particular hepatocitos y colangiocitos.

2- Los niveles de expresión de ARNm de KLF15 están disminuidos en tejido de CCA humano en comparación a tejido hepático adyacente no tumoral y/o conductos biliares normales en 6 cohortes internacionales de pacientes.

3- El descenso de los niveles de expresión de KLF15 en tejido de CCA humano es independiente del perfil mutacional del tumor, estando igualmente disminuidos en tumores con mutaciones en *TP53*, *KRAS*, *IDH1/2* o en ninguna de ellas, en comparación a tejido hepático adyacente no tumoral y/o conductos biliares normales, indicando que la disminución de *KLF15* es un evento común durante colangiocarcinogénesis.

4- Los niveles de expresión (ARNm y proteína) de KLF15 están disminuidos en líneas celulares de CCA humano en comparación con colangiocitos humanos normales en cultivo.

5- El descenso de expresión de *KLF15* en tumores humanos es particularmente evidente en pacientes con tumores poco diferenciados, invasión de los nódulos

linfáticos y estadios tumorales avanzados, correlacionándose con menor supervivencia global y supervivencia libre de recurrencia.

6- La expresión de *KLF15* es, al menos parcialmente, regulada epigenéticamente por mecanismos de metilación del ADN, pero no es afectada por modulación de la acetilación de histonas en células de CCA.

7- La sobreexpresión experimental de KLF15 en líneas celulares de CCA *in vitro* disminuyó la viabilidad y proliferación celular, induciendo una detención del ciclo celular en las fases G_2/M.

8- Las células de CCA con sobreexpresión de KLF15 presentan menor capacidad de formación de colonias y menor actividad migratoria, así como niveles de expresión de marcadores de EMT disminuidos.

9- La sobrexpresión experimental de KLF15 en células de CCA reduce la actividad energética mitocondrial, potencialmente induciendo una remodelación metabólica en CCA.

10- El análisis proteómico de las células de CCA con sobreexpresión de KLF15 reveló alteraciones en proteínas involucradas en procesos relacionados con proliferación, EMT y metabolismo celular.

11- La sobrexpresión de KLF15 en células de CCA indujo una normalización de expresión de proteínas asociadas con la regulación de crecimiento celular, mostrando niveles similares a los detectados en colangiocitos humanos.

12- Las células con sobreexpresión de KLF15 presentan menor capacidad tumorigénica tras su inyección subcutánea en ratones inmunodeficientes, en comparación con células de CCA control.

13- En un modelo de CCA subcutáneo en ratones inmunodeficientes, la sobreexpresión de KLF15 mediante inyección intratumoral de lentivirus recombinantes provocó un descenso del crecimiento tumoral en comparación con el grupo control.

Nuestros datos indican que KLF15 actúa como supresor tumoral en CCA. Asimismo, KLF15 se presenta como un posible biomarcador diagnóstico y pronóstico en el entorno

clínico, así como una importante diana terapéutica. Así, la investigación exhaustiva de los mecanismos que regulan la expresión de KLF15 en CCA, sus mecanismos precisos de acción y el desarrollo de nuevas estrategias farmacológicas y/o moléculas capaces de restablecer la expresión de KLF15 en CCA pueden tener un impacto futuro en la patogenia de esta enfermedad.

References

1. Juza RM, Pauli EM. Clinical and surgical anatomy of the liver: a review for clinicians. Clin Anat 2014;27:764–769.

2. Trefts E, Gannon M, Wasserman DH. The liver. Curr Biol 2017;27:R1147–R1151.

3. Boyer JL. Bile formation and secretion. Compr Physiol 2013;3:1035–1078.

4. Kubes P, Jenne C. Immune Responses in the Liver. Annu Rev Immunol 2018;36:247–277.

5. Bhatia SN, Underhill GH, Zaret KS, et al. Cell and Tissue Engineering for Liver Disease. Sci Transl Med 2014;6:245sr2.

6. Cotoi CG, Quaglia A. Normal Liver Anatomy and Introduction to Liver Histology. In: *Textbook of Pediatric Gastroenterology, Hepatology and Nutrition: A Comprehensive Guide to Practice.* 1st ed. Springer International Publishing; 2016:609–6012.

7. Mescher AL, Junqueira LCU. *Junqueira's Basic Histology: Text and Atlas*. McGraw-Hill Medical; 2013.

8. Han Y, Glaser S, Meng F, et al. Recent advances in the morphological and functional heterogeneity of the biliary epithelium. Exp Biol Med (Maywood) 2013;238:549–565.

9. Tabibian JH, Masyuk AI, Masyuk TV, et al. Physiology of cholangiocytes. Compr Physiol 2013;3:541–565.

10. Anon. The Biliary Tree. Radiology Key 2016. Available at: https://radiologykey.com/the-biliary-tree/ [Accessed June 20, 2022].

11. Jensen K, Marzioni M, Munshi K, et al. Autocrine regulation of biliary pathology by activated cholangiocytes. Am J Physiol Gastrointest Liver Physiol 2012;302:G473-483.

12. Bogert PT, LaRusso NF. Cholangiocyte biology. Curr Opin Gastroenterol 2007;23:299–305.

13. Lazaridis KN, Strazzabosco M, Larusso NF. The cholangiopathies: disorders of biliary epithelia. Gastroenterology 2004;127:1565–1577.

14. Beuers U, Hohenester S, Buy Wenniger LJM de, et al. The biliary HCO(3)(-) umbrella: a unifying hypothesis on pathogenetic and therapeutic aspects of fibrosing cholangiopathies. Hepatology 2010;52:1489–1496.

15. Maroni L, Haibo B, Ray D, et al. Functional and structural features of cholangiocytes in health and disease. Cell Mol Gastroenterol Hepatol 2015;1:368–380.

16. Goetz SC, Anderson KV. The primary cilium: a signalling centre during vertebrate development. Nat Rev Genet 2010;11:331–344.

17. Wheway G, Nazlamova L, Hancock JT. Signaling through the Primary Cilium. Front Cell Dev Biol 2018;6:8.

18. Wheatley DN, Wang AM, Strugnell GE. Expression of primary cilia in mammalian cells. Cell Biol Int 1996;20:73–81.

19. Gradilone SA, Masyuk AI, Splinter PL, et al. Cholangiocyte cilia express TRPV4 and detect changes in luminal tonicity inducing bicarbonate secretion. Proc Natl Acad Sci U S A 2007;104:19138–19143.

20. Masyuk AI, Masyuk TV, Splinter PL, et al. Cholangiocyte cilia detect changes in luminal fluid flow and transmit them into intracellular Ca2+ and cAMP signaling. Gastroenterology 2006;131:911–920.

21. Larusso NF, Masyuk TV. The role of cilia in the regulation of bile flow. Dig Dis 2011;29:6–12.

22. Lazaridis KN, LaRusso NF. The Cholangiopathies. Mayo Clin Proc 2015;90:791–800.

23. Eaton JE, Talwalkar JA, Lazaridis KN, et al. Pathogenesis of primary sclerosing cholangitis and advances in diagnosis and management. Gastroenterology 2013;145:521–536.

24. O'Hara SP, Small AJ, Gajdos GB, et al. HIV-1 Tat protein suppresses cholangiocyte toll-like receptor 4 expression and defense against Cryptosporidium parvum. J Infect Dis 2009;199:1195–1204.

25. Gevers TJG, Drenth JPH. Diagnosis and management of polycystic liver disease. Nat Rev Gastroenterol Hepatol 2013;10:101–108.

26. Elborn JS. Cystic fibrosis. Lancet 2016;388:2519–2531.

27. Saleh M, Kamath BM, Chitayat D. Alagille syndrome: clinical perspectives. Appl Clin Genet 2016;9:75–82.

28. Deltenre P, Valla D-C. Ischemic cholangiopathy. Semin Liver Dis 2008;28:235–246.

29. Razumilava N, Gores GJ. Cholangiocarcinoma. Lancet 2014;383:2168–2179.

30. Visentin M, Lenggenhager D, Gai Z, et al. Drug-induced bile duct injury. Biochim Biophys Acta Mol Basis Dis 2018;1864:1498–1506.

31. Rajapaksha IG, Angus PW, Herath CB. Current therapies and novel approaches for biliary diseases. World J Gastrointest Pathophysiol 2019;10:1–10.

32. Tam PKH, Yiu RS, Lendahl U, et al. Cholangiopathies - Towards a molecular understanding. EBioMedicine 2018;35:381–393.

33. Cardinale V, Carpino G, Reid L, et al. Multiple cells of origin in cholangiocarcinoma underlie biological, epidemiological and clinical heterogeneity. World J Gastrointest Oncol 2012;4:94–102.

34. Fabris L, Perugorria MJ, Mertens J, et al. The tumour microenvironment and immune milieu of cholangiocarcinoma. Liver Int 2019;39 Suppl 1:63–78.

35. Blechacz B, Komuta M, Roskams T, et al. Clinical diagnosis and staging of cholangiocarcinoma. Nat Rev Gastroenterol Hepatol 2011;8:512–522.

36. Banales JM, Marin JJG, Lamarca A, et al. Cholangiocarcinoma 2020: the next horizon in mechanisms and management. Nat Rev Gastroenterol Hepatol 2020;17:557–588.

37. Klatskin G. ADENOCARCINOMA OF THE HEPATIC DUCT AT ITS BIFURCATION WITHIN THE PORTA HEPATIS. AN UNUSUAL TUMOR WITH DISTINCTIVE CLINICAL AND PATHOLOGICAL FEATURES. Am J Med 1965;38:241–256.

38. Yamasaki S. Intrahepatic cholangiocarcinoma: macroscopic type and stage classification. J Hepatobiliary Pancreat Surg 2003;10:288–291.

39. Vijgen S, Terris B, Rubbia-Brandt L. Pathology of intrahepatic cholangiocarcinoma. Hepatobiliary Surg Nutr 2017;6:22–34.

40. Nakanuma Y, Sato Y, Harada K, et al. Pathological classification of intrahepatic cholangiocarcinoma based on a new concept. World J Hepatol 2010;2:419–427.

41. Nakanuma Y, Kakuda Y. Pathologic classification of cholangiocarcinoma: New concepts. Best Pract Res Clin Gastroenterol 2015;29:277–293.

42. Aishima S, Oda Y. Pathogenesis and classification of intrahepatic cholangiocarcinoma: different characters of perihilar large duct type versus peripheral small duct type. J Hepatobiliary Pancreat Sci 2015;22:94–100.

43. Alvaro D, Bragazzi MC, Benedetti A, et al. Cholangiocarcinoma in Italy: A national survey on clinical characteristics, diagnostic modalities and treatment. Results from the “Cholangiocarcinoma” committee of the Italian Association for the Study of Liver disease. Dig Liver Dis 2011;43:60–65.

44. De Rose AM, Cucchetti A, Clemente G, et al. Prognostic significance of tumor doubling time in mass-forming type cholangiocarcinoma. J Gastrointest Surg 2013;17:739–747.

45. Krasinskas AM. Cholangiocarcinoma. Surg Pathol Clin 2018;11:403–429.

46. Liau J-Y, Tsai J-H, Yuan R-H, et al. Morphological subclassification of intrahepatic cholangiocarcinoma: etiological, clinicopathological, and molecular features. Mod Pathol 2014;27:1163–1173.

47. Komuta M, Govaere O, Vandecaveye V, et al. Histological diversity in cholangiocellular carcinoma reflects the different cholangiocyte phenotypes. Hepatology 2012;55:1876–1888.

48. Akita M, Fujikura K, Ajiki T, et al. Dichotomy in intrahepatic cholangiocarcinomas based on histologic similarities to hilar cholangiocarcinomas. Mod Pathol 2017;30:986–997.

49. Hayashi A, Misumi K, Shibahara J, et al. Distinct Clinicopathologic and Genetic Features of 2 Histologic Subtypes of Intrahepatic Cholangiocarcinoma. Am J Surg Pathol 2016;40:1021–1030.

50. Aishima S, Kuroda Y, Nishihara Y, et al. Proposal of progression model for intrahepatic cholangiocarcinoma: clinicopathologic differences between hilar type and peripheral type. Am J Surg Pathol 2007;31:1059–1067.

51. Igarashi S, Sato Y, Ren XS, et al. Participation of peribiliary glands in biliary tract pathophysiologies. World J Hepatol 2013;5:425–432.

52. Cardinale V, Wang Y, Carpino G, et al. Mucin-producing cholangiocarcinoma might derive from biliary tree stem/progenitor cells located in peribiliary glands. Hepatology 2012;55:2041–2042.

53. Carpino G, Cardinale V, Folseraas T, et al. Neoplastic Transformation of the Peribiliary Stem Cell Niche in Cholangiocarcinoma Arisen in Primary Sclerosing Cholangitis. Hepatology 2019;69:622–638.

54. Khan SA, Toledano MB, Taylor-Robinson SD. Epidemiology, risk factors, and pathogenesis of cholangiocarcinoma. HPB (Oxford) 2008;10:77–82.

55. Khan SA, Tavolari S, Brandi G. Cholangiocarcinoma: Epidemiology and risk factors. Liver Int 2019;39 Suppl 1:19–31.

56. Shaib YH, Davila JA, McGlynn K, et al. Rising incidence of intrahepatic cholangiocarcinoma in the United States: a true increase? J Hepatol 2004;40:472–477.

57. Nakeeb A, Pitt HA, Sohn TA, et al. Cholangiocarcinoma. A spectrum of intrahepatic, perihilar, and distal tumors. Ann Surg 1996;224:463–473; discussion 473-475.

58. Banales JM, Cardinale V, Carpino G, et al. Expert consensus document: Cholangiocarcinoma: current knowledge and future perspectives consensus statement from the European Network for the Study of Cholangiocarcinoma (ENS-CCA). Nat Rev Gastroenterol Hepatol 2016;13:261–280.

59. Bertuccio P, Malvezzi M, Carioli G, et al. Global trends in mortality from intrahepatic and extrahepatic cholangiocarcinoma. J Hepatol 2019;71:104–114.

60. Bridgewater J, Galle PR, Khan SA, et al. Guidelines for the diagnosis and management of intrahepatic cholangiocarcinoma. J Hepatol 2014;60:1268–1289.

61. Cardinale V, Semeraro R, Torrice A, et al. Intra-hepatic and extra-hepatic cholangiocarcinoma: New insight into epidemiology and risk factors. World J Gastrointest Oncol 2010;2:407–416.

62. Khan SA, Emadossadaty S, Ladep NG, et al. Rising trends in cholangiocarcinoma: is the ICD classification system misleading us? J Hepatol 2012;56:848–854.

63. Clements O, Eliahoo J, Kim JU, et al. Risk factors for intrahepatic and extrahepatic cholangiocarcinoma: A systematic review and meta-analysis. J Hepatol 2020;72:95–103.

64. Baison GN, Bonds MM, Helton WS, et al. Choledochal cysts: Similarities and differences between Asian and Western countries. World J Gastroenterol 2019;25:3334–3343.

65. Kim HJ, Kim JS, Joo MK, et al. Hepatolithiasis and intrahepatic cholangiocarcinoma: A review. World J Gastroenterol 2015;21:13418–13431.

66. Karlsen TH, Folseraas T, Thorburn D, et al. Primary sclerosing cholangitis - a comprehensive review. J Hepatol 2017;67:1298–1323.

67. Boonstra K, Weersma RK, Erpecum KJ van, et al. Population-based epidemiology, malignancy risk, and outcome of primary sclerosing cholangitis. Hepatology 2013;58:2045–2055.

68. Yonem O, Bayraktar Y. Clinical characteristics of Caroli's disease. World J Gastroenterol 2007;13:1930–1933.

69. Petrick JL, Yang B, Altekruse SF, et al. Risk factors for intrahepatic and extrahepatic cholangiocarcinoma in the United States: A population-based study in SEER-Medicare. PLoS One 2017;12:e0186643.

70. Lim MK, Ju Y-H, Franceschi S, et al. Clonorchis sinensis infection and increasing risk of cholangiocarcinoma in the Republic of Korea. Am J Trop Med Hyg 2006;75:93–96.

71. Lee TY, Lee SS, Jung SW, et al. Hepatitis B virus infection and intrahepatic cholangiocarcinoma in Korea: a case-control study. Am J Gastroenterol 2008;103:1716–1720.

72. Hughes T, O'Connor T, Techasen A, et al. Opisthorchiasis and cholangiocarcinoma in Southeast Asia: an unresolved problem. Int J Gen Med 2017;10:227–237.

73. Shin H-R, Oh J-K, Masuyer E, et al. Epidemiology of cholangiocarcinoma: an update focusing on risk factors. Cancer Sci 2010;101:579–585.

74. Beyer G, Habtezion A, Werner J, et al. Chronic pancreatitis. Lancet 2020;396:499–512.

75. Jing W, Jin G, Zhou X, et al. Diabetes mellitus and increased risk of cholangiocarcinoma: a meta-analysis. Eur J Cancer Prev 2012;21:24–31.

76. Byrne CD, Targher G. NAFLD: a multisystem disease. J Hepatol 2015;62:S47-64.

77. Wongjarupong N, Assavapongpaiboon B, Susantitaphong P, et al. Non-alcoholic fatty liver disease as a risk factor for cholangiocarcinoma: a systematic review and meta-analysis. BMC Gastroenterol 2017;17:149.

78. Rodrigues PM, Olaizola P, Paiva NA, et al. Pathogenesis of Cholangiocarcinoma. Annu Rev Pathol 2021;16:433–463.

79. Li J-S, Han T-J, Jing N, et al. Obesity and the risk of cholangiocarcinoma: a meta-analysis. Tumour Biol 2014;35:6831–6838.

80. Petrick JL, Thistle JE, Zeleniuch-Jacquotte A, et al. Body Mass Index, Diabetes and Intrahepatic Cholangiocarcinoma Risk: The Liver Cancer Pooling Project and Meta-analysis. Am J Gastroenterol 2018;113:1494–1505.

81. Palmer WC, Patel T. Are common factors involved in the pathogenesis of primary liver cancers? A meta-analysis of risk factors for intrahepatic cholangiocarcinoma. J Hepatol 2012;57:69–76.

82. Osataphan S, Mahankasuwan T, Saengboonmee C. Obesity and cholangiocarcinoma: A review of epidemiological and molecular associations. J Hepatobiliary Pancreat Sci 2021;28:1047–1059.

83. Kato I, Kido C. Increased risk of death in thorotrast-exposed patients during the late follow-up period. Jpn J Cancer Res 1987;78:1187–1192.

84. Ishikawa Y, Wada I, Fukumoto M. Alpha-particle carcinogenesis in Thorotrast patients: epidemiology, dosimetry, pathology, and molecular analysis. J Environ Pathol Toxicol Oncol 2001;20:311–315.

85. Brandi G, Di Girolamo S, Farioli A, et al. Asbestos: a hidden player behind the cholangiocarcinoma increase? Findings from a case-control analysis. Cancer Causes Control 2013;24:911–918.

86. Farioli A, Straif K, Brandi G, et al. Occupational exposure to asbestos and risk of cholangiocarcinoma: a population-based case-control study in four Nordic countries. Occup Environ Med 2018;75:191–198.

87. Kumagai S, Sobue T, Makiuchi T, et al. Relationship between cumulative exposure to 1,2-dichloropropane and incidence risk of cholangiocarcinoma among offset printing workers. Occup Environ Med 2016;73:545–552.

88. Huang Y, You L, Xie W, et al. Smoking and risk of cholangiocarcinoma: a systematic review and meta-analysis. Oncotarget 2017;8:100570–100581.

89. Forner A, Vidili G, Rengo M, et al. Clinical presentation, diagnosis and staging of cholangiocarcinoma. Liver Int 2019;39 Suppl 1:98–107.

90. Cardinale V, Bragazzi MC, Carpino G, et al. Intrahepatic cholangiocarcinoma: review and update. HR 2018;4:20.

91. Joo I, Lee JM, Yoon JH. Imaging Diagnosis of Intrahepatic and Perihilar Cholangiocarcinoma: Recent Advances and Challenges. Radiology 2018;288:7–13.

92. Yamashita S, Passot G, Aloia TA, et al. Prognostic value of carbohydrate antigen 19-9 in patients undergoing resection of biliary tract cancer. Br J Surg 2017;104:267–277.

93. Macias RIR, Banales JM, Sangro B, et al. The search for novel diagnostic and prognostic biomarkers in cholangiocarcinoma. Biochim Biophys Acta Mol Basis Dis 2018;1864:1468–1477.

94. Onal C, Colakoglu T, Ulusan SN, et al. Biliary obstruction induces extremely elevated serum CA 19-9 levels: case report. Onkologie 2012;35:780–782.

95. Wannhoff A, Hov JR, Folseraas T, et al. FUT2 and FUT3 genotype determines CA19-9 cut-off values for detection of cholangiocarcinoma in patients with primary sclerosing cholangitis. J Hepatol 2013;59:1278–1284.

96. Kondo N, Murakami Y, Uemura K, et al. Elevated perioperative serum CA 19-9 levels are independent predictors of poor survival in patients with resectable cholangiocarcinoma. J Surg Oncol 2014;110:422–429.

97. Luo X, Yuan L, Wang Y, et al. Survival outcomes and prognostic factors of surgical therapy for all potentially resectable intrahepatic cholangiocarcinoma: a large single-center cohort study. J Gastrointest Surg 2014;18:562–572.

98. Qiang Z, Zhang W, Jin S, et al. Carcinoembryonic antigen, α-fetoprotein, and Ki67 as biomarkers and prognostic factors in intrahepatic cholangiocarcinoma: A retrospective cohort study. Ann Hepatol 2021;20:100242.

99. Lee BS, Lee SH, Son JH, et al. Prognostic value of CA 19-9 kinetics during gemcitabine-based chemotherapy in patients with advanced cholangiocarcinoma. J Gastroenterol Hepatol 2016;31:493–500.

100. Vilana R, Forner A, Bianchi L, et al. Intrahepatic peripheral cholangiocarcinoma in cirrhosis patients may display a vascular pattern similar to hepatocellular carcinoma on contrast-enhanced ultrasound. Hepatology 2010;51:2020–2029.

101. Mar WA, Shon AM, Lu Y, et al. Imaging spectrum of cholangiocarcinoma: role in diagnosis, staging, and posttreatment evaluation. Abdom Radiol (NY) 2016;41:553–567.

102. Lo EC, N Rucker A, Federle MP. Hepatocellular Carcinoma and Intrahepatic Cholangiocarcinoma: Imaging for Diagnosis, Tumor Response to Treatment and Liver Response to Radiation. Semin Radiat Oncol 2018;28:267–276.

103. Vanderveen KA, Hussain HK. Magnetic resonance imaging of cholangiocarcinoma. Cancer Imaging 2004;4:104–115.

104. Lamarca A, Barriuso J, Chander A, et al. 18F-fluorodeoxyglucose positron emission tomography (18FDG-PET) for patients with biliary tract cancer: Systematic review and meta-analysis. J Hepatol 2019;71:115–129.

105. Florescu LM, Florescu DN, Gheonea IA. The Importance of Imaging Techniques in the Assessment of Biliary Tract Cancer. Curr Health Sci J 2017;43:201–208.

106. Romagnuolo J, Bardou M, Rahme E, et al. Magnetic resonance cholangiopancreatography: a meta-analysis of test performance in suspected biliary disease. Ann Intern Med 2003;139:547–557.

107. Weber A, Schmid R-M, Prinz C. Diagnostic approaches for cholangiocarcinoma. World J Gastroenterol 2008;14:4131–4136.

108. Liew ZH, Loh TJ, Lim TKH, et al. Role of fluorescence in situ hybridization in diagnosing cholangiocarcinoma in indeterminate biliary strictures. J Gastroenterol Hepatol 2018;33:315–319.

109. Mirallas O, López-Valbuena D, García-Illescas D, et al. Advances in the systemic treatment of therapeutic approaches in biliary tract cancer. ESMO Open 2022;7:100503.

110. Alabraba E, Joshi H, Bird N, et al. Increased multimodality treatment options has improved survival for Hepatocellular carcinoma but poor survival for biliary tract cancers remains unchanged. Eur J Surg Oncol 2019;45:1660–1667.

111. Spolverato G, Kim Y, Alexandrescu S, et al. Management and Outcomes of Patients with Recurrent Intrahepatic Cholangiocarcinoma Following Previous Curative-Intent Surgical Resection. Ann Surg Oncol 2016;23:235–243.

112. Mocan L-P, Ilieș M, Melincovici CS, et al. Novel approaches in search for biomarkers of cholangiocarcinoma. World J Gastroenterol 2022;28:1508–1525.

113. Endo I, Gonen M, Yopp AC, et al. Intrahepatic cholangiocarcinoma: rising frequency, improved survival, and determinants of outcome after resection. Ann Surg 2008;248:84–96.

114. From the American Association of Neurological Surgeons (AANS), American Society of Neuroradiology (ASNR), Cardiovascular and Interventional Radiology Society of Europe (CIRSE), Canadian Interventional Radiology Association (CIRA), Congress of Neurological Surgeons (CNS), European Society of Minimally Invasive Neurological Therapy (ESMINT), European Society of Neuroradiology (ESNR), European Stroke Organization (ESO), Society for Cardiovascular Angiography and Interventions (SCAI), Society of Interventional Radiology (SIR), Society of NeuroInterventional Surgery (SNIS), and World Stroke Organization (WSO), Sacks D, Baxter B, et al. Multisociety Consensus Quality Improvement Revised Consensus Statement for Endovascular Therapy of Acute Ischemic Stroke. Int J Stroke 2018;13:612–632.

115. Ong CK, Subimerb C, Pairojkul C, et al. Exome sequencing of liver fluke-associated cholangiocarcinoma. Nat Genet 2012;44:690–693.

116. Chan-On W, Nairismägi M-L, Ong CK, et al. Exome sequencing identifies distinct mutational patterns in liver fluke-related and non-infection-related bile duct cancers. Nat Genet 2013;45:1474–1478.

117. Perugorria MJ, Olaizola P, Labiano I, et al. Wnt–β-catenin signalling in liver development, health and disease. Nat Rev Gastroenterol Hepatol 2019;16:121–136.

118. Gu T-L, Deng X, Huang F, et al. Survey of Tyrosine Kinase Signaling Reveals ROS Kinase Fusions in Human Cholangiocarcinoma. PLoS One 2011;6:e15640.

119. Nakamura H, Arai Y, Totoki Y, et al. Genomic spectra of biliary tract cancer. Nat Genet 2015;47:1003–1010.

120. Nepal C, O'Rourke CJ, Oliveira DVNP, et al. Genomic perturbations reveal distinct regulatory networks in intrahepatic cholangiocarcinoma. Hepatology 2018;68:949–963.

121. Sia D, Hoshida Y, Villanueva A, et al. Integrative molecular analysis of intrahepatic cholangiocarcinoma reveals 2 classes that have different outcomes. Gastroenterology 2013;144:829–840.

122. Andersen JB, Spee B, Blechacz BR, et al. Genomic and genetic characterization of cholangiocarcinoma identifies therapeutic targets for tyrosine kinase inhibitors. Gastroenterology 2012;142:1021-1031.e15.

123. Maynard H, Stadler ZK, Berger MF, et al. Germline alterations in patients with biliary tract cancers: A spectrum of significant and previously underappreciated findings. Cancer 2020;126:1995–2002.

124. Lin J, Shi J, Guo H, et al. Alterations in DNA Damage Repair Genes in Primary Liver Cancer. Clin Cancer Res 2019;25:4701–4711.

125. O'Rourke CJ, Munoz-Garrido P, Aguayo EL, et al. Epigenome dysregulation in cholangiocarcinoma. Biochim Biophys Acta Mol Basis Dis 2018;1864:1423–1434.

126. Luczak MW, Jagodziński PP. The role of DNA methylation in cancer development. Folia Histochem Cytobiol 2006;44:143–154.

127. Jusakul A, Cutcutache I, Yong CH, et al. Whole-Genome and Epigenomic Landscapes of Etiologically Distinct Subtypes of Cholangiocarcinoma. Cancer Discov 2017;7:1116–1135.

128. Goeppert B, Toth R, Singer S, et al. Integrative Analysis Defines Distinct Prognostic Subgroups of Intrahepatic Cholangiocarcinoma. Hepatology 2019;69:2091–2106.

129. Morine Y, Shimada M, Iwahashi S, et al. Role of histone deacetylase expression in intrahepatic cholangiocarcinoma. Surgery 2012;151:412–419.

130. He J, Yao W, Wang J, et al. TACC3 overexpression in cholangiocarcinoma correlates with poor prognosis and is a potential anti-cancer molecular drug target for HDAC inhibitors. Oncotarget 2016;7:75441–75456.

131. Lu L, Byrnes K, Han C, et al. miR-21 targets 15-PGDH and promotes cholangiocarcinoma growth. Mol Cancer Res 2014;12:890–900.

132. Li H, Zhou Z-Q, Yang Z-R, et al. MicroRNA-191 acts as a tumor promoter by modulating the TET1-p53 pathway in intrahepatic cholangiocarcinoma. Hepatology 2017;66:136–151.

133. Kwon H, Song K, Han C, et al. Epigenetic Silencing of miRNA-34a in Human Cholangiocarcinoma via EZH2 and DNA Methylation: Impact on Regulation of Notch Pathway. Am J Pathol 2017;187:2288–2299.

134. Peng C, Sun Z, Li O, et al. Leptin stimulates the epithelial-mesenchymal transition and pro-angiogenic capability of cholangiocarcinoma cells through the miR-122/PKM2 axis. Int J Oncol 2019;55:298–308.

135. Mansini AP, Lorenzo Pisarello MJ, Thelen KM, et al. MiR-433 and miR-22 dysregulations induce HDAC6 overexpression and ciliary loss in cholangiocarcinoma. Hepatology 2018;68:561–573.

136. Zabron A, Edwards RJ, Khan SA. The challenge of cholangiocarcinoma: dissecting the molecular mechanisms of an insidious cancer. Dis Model Mech 2013;6:281–292.

137. Jaiswal M, LaRusso NF, Burgart LJ, et al. Inflammatory cytokines induce DNA damage and inhibit DNA repair in cholangiocarcinoma cells by a nitric oxide-dependent mechanism. Cancer Res 2000;60:184–190.

138. Frampton G, Invernizzi P, Bernuzzi F, et al. Interleukin-6-driven progranulin expression increases cholangiocarcinoma growth by an Akt-dependent mechanism. Gut 2012;61:268–277.

139. Tadlock L, Patel T. Involvement of p38 mitogen-activated protein kinase signaling in transformed growth of a cholangiocarcinoma cell line. Hepatology 2001;33:43–51.

140. Sia D, Tovar V, Moeini A, et al. Intrahepatic cholangiocarcinoma: pathogenesis and rationale for molecular therapies. Oncogene 2013;32:4861–4870.

141. Andersen JB. Molecular pathogenesis of intrahepatic cholangiocarcinoma. J Hepatobiliary Pancreat Sci 2015;22:101–113.

142. Yoon J-H, Canbay AE, Werneburg NW, et al. Oxysterols induce cyclooxygenase-2 expression in cholangiocytes: implications for biliary tract carcinogenesis. Hepatology 2004;39:732–738.

143. Aishima S, Mano Y, Tanaka Y, et al. Different roles of inducible nitric oxide synthase and cyclooxygenase-2 in carcinogenesis and metastasis of intrahepatic cholangiocarcinoma. Hum Pathol 2013;44:1031–1037.

144. Zhang Z, Lai G-H, Sirica AE. Celecoxib-induced apoptosis in rat cholangiocarcinoma cells mediated by Akt inactivation and Bax translocation. Hepatology 2004;39:1028–1037.

145. Lai G-H, Zhang Z, Sirica AE. Celecoxib acts in a cyclooxygenase-2-independent manner and in synergy with emodin to suppress rat cholangiocarcinoma growth in vitro through a mechanism involving enhanced Akt inactivation and increased activation of caspases-9 and -3. Mol Cancer Ther 2003;2:265–271.

146. Banales JM, Huebert RC, Karlsen T, et al. Cholangiocyte pathobiology. Nat Rev Gastroenterol Hepatol 2019;16:269–281.

147. Xue T-C, Zhang B-H, Ye S-L, et al. Differentially expressed gene profiles of intrahepatic cholangiocarcinoma, hepatocellular carcinoma, and combined hepatocellular-cholangiocarcinoma by integrated microarray analysis. Tumour Biol 2015;36:5891–5899.

148. Sekiya S, Suzuki A. Intrahepatic cholangiocarcinoma can arise from Notch-mediated conversion of hepatocytes. J Clin Invest 2012;122:3914–3918.

149. Gil-García B, Baladrón V. The complex role of NOTCH receptors and their ligands in the development of hepatoblastoma, cholangiocarcinoma and hepatocellular carcinoma. Biol Cell 2016;108:29–40.

150. Wu W-R, Shi X-D, Zhang R, et al. Clinicopathological significance of aberrant Notch receptors in intrahepatic cholangiocarcinoma. Int J Clin Exp Pathol 2014;7:3272–3279.

151. Wu W-R, Zhang R, Shi X-D, et al. Notch1 is overexpressed in human intrahepatic cholangiocarcinoma and is associated with its proliferation, invasiveness and sensitivity to 5-fluorouracil in vitro. Oncol Rep 2014;31:2515–2524.

152. Aoki S, Mizuma M, Takahashi Y, et al. Aberrant activation of Notch signaling in extrahepatic cholangiocarcinoma: clinicopathological features and therapeutic potential for cancer stem cell-like properties. BMC Cancer 2016;16:854.

153. Guest RV, Boulter L, Dwyer BJ, et al. Notch3 drives development and progression of cholangiocarcinoma. Proc Natl Acad Sci U S A 2016;113:12250–12255.

154. Fan B, Malato Y, Calvisi DF, et al. Cholangiocarcinomas can originate from hepatocytes in mice. J Clin Invest 2012;122:2911–2915.

155. Wang J, Dong M, Xu Z, et al. Notch2 controls hepatocyte-derived cholangiocarcinoma formation in mice. Oncogene 2018;37:3229–3242.

156. De Jesus-Acosta A, Laheru D, Maitra A, et al. A phase II study of the gamma secretase inhibitor RO4929097 in patients with previously treated metastatic pancreatic adenocarcinoma. Invest New Drugs 2014;32:739–745.

157. Piha-Paul SA, Munster PN, Hollebecque A, et al. Results of a phase 1 trial combining ridaforolimus and MK-0752 in patients with advanced solid tumours. Eur J Cancer 2015;51:1865–1873.

158. Pant S, Jones SF, Kurkjian CD, et al. A first-in-human phase I study of the oral Notch inhibitor, LY900009, in patients with advanced cancer. Eur J Cancer 2016;56:1–9.

159. Locatelli MA, Aftimos P, Dees EC, et al. Phase I study of the gamma secretase inhibitor PF-03084014 in combination with docetaxel in patients with advanced triple-negative breast cancer. Oncotarget 2017;8:2320–2328.

160. Massard C, Azaro A, Soria J-C, et al. First-in-human study of LY3039478, an oral Notch signaling inhibitor in advanced or metastatic cancer. Ann Oncol 2018;29:1911–1917.

161. Ferrarotto R, Eckhardt G, Patnaik A, et al. A phase I dose-escalation and dose-expansion study of brontictuzumab in subjects with selected solid tumors. Ann Oncol 2018;29:1561–1568.

162. Hu ZI, Bendell JC, Bullock A, et al. A randomized phase II trial of nab-paclitaxel and gemcitabine with tarextumab or placebo in patients with untreated metastatic pancreatic cancer. Cancer Med 2019;8:5148–5157.

163. Chiorean EG, LoRusso P, Strother RM, et al. A Phase I First-in-Human Study of Enoticumab (REGN421), a Fully Human Delta-like Ligand 4 (Dll4) Monoclonal Antibody in Patients with Advanced Solid Tumors. Clin Cancer Res 2015;21:2695–2703.

164. McKeage MJ, Kotasek D, Markman B, et al. Phase IB Trial of the Anti-Cancer Stem Cell DLL4-Binding Agent Demcizumab with Pemetrexed and Carboplatin as First-Line Treatment of Metastatic Non-Squamous NSCLC. Target Oncol 2018;13:89–98.

165. Boulter L, Guest RV, Kendall TJ, et al. WNT signaling drives cholangiocarcinoma growth and can be pharmacologically inhibited. J Clin Invest 2015;125:1269–1285.

166. Loilome W, Bungkanjana P, Techasen A, et al. Activated macrophages promote Wnt/β-catenin signaling in cholangiocarcinoma cells. Tumour Biol 2014;35:5357–5367.

167. Goeppert B, Konermann C, Schmidt CR, et al. Global alterations of DNA methylation in cholangiocarcinoma target the Wnt signaling pathway. Hepatology 2014;59:544–554.

168. Merino-Azpitarte M, Lozano E, Perugorria MJ, et al. SOX17 regulates cholangiocyte differentiation and acts as a tumor suppressor in cholangiocarcinoma. J Hepatol 2017;67:72–83.

169. Riedlinger D, Bahra M, Boas-Knoop S, et al. Hedgehog pathway as a potential treatment target in human cholangiocarcinoma. J Hepatobiliary Pancreat Sci 2014;21:607–615.

170. El Khatib M, Kalnytska A, Palagani V, et al. Inhibition of hedgehog signaling attenuates carcinogenesis in vitro and increases necrosis of cholangiocellular carcinoma. Hepatology 2013;57:1035–1045.

171. Fingas CD, Bronk SF, Werneburg NW, et al. Myofibroblast-derived PDGF-BB promotes Hedgehog survival signaling in cholangiocarcinoma cells. Hepatology 2011;54:2076–2088.

172. Kim Y, Kim M-O, Shin JS, et al. Hedgehog signaling between cancer cells and hepatic stellate cells in promoting cholangiocarcinoma. Ann Surg Oncol 2014;21:2684–2698.

173. Pan D. Hippo signaling in organ size control. Genes Dev 2007;21:886–897.

174. Li H, Wolfe A, Septer S, et al. Deregulation of Hippo kinase signalling in human hepatic malignancies. Liver Int 2012;32:38–47.

175. Tao J, Calvisi DF, Ranganathan S, et al. Activation of β-catenin and Yap1 in human hepatoblastoma and induction of hepatocarcinogenesis in mice. Gastroenterology 2014;147:690–701.

176. Pei T, Li Y, Wang J, et al. YAP is a critical oncogene in human cholangiocarcinoma. Oncotarget 2015;6:17206–17220.

177. Wu H, Liu Y, Jiang X-W, et al. Clinicopathological and prognostic significance of Yes-associated protein expression in hepatocellular carcinoma and hepatic cholangiocarcinoma. Tumor Biol 2016;37:13499–13508.

178. Sugimachi K, Nishio M, Aishima S, et al. Altered Expression of Hippo Signaling Pathway Molecules in Intrahepatic Cholangiocarcinoma. Oncology 2017;93:67–74.

179. Farshidfar F, Zheng S, Gingras M-C, et al. Integrative Genomic Analysis of Cholangiocarcinoma Identifies Distinct IDH-Mutant Molecular Profiles. Cell Rep 2017;18:2780–2794.

180. Moeini A, Sia D, Bardeesy N, et al. Molecular Pathogenesis and Targeted Therapies for Intrahepatic Cholangiocarcinoma. Clin Cancer Res 2016;22:291–300.

181. Leone F, Cavalloni G, Pignochino Y, et al. Somatic mutations of epidermal growth factor receptor in bile duct and gallbladder carcinoma. Clin Cancer Res 2006;12:1680–1685.

182. Radtke A, Königsrainer A. Surgical Therapy of Cholangiocarcinoma. Visc Med 2016;32:422–426.

183. Khan SA, Davidson BR, Goldin RD, et al. Guidelines for the diagnosis and treatment of cholangiocarcinoma: an update. Gut 2012;61:1657–1669.

184. Primrose JN, Fox RP, Palmer DH, et al. Capecitabine compared with observation in resected biliary tract cancer (BILCAP): a randomised, controlled, multicentre, phase 3 study. Lancet Oncol 2019;20:663–673.

185. Sapisochin G, Facciuto M, Rubbia-Brandt L, et al. Liver transplantation for “very early” intrahepatic cholangiocarcinoma: International retrospective study supporting a prospective assessment. Hepatology 2016;64:1178–1188.

186. Sapisochin G, Lope CR de, Gastaca M, et al. Intrahepatic cholangiocarcinoma or mixed hepatocellular-cholangiocarcinoma in patients undergoing liver transplantation: a Spanish matched cohort multicenter study. Ann Surg 2014;259:944–952.

187. Ethun CG, Lopez-Aguiar AG, Anderson DJ, et al. Transplantation Versus Resection for Hilar Cholangiocarcinoma: An Argument for Shifting Treatment Paradigms for Resectable Disease. Ann Surg 2018;267:797–805.

188. Darwish Murad S, Kim WR, Harnois DM, et al. Efficacy of neoadjuvant chemoradiation, followed by liver transplantation, for perihilar cholangiocarcinoma at 12 US centers. Gastroenterology 2012;143:88-98.e3; quiz e14.

189. Okusaka T, Nakachi K, Fukutomi A, et al. Gemcitabine alone or in combination with cisplatin in patients with biliary tract cancer: a comparative multicentre study in Japan. Br J Cancer 2010;103:469–474.

190. Valle J, Wasan H, Palmer DH, et al. Cisplatin plus gemcitabine versus gemcitabine for biliary tract cancer. N Engl J Med 2010;362:1273–1281.

191. Lamarca A, Palmer DH, Wasan HS, et al. Second-line FOLFOX chemotherapy versus active symptom control for advanced biliary tract cancer (ABC-06): a phase 3, open-label, randomised, controlled trial. Lancet Oncol 2021;22:690–701.

192. Park JO, Feng Y-H, Chen Y-Y, et al. Updated results of a phase IIa study to evaluate the clinical efficacy and safety of erdafitinib in Asian advanced cholangiocarcinoma (CCA) patients with FGFR alterations. JCO 2019;37:4117–4117.

193. Shroff RT, Javle MM, Xiao L, et al. Gemcitabine, Cisplatin, and nab-Paclitaxel for the Treatment of Advanced Biliary Tract Cancers: A Phase 2 Clinical Trial. JAMA Oncol 2019;5:824–830.

194. Schönfeld L, Hinrichs JB, Marquardt S, et al. Chemosaturation with percutaneous hepatic perfusion is effective in patients with ocular melanoma and cholangiocarcinoma. J Cancer Res Clin Oncol 2020;146:3003–3012.

195. Al-Adra DP, Gill RS, Axford SJ, et al. Treatment of unresectable intrahepatic cholangiocarcinoma with yttrium-90 radioembolization: a systematic review and pooled analysis. Eur J Surg Oncol 2015;41:120–127.

196. Park S-Y, Kim JH, Yoon H-J, et al. Transarterial chemoembolization versus supportive therapy in the palliative treatment of unresectable intrahepatic cholangiocarcinoma. Clin Radiol 2011;66:322–328.

197. Abou-Alfa GK, Sahai V, Hollebecque A, et al. Pemigatinib for previously treated, locally advanced or metastatic cholangiocarcinoma: a multicentre, open-label, phase 2 study. Lancet Oncol 2020;21:671–684.

198. Hoy SM. Pemigatinib: First Approval. Drugs 2020;80:923–929.

199. Bibeau K, Féliz L, Lihou CF, et al. Progression-Free Survival in Patients With Cholangiocarcinoma With or Without FGF/FGFR Alterations: A FIGHT-202 Post Hoc Analysis of Prior Systemic Therapy Response. JCO Precis Oncol 2022;6:e2100414.

200. Bekaii-Saab TS, Valle JW, Van Cutsem E, et al. FIGHT-302: first-line pemigatinib vs gemcitabine plus cisplatin for advanced cholangiocarcinoma with FGFR2 rearrangements. Future Oncol 2020;16:2385–2399.

201. Makawita S, K Abou-Alfa G, Roychowdhury S, et al. Infigratinib in patients with advanced cholangiocarcinoma with FGFR2 gene fusions/translocations: the PROOF 301 trial. Future Oncol 2020;16:2375–2384.

202. Javle M, Roychowdhury S, Kelley RK, et al. Infigratinib (BGJ398) in previously treated patients with advanced or metastatic cholangiocarcinoma with FGFR2 fusions or rearrangements: mature results from a multicentre, open-label, single-arm, phase 2 study. Lancet Gastroenterol Hepatol 2021;6:803–815.

203. Kang C. Infigratinib: First Approval. Drugs 2021;81:1355–1360.

204. Mazzaferro V, El-Rayes BF, Droz Dit Busset M, et al. Derazantinib (ARQ 087) in advanced or inoperable FGFR2 gene fusion-positive intrahepatic cholangiocarcinoma. Br J Cancer 2019;120:165–171.

205. Bahleda R, Italiano A, Hierro C, et al. Multicenter Phase I Study of Erdafitinib (JNJ-42756493), Oral Pan-Fibroblast Growth Factor Receptor Inhibitor, in Patients with Advanced or Refractory Solid Tumors. Clin Cancer Res 2019;25:4888–4897.

206. Markham A. Erdafitinib: First Global Approval. Drugs 2019;79:1017–1021.

207. Bahleda R, Meric-Bernstam F, Goyal L, et al. Phase I, first-in-human study of futibatinib, a highly selective, irreversible FGFR1-4 inhibitor in patients with advanced solid tumors. Ann Oncol 2020;31:1405–1412.

208. Abou-Alfa GK, Macarulla T, Javle MM, et al. Ivosidenib in IDH1-mutant, chemotherapy-refractory cholangiocarcinoma (ClarIDHy): a multicentre, randomised, double-blind, placebo-controlled, phase 3 study. Lancet Oncol 2020;21:796–807.

209. Zhu AX, Macarulla T, Javle MM, et al. Final Overall Survival Efficacy Results of Ivosidenib for Patients With Advanced Cholangiocarcinoma With IDH1 Mutation: The Phase 3 Randomized Clinical ClarIDHy Trial. JAMA Oncol 2021;7:1669–1677.

210. Casak SJ, Pradhan S, Fashoyin-Aje LA, et al. FDA Approval Summary: Ivosidenib for the Treatment of Patients with Advanced Unresectable or Metastatic, Chemotherapy Refractory Cholangiocarcinoma with an IDH1 Mutation. Clin Cancer Res 2022;28:2733–2737.

211. Rizzo A, Ricci AD, Brandi G. IDH inhibitors in advanced cholangiocarcinoma: Another arrow in the quiver? Cancer Treat Res Commun 2021;27:100356.

212. Subbiah V, Lassen U, Élez E, et al. Dabrafenib plus trametinib in patients with BRAFV600E-mutated biliary tract cancer (ROAR): a phase 2, open-label, single-arm, multicentre basket trial. Lancet Oncol 2020;21:1234–1243.

213. Center for Drug Evaluation and Research. *FDA grants accelerated approval to dabrafenib in combination with trametinib for unresectable or metastatic solid tumors with BRAF V600E mutation*. FDA; 2022. Available at: https://www.fda.gov/drugs/resources-information-approved-drugs/fda-grants-accelerated-approval-dabrafenib-combination-trametinib-unresectable-or-metastatic-solid [Accessed July 14, 2022].

214. Milbury CA, Creeden J, Yip W-K, et al. Clinical and analytical validation of FoundationOne®CDx, a comprehensive genomic profiling assay for solid tumors. PLoS One 2022;17:e0264138.

215. Silverman IM, Li M, Murugesan K, et al. Validation and Characterization of FGFR2 Rearrangements in Cholangiocarcinoma with Comprehensive Genomic Profiling. The Journal of Molecular Diagnostics 2022;24:351–364.

216. Chen C, Wang T, Yang M, et al. Genomic Profiling of Blood-Derived Circulating Tumor DNA from Patients with Advanced Biliary Tract Cancer. Pathol Oncol Res 2021;27:1609879.

217. Feng K-C, Guo Y-L, Liu Y, et al. Cocktail treatment with EGFR-specific and CD133-specific chimeric antigen receptor-modified T cells in a patient with advanced cholangiocarcinoma. J Hematol Oncol 2017;10:4.

218. Guo Y, Feng K, Liu Y, et al. Phase I Study of Chimeric Antigen Receptor-Modified T Cells in Patients with EGFR-Positive Advanced Biliary Tract Cancers. Clin Cancer Res 2018;24:1277–1286.

219. Feng K, Liu Y, Guo Y, et al. Phase I study of chimeric antigen receptor modified T cells in treating HER2-positive advanced biliary tract cancers and pancreatic cancers. Protein Cell 2018;9:838–847.

220. Piha-Paul SA, Oh D-Y, Ueno M, et al. Efficacy and safety of pembrolizumab for the treatment of advanced biliary cancer: Results from the KEYNOTE-158 and KEYNOTE-028 studies. Int J Cancer 2020;147:2190–2198.

221. Kim RD, Chung V, Alese OB, et al. A Phase 2 Multi-institutional Study of Nivolumab for Patients With Advanced Refractory Biliary Tract Cancer. JAMA Oncol 2020;6:1–8.

222. Oh D-Y, Ruth HA, Qin S, et al. Durvalumab plus Gemcitabine and Cisplatin in Advanced Biliary Tract Cancer. NEJM Evidence 2022:EVIDoa2200015.

223. Anon. Imfinzi plus chemotherapy granted Priority Review in the US for patients with locally advanced or metastatic biliary tract cancer based on TOPAZ-1 Phase III trial. Available at: https://www.astrazeneca-us.com/media/press-releases/2022/imfinzi-plus-chemotherapy-granted-priority-review-in-the-us-for-patients-with-locally-advanced-or-metastatic-biliary-tract-cancer-based-on-topaz-1-phase-iii-trial-05042022.html [Accessed July 15, 2022].

224. Doki Y, Ueno M, Hsu C-H, et al. Tolerability and efficacy of durvalumab, either as monotherapy or in combination with tremelimumab, in patients from Asia with advanced biliary tract, esophageal, or head-and-neck cancer. Cancer Med 2022;11:2550–2560.

225. Oh D-Y, Lee K-H, Lee D-W, et al. Gemcitabine and cisplatin plus durvalumab with or without tremelimumab in chemotherapy-naive patients with advanced biliary tract cancer: an open-label, single-centre, phase 2 study. Lancet Gastroenterol Hepatol 2022;7:522–532.

226. Boilève A, Hilmi M, Gougis P, et al. Triplet combination of durvalumab, tremelimumab, and paclitaxel in biliary tract carcinomas: Safety run-in results of the randomized IMMUNOBIL PRODIGE 57 phase II trial. Eur J Cancer 2021;143:55–63.

227. Hong M, Clubb JD, Chen YY. Engineering CAR-T Cells for Next-Generation Cancer Therapy. Cancer Cell 2020;38:473–488.

228. Tran E, Turcotte S, Gros A, et al. Cancer immunotherapy based on mutation-specific CD4+ T cells in a patient with epithelial cancer. Science 2014;344:641–645.

229. McConnell BB, Yang VW. Mammalian Krüppel-Like Factors in Health and Diseases. Physiol Rev 2010;90:1337–1381.

230. Nagai R, Friedman SL, Kasuga M. *The Biology of Krüppel-like Factors*. 1st ed. Tokyo: Springer; 2009.

231. Pei J, Grishin NV. A new family of predicted Krüppel-like factor genes and pseudogenes in placental mammals. PLoS One 2013;8:e81109.

232. Liao Z, Wang X, Chen X, et al. Prediction and Identification of Krüppel-Like Transcription Factors by Machine Learning Method. Comb Chem High Throughput Screen 2017;20:594–602.

233. Prosdocimo DA, Sabeh MK, Jain MK. Kruppel-like factors in muscle health and disease. Trends Cardiovasc Med 2015;25:278–287.

234. Yoshida T, Yamashita M, Horimai C, et al. Kruppel-like factor 4 protein regulates isoproterenol-induced cardiac hypertrophy by modulating myocardin expression and activity. J Biol Chem 2014;289:26107–26118.

235. Waye JS, Eng B. Krüppel-like factor 1: hematologic phenotypes associated with KLF1 gene mutations. Int J Lab Hematol 2015;37 Suppl 1:78–84.

236. Wan H, Luo F, Wert SE, et al. Kruppel-like factor 5 is required for perinatal lung morphogenesis and function. Development 2008;135:2563–2572.

237. Wani MA, Wert SE, Lingrel JB. Lung Kruppel-like factor, a zinc finger transcription factor, is essential for normal lung development. J Biol Chem 1999;274:21180–21185.

238. Flandez M, Guilmeau S, Blache P, et al. KLF4 regulation in intestinal epithelial cell maturation. Exp Cell Res 2008;314:3712–3723.

239. Yu T, Chen X, Zhang W, et al. Krüppel-like factor 4 regulates intestinal epithelial cell morphology and polarity. PLoS One 2012;7:e32492.

240. Hart GT, Hogquist KA, Jameson SC. Krüppel-like factors in lymphocyte biology. J Immunol 2012;188:521–526.

241. Shields JM, Christy RJ, Yang VW. Identification and characterization of a gene encoding a gut-enriched Krüppel-like factor expressed during growth arrest. J Biol Chem 1996;271:20009–20017.

242. Panigada M, Porcellini S, Sutti F, et al. GKLF in thymus epithelium as a developmentally regulated element of thymocyte-stroma cross-talk. Mech Dev 1999;81:103–113.

243. Fruman DA, Ferl GZ, An SS, et al. Phosphoinositide 3-kinase and Bruton's tyrosine kinase regulate overlapping sets of genes in B lymphocytes. Proc Natl Acad Sci U S A 2002;99:359–364.

244. Chiambaretta F, De Graeve F, Turet G, et al. Cell and tissue specific expression of human Krüppel-like transcription factors in human ocular surface. Mol Vis 2004;10:901–909.

245. Cullingford TE, Butler MJ, Marshall AK, et al. Differential regulation of Krüppel-like factor family transcription factor expression in neonatal rat cardiac myocytes: effects of endothelin-1, oxidative stress and cytokines. Biochim Biophys Acta 2008;1783:1229–1236.

246. Anderson KP, Kern CB, Crable SC, et al. Isolation of a gene encoding a functional zinc finger protein homologous to erythroid Krüppel-like factor: identification of a new multigene family. Mol Cell Biol 1995;15:5957–5965.

247. Carlson CM, Endrizzi BT, Wu J, et al. Kruppel-like factor 2 regulates thymocyte and T-cell migration. Nature 2006;442:299–302.

248. Matsumoto N, Kubo A, Liu H, et al. Developmental regulation of yolk sac hematopoiesis by Kruppel-like factor 6. Blood 2006;107:1357–1365.

249. Martin KM, Metcalfe JC, Kemp PR. Expression of Klf9 and Klf13 in mouse development. Mech Dev 2001;103:149–151.

250. Hodge D, Coghill E, Keys J, et al. A global role for EKLF in definitive and primitive erythropoiesis. Blood 2006;107:3359–3370.

251. Ton-That H, Kaestner KH, Shields JM, et al. Expression of the gut-enriched Krüppel-like factor gene during development and intestinal tumorigenesis. FEBS Lett 1997;419:239–243.

252. Laub F, Lei L, Sumiyoshi H, et al. Transcription factor KLF7 is important for neuronal morphogenesis in selected regions of the nervous system. Mol Cell Biol 2005;25:5699–5711.

253. Miller IJ, Bieker JJ. A novel, erythroid cell-specific murine transcription factor that binds to the CACCC element and is related to the Krüppel family of nuclear proteins. Mol Cell Biol 1993;13:2776–2786.

254. Ree JH van, Roskrow MA, Becher AM, et al. The human erythroid-specific transcription factor EKLF localizes to chromosome 19p13.12-p13.13. Genomics 1997;39:393–395.

255. Matsumoto N, Laub F, Aldabe R, et al. Cloning the cDNA for a new human zinc finger protein defines a group of closely related Krüppel-like transcription factors. J Biol Chem 1998;273:28229–28237.

256. Patel SK, Velkoska E, Gayed D, et al. Left ventricular hypertrophy in experimental chronic kidney disease is associated with reduced expression of cardiac Kruppel-like factor 15. BMC Nephrol 2018;19:159.

257. Leenders JJ, Wijnen WJ, Hiller M, et al. Regulation of cardiac gene expression by KLF15, a repressor of myocardin activity. J Biol Chem 2010;285:27449–27456.

258. Li Z, Martin M, Zhang J, et al. Krüppel-Like Factor 4 Regulation of Cholesterol-25-Hydroxylase and Liver X Receptor Mitigates Atherosclerosis Susceptibility. Circulation 2017;136:1315–1330.

259. Hergenreider E, Heydt S, Tréguer K, et al. Atheroprotective communication between endothelial cells and smooth muscle cells through miRNAs. Nat Cell Biol 2012;14:249–256.

260. Mreich E, Chen X-M, Zaky A, et al. The role of Krüppel-like factor 4 in transforming growth factor-β-induced inflammatory and fibrotic responses in human proximal tubule cells. Clin Exp Pharmacol Physiol 2015;42:680–686.

261. Chen W-C, Lin H-H, Tang M-J. Matrix-Stiffness-Regulated Inverse Expression of Krüppel-Like Factor 5 and Krüppel-Like Factor 4 in the Pathogenesis of Renal Fibrosis. Am J Pathol 2015;185:2468–2481.

262. Liao X, Sharma N, Kapadia F, et al. Krüppel-like factor 4 regulates macrophage polarization. J Clin Invest 2011;121:2736–2749.

263. Small KS, Todorčević M, Civelek M, et al. Regulatory variants at KLF14 influence type 2 diabetes risk via a female-specific effect on adipocyte size and body composition. Nat Genet 2018;50:572–580.

264. Small KS, Hedman AK, Grundberg E, et al. Identification of an imprinted master trans regulator at the KLF14 locus related to multiple metabolic phenotypes. Nat Genet 2011;43:561–564.

265. Bacos K, Gillberg L, Volkov P, et al. Blood-based biomarkers of age-associated epigenetic changes in human islets associate with insulin secretion and diabetes. Nat Commun 2016;7:11089.

266. Zobel DP, Andreasen CH, Burgdorf KS, et al. Variation in the gene encoding Krüppel-like factor 7 influences body fat: studies of 14 818 Danes. Eur J Endocrinol 2009;160:603–609.

267. Salinas YD, Wang L, DeWan AT. Multiethnic genome-wide association study identifies ethnic-specific associations with body mass index in Hispanics and African Americans. BMC Genet 2016;17:78.

268. Pettersson M, Viljakainen H, Loid P, et al. Copy Number Variants Are Enriched in Individuals With Early-Onset Obesity and Highlight Novel Pathogenic Pathways. J Clin Endocrinol Metab 2017;102:3029–3039.

269. Koh I-U, Lee H-J, Hwang J-Y, et al. Obesity-related CpG Methylation (cg07814318) of Kruppel-like Factor-13 (KLF13) Gene with Childhood Obesity and its cis-Methylation Quantitative Loci. Sci Rep 2017;7:45368.

270. Spörl F, Korge S, Jürchott K, et al. Krüppel-like factor 9 is a circadian transcription factor in human epidermis that controls proliferation of keratinocytes. Proc Natl Acad Sci U S A 2012;109:10903–10908.

271. Simmen FA, Xiao R, Velarde MC, et al. Dysregulation of intestinal crypt cell proliferation and villus cell migration in mice lacking Kruppel-like factor 9. Am J Physiol Gastrointest Liver Physiol 2007;292:G1757-1769.

272. Li R, Liang J, Ni S, et al. A mesenchymal-to-epithelial transition initiates and is required for the nuclear reprogramming of mouse fibroblasts. Cell Stem Cell 2010;7:51–63.

273. Narla G, Heath KE, Reeves HL, et al. KLF6, a candidate tumor suppressor gene mutated in prostate cancer. Science 2001;294:2563–2566.

274. Gumireddy K, Li A, Gimotty PA, et al. KLF17 is a negative regulator of epithelial-mesenchymal transition and metastasis in breast cancer. Nat Cell Biol 2009;11:1297–1304.

275. Wang X, Zheng M, Liu G, et al. Krüppel-like factor 8 induces epithelial to mesenchymal transition and epithelial cell invasion. Cancer Res 2007;67:7184–7193.

276. Kumar S, Behera A, Saha P, et al. The role of Krüppel-like factor 8 in cancer biology: Current research and its clinical relevance. Biochemical Pharmacology 2021;183:114351.

277. Vliet J van, Crofts LA, Quinlan KGR, et al. Human KLF17 is a new member of the Sp/KLF family of transcription factors. Genomics 2006;87:474–482.

278. Onyango P, Koritschoner NP, Patrito LC, et al. Assignment of the gene encoding the core promoter element binding protein (COPEB) to human chromosome 10p15 by somatic hybrid analysis and fluorescence in situ hybridization. Genomics 1998;48:143–144.

279. Yoon HS, Chen X, Yang VW. Krüppel-like Factor 4 Mediates p53-dependent G1/S Cell Cycle Arrest in Response to DNA Damage. J Biol Chem 2003;278:2101–2105.

280. Yoon HS, Yang VW. Requirement of Krüppel-like Factor 4 in Preventing Entry into Mitosis following DNA Damage. J Biol Chem 2004;279:5035–5041.

281. Foster KW, Liu Z, Nail CD, et al. Induction of KLF4 in basal keratinocytes blocks the proliferation-differentiation switch and initiates squamous epithelial dysplasia. Oncogene 2005;24:1491–1500.

282. Gray S, Feinberg MW, Hull S, et al. The Krüppel-like factor KLF15 regulates the insulin-sensitive glucose transporter GLUT4. J Biol Chem 2002;277:34322–34328.

283. Uchida S, Sasaki S, Marumo F. Isolation of a novel zinc finger repressor that regulates the kidney-specific CLC-K1 promoter. Kidney Int 2001;60:416–421.

284. Gray S, Wang B, Orihuela Y, et al. Regulation of Gluconeogenesis by Krüppel-like Factor 15. Cell Metab 2007;5:305–312.

285. Takashima M, Ogawa W, Hayashi K, et al. Role of KLF15 in Regulation of Hepatic Gluconeogenesis and Metformin Action. Diabetes 2010;59:1608–1615.

286. Takeuchi Y, Yahagi N, Aita Y, et al. KLF15 Enables Rapid Switching between Lipogenesis and Gluconeogenesis during Fasting. Cell Rep 2016;16:2373–2386.

287. Prosdocimo DA, Anand P, Liao X, et al. Kruppel-like factor 15 is a critical regulator of cardiac lipid metabolism. J Biol Chem 2014;289:5914–5924.

288. Jeyaraj D, Haldar SM, Wan X, et al. Circadian rhythms govern cardiac repolarization and arrhythmogenesis. Nature 2012;483:96–99.

289. Haldar SM, Lu Y, Jeyaraj D, et al. Klf15 deficiency is a molecular link between heart failure and aortic aneurysm formation. Sci Transl Med 2010;2:26ra26.

290. Mori T, Sakaue H, Iguchi H, et al. Role of Krüppel-like Factor 15 (KLF15) in Transcriptional Regulation of Adipogenesis. Journal of Biological Chemistry 2005;280:12867–12875.

291. Han S, Han SS, Zhang R, et al. Circadian control of bile acid synthesis by a KLF15-Fgf15 axis. Nat Commun 2015;6:7231.

292. Mallipattu SK, Liu R, Zheng F, et al. Kruppel-like factor 15 (KLF15) is a key regulator of podocyte differentiation. J Biol Chem 2012;287:19122–19135.

293. Zhou L, Li Q, Chen A, et al. KLF15-activating Twist2 ameliorated hepatic steatosis by inhibiting inflammation and improving mitochondrial dysfunction via NF-κB-FGF21 or SREBP1c-FGF21 pathway. FASEB J 2019;33:14254–14269.

294. Jung DY, Chalasani U, Pan N, et al. KLF15 is a molecular link between endoplasmic reticulum stress and insulin resistance. PLoS One 2013;8:e77851.

295. Anzai K, Tsuruya K, Ida K, et al. Kruppel-like factor 15 induces the development of mature hepatocyte-like cells from hepatoblasts. Sci Rep 2021;11:18551.

296. Wade HE, Kobayashi S, Eaton ML, et al. Multimodal regulation of E2F1 gene expression by progestins. Mol Cell Biol 2010;30:1866–1877.

297. Ray S, Pollard JW. KLF15 negatively regulates estrogen-induced epithelial cell proliferation by inhibition of DNA replication licensing. Proc Natl Acad Sci U S A 2012;109:E1334-1343.

298. Zhu K-Y, Tian Y, Li Y-X, et al. The functions and prognostic value of Krüppel-like factors in breast cancer. Cancer Cell Int 2022;22:23.

299. Sun C, Ma P, Wang Y, et al. KLF15 Inhibits Cell Proliferation in Gastric Cancer Cells via Up-Regulating CDKN1A/p21 and CDKN1C/p57 Expression. Dig Dis Sci 2017;62:1518–1526.

300. Wang N, Cao Q-X, Tian J, et al. Circular RNA MTO1 Inhibits the Proliferation and Invasion of Ovarian Cancer Cells Through the miR-182-5p/KLF15 Axis. Cell Transplant 2020;29:963689720943613.

301. Sun CX, Liu BJ, Su Y, et al. MiR-181a promotes cell proliferation and migration through targeting KLF15 in papillary thyroid cancer. Clin Transl Oncol 2022;24:66–75.

302. Chen L, Jing S-Y, Liu N, et al. MiR-376a-3p alleviates the development of glioma through negatively regulating KLF15. Eur Rev Med Pharmacol Sci 2020;24:11666–11674.

303. Wang Y, Jiang F, Xiong Y, et al. LncRNA TTN-AS1 sponges miR-376a-3p to promote colorectal cancer progression via upregulating KLF15. Life Sci 2020;244:116936.

304. Gao L, Qiu H, Liu J, et al. KLF15 promotes the proliferation and metastasis of lung adenocarcinoma cells and has potential as a cancer prognostic marker. Oncotarget 2017;8:109952–109961.

305. Wang X, He M, Li J, et al. KLF15 suppresses cell growth and predicts prognosis in lung adenocarcinoma. Biomed Pharmacother 2018;106:672–677.

306. Montal R, Sia D, Montironi C, et al. Molecular classification and therapeutic targets in extrahepatic cholangiocarcinoma. J Hepatol 2020;73:315–327.

307. O'Rourke CJ, Matter MS, Nepal C, et al. Identification of a Pan-Gamma-Secretase Inhibitor Response Signature for Notch-Driven Cholangiocarcinoma. Hepatology 2020;71:196–213.

308. Chaisaingmongkol J, Budhu A, Dang H, et al. Common Molecular Subtypes Among Asian Hepatocellular Carcinoma and Cholangiocarcinoma. Cancer Cell 2017;32:57-70.e3.

309. Job S, Rapoud D, Dos Santos A, et al. Identification of Four Immune Subtypes Characterized by Distinct Composition and Functions of Tumor Microenvironment in Intrahepatic Cholangiocarcinoma. Hepatology 2020;72:965–981.

310. Banales JM, Sáez E, Uriz M, et al. Up-regulation of microRNA 506 leads to decreased Cl-/HCO3- anion exchanger 2 expression in biliary epithelium of patients with primary biliary cirrhosis. Hepatology 2012;56:687–697.

311. Perugorria MJ, Wilson CL, Zeybel M, et al. Histone methyltransferase ASH1 orchestrates fibrogenic gene transcription during myofibroblast transdifferentiation. Hepatology 2012;56:1129–1139.

312. Chen Q, Kang J, Fu C. The independence of and associations among apoptosis, autophagy, and necrosis. Sig Transduct Target Ther 2018;3:1–11.

313. Poon IKH, Hulett MD, Parish CR. Molecular mechanisms of late apoptotic/necrotic cell clearance. Cell Death Differ 2010;17:381–397.

314. Divakaruni AS, Paradyse A, Ferrick DA, et al. Analysis and interpretation of microplate-based oxygen consumption and pH data. Methods Enzymol 2014;547:309–354.

315. Wiśniewski JR. Filter-Aided Sample Preparation for Proteome Analysis. Methods Mol Biol 2018;1841:3–10.

316. Meier F, Beck S, Grassl N, et al. Parallel Accumulation–Serial Fragmentation (PASEF): Multiplying Sequencing Speed and Sensitivity by Synchronized Scans in a Trapped Ion Mobility Device. J Proteome Res 2015;14:5378–5387.

317. Meier F, Brunner A-D, Koch S, et al. Online Parallel Accumulation-Serial Fragmentation (PASEF) with a Novel Trapped Ion Mobility Mass Spectrometer. Mol Cell Proteomics 2018;17:2534–2545.

318. Szklarczyk D, Gable AL, Lyon D, et al. STRING v11: Protein-protein association networks with increased coverage, supporting functional discovery in genome-wide experimental datasets. Nucleic Acids Research 2019;47:D607–D613.

319. Huang DW, Sherman BT, Lempicki RA. Systematic and integrative analysis of large gene lists using DAVID bioinformatics resources. Nature Protocols 2009;4:44–57.

320. Babicki S, Arndt D, Marcu A, et al. Heatmapper: web-enabled heat mapping for all. Nucleic acids research 2016;44:W147–W153.

321. Karlsson M, Zhang C, Méar L, et al. A single-cell type transcriptomics map of human tissues. Sci Adv 2021;7:eabh2169.

322. Jjingo D, Conley AB, Yi SV, et al. On the presence and role of human gene-body DNA methylation. Oncotarget 2012;3:462–474.

323. Quan Y, Liang F, Deng S-M, et al. Mining the Selective Remodeling of DNA Methylation in Promoter Regions to Identify Robust Gene-Level Associations With Phenotype. Front Mol Biosci 2021;8:597513.

324. Horibata S, Vo TV, Subramanian V, et al. Utilization of the Soft Agar Colony Formation Assay to Identify Inhibitors of Tumorigenicity in Breast Cancer Cells. J Vis Exp 2015:e52727.

325. Mehrazad-Saber Z, Takeuchi Y, Sawada Y, et al. High protein diet-induced metabolic changes are transcriptionally regulated via KLF15-dependent and independent pathways. Biochem Biophys Res Commun 2021;582:35–42.

326. Chattopadhyay E, Roy B. Altered Mitochondrial Signalling and Metabolism in Cancer. Front Oncol 2017;7:43.

327. Rizvi S, Khan SA, Hallemeier CL, et al. Cholangiocarcinoma - evolving concepts and therapeutic strategies. Nat Rev Clin Oncol 2018;15:95–111.

328. Dabney RS, Khalife M, Shahid K, et al. Molecular pathways and targeted therapy in cholangiocarcinoma. Clin Adv Hematol Oncol 2019;17:630–637.

329. Ruzzenente A, Fassan M, Conci S, et al. Cholangiocarcinoma Heterogeneity Revealed by Multigene Mutational Profiling: Clinical and Prognostic Relevance in Surgically Resected Patients. Ann Surg Oncol 2016;23:1699–1707.

330. Rizvi S, Borad MJ. The rise of the FGFR inhibitor in advanced biliary cancer: the next cover of time magazine? Journal of Gastrointestinal Oncology 2016;7:789.

331. Li X, Cao X. BMP signaling and HOX transcription factors in limb development. Front Biosci 2003;8:s805-812.

332. Priya Dharshini LC, Vishnupriya S, Sakthivel KM, et al. Oxidative stress responsive transcription factors in cellular signalling transduction mechanisms. Cellular Signalling 2020;72:109670.

333. Ibar C, Irvine KD. Integration of Hippo-YAP signaling with metabolism. Dev Cell 2020;54:256–267.

334. Chronis C, Fiziev P, Papp B, et al. Cooperative Binding of Transcription Factors Orchestrates Reprogramming. Cell 2017;168:442-459.e20.

335. Safe S, Karki K. The Paradoxical Roles of Orphan Nuclear Receptor 4A (NR4A) in Cancer. Mol Cancer Res 2021;19:180–191.

336. Beckerman R, Prives C. Transcriptional Regulation by P53. Cold Spring Harb Perspect Biol 2010;2:a000935.

337. Dang CV. MYC on the Path to Cancer. Cell 2012;149:22–35.

338. Wang Y, Lu T, Sun G, et al. Targeting of apoptosis gene loci by reprogramming factors leads to selective eradication of leukemia cells. Nat Commun 2019;10:5594.

339. Illendula A, Pulikkan JA, Zong H, et al. A small-molecule inhibitor of the aberrant transcription factor CBFβ-SMMHC delays leukemia in mice. Science 2015;347:779–784.

340. Wan T, Shao J, Hu B, et al. Prognostic role of HSF1 overexpression in solid tumors: a pooled analysis of 3,159 patients. Onco Targets Ther 2018;11:383–393.

341. Yin J, Xie X, Ye Y, et al. BCL11A: a potential diagnostic biomarker and therapeutic target in human diseases. Biosci Rep 2019;39:BSR20190604.

342. Pepin ME, Ha C-M, Crossman DK, et al. Genome-wide DNA methylation encodes cardiac transcriptional reprogramming in human ischemic heart failure. Lab Invest 2019;99:371–386.

343. Pei J, Schuldt M, Nagyova E, et al. Multi-omics integration identifies key upstream regulators of pathomechanisms in hypertrophic cardiomyopathy due to truncating MYBPC3 mutations. Clin Epigenetics 2021;13:61.

344. Yang L, Wei Q-M, Zhang X-W, et al. MiR-376a promotion of proliferation and metastases in ovarian cancer: Potential role as a biomarker. Life Sci 2017;173:62–67.

345. Zhao T, Qiu Z, Gao Y. MiR-137-3p exacerbates the ischemia-reperfusion injured cardiomyocyte apoptosis by targeting KLF15. Naunyn Schmiedebergs Arch Pharmacol 2020;393:1013–1024.

346. Chen T, Lei S, Zeng Z, et al. MicroRNA-137 suppresses the proliferation, migration and invasion of cholangiocarcinoma cells by targeting WNT2B. Int J Mol Med 2020;45:886–896.

347. Lim S, Kaldis P. Cdks, cyclins and CKIs: roles beyond cell cycle regulation. Development 2013;140:3079–3093.

348. Rhind N, Russell P. Tyrosine phosphorylation of cdc2 is required for the replication checkpoint in Schizosaccharomyces pombe. Mol Cell Biol 1998;18:3782–3787.

349. Zhang J, Zhong H-B, Lin Y, et al. KLF15 suppresses cell proliferation and extracellular matrix expression in mesangial cells under high glucose. Int J Clin Exp Med 2015;8:20330–20336.

350. Yoda T, McNamara KM, Miki Y, et al. KLF15 in breast cancer: a novel tumor suppressor? Cell Oncol (Dordr) 2015;38:227–235.

351. Noack C, Zafiriou M-P, Schaeffer H-J, et al. Krueppel-like factor 15 regulates Wnt/β-catenin transcription and controls cardiac progenitor cell fate in the postnatal heart. EMBO Mol Med 2012;4:992–1007.

352. Wang B, Xu H, Kong J, et al. Krüppel-Like Factor 15 Reduces Ischemia-Induced Apoptosis Involving Regulation of p38/MAPK Signaling. Human Gene Therapy 2021;32:1471–1480.

353. Wood MA, McMahon SB, Cole MD. An ATPase/Helicase Complex Is an Essential Cofactor for Oncogenic Transformation by c-Myc. Molecular Cell 2000;5:321–330.

354. Shin SH, Lee JS, Zhang J-M, et al. Synthetic lethality by targeting the RUVBL1/2-TTT complex in mTORC1-hyperactive cancer cells. Sci Adv 2020;6:eaay9131.

355. Hsu K-W, Hsieh R-H, Lee Y-HW, et al. The Activated Notch1 Receptor Cooperates with α-Enolase and MBP-1 in Modulating c-myc Activity. Mol Cell Biol 2008;28:4829–4842.

356. Subramanian A, Miller DM. Structural analysis of alpha-enolase. Mapping the functional domains involved in down-regulation of the c-myc protooncogene. J Biol Chem 2000;275:5958–5965.

357. Cui C, Ren X, Liu D, et al. 14-3-3 epsilon prevents G2/M transition of fertilized mouse eggs by binding with CDC25B. BMC Dev Biol 2014;14:33.

358. Konishi H, Nakagawa T, Harano T, et al. Identification of frequent G(2) checkpoint impairment and a homozygous deletion of 14-3-3epsilon at 17p13.3 in small cell lung cancers. Cancer Res 2002;62:271–276.

359. Kosaka Y, Cieslik KA, Li L, et al. 14-3-3ε plays a role in cardiac ventricular compaction by regulating the cardiomyocyte cell cycle. Mol Cell Biol 2012;32:5089–5102.

360. Liu M, Yu T, Li M, et al. Apoptosis repressor with caspase recruitment domain promotes cell proliferation and phenotypic modulation through 14-3-3ε/YAP signaling in vascular smooth muscle cells. J Mol Cell Cardiol 2020;147:35–48.

361. Ren F, Zhang L, Jiang J. Hippo signaling regulates Yorkie nuclear localization and activity through 14-3-3 dependent and independent mechanisms. Dev Biol 2010;337:303–312.

362. Sugihara T, Isomoto H, Gores G, et al. YAP and the Hippo pathway in cholangiocarcinoma. J Gastroenterol 2019;54:485–491.

363. Desplat A, Penalba V, Gros E, et al. Piezo1–Pannexin1 complex couples force detection to ATP secretion in cholangiocytes. J Gen Physiol 2021;153:e202112871.

364. Hirata Y, Nomura K, Kato D, et al. A Piezo1/KLF15/IL-6 axis mediates immobilization-induced muscle atrophy. J Clin Invest 2022;132. Available at: https://www.jci.org/articles/view/154611 [Accessed June 16, 2022].

365. Zhu B, Qian W, Han C, et al. Piezo 1 activation facilitates cholangiocarcinoma metastasis via Hippo/YAP signaling axis. Mol Ther Nucleic Acids 2021;24:241–252.

366. Chung BK, Karlsen TH, Folseraas T. Cholangiocytes in the pathogenesis of primary sclerosing cholangitis and development of cholangiocarcinoma. Biochimica et Biophysica Acta (BBA) - Molecular Basis of Disease 2018;1864:1390–1400.

367. Loeuillard E, Fischbach SR, Gores GJ, et al. Animal Models of Cholangiocarcinoma. Biochim Biophys Acta Mol Basis Dis 2019;1865:982–992.

368. Wang Z, Zhou Z, Zhang Y, et al. Diacylglycerol kinase epsilon protects against renal ischemia/reperfusion injury in mice through Krüppel-like factor 15/klotho pathway. Renal Failure 2022;44:902.

369. Xie B, Chen J, Liu B, et al. Klotho acts as a tumor suppressor in cancers. Pathol Oncol Res 2013;19:611–617.

370. Tang X, Wang Y, Fan Z, et al. Klotho: a tumor suppressor and modulator of the Wnt/β-catenin pathway in human hepatocellular carcinoma. Lab Invest 2016;96:197–205.

371. Liu H, Fergusson MM, Castilho RM, et al. Augmented Wnt signaling in a mammalian model of accelerated aging. Science 2007;317:803–806.

372. Yang H-G, Wang T, Hu S, et al. Long Non-coding RNA SNHG12, a New Therapeutic Target, Regulates miR-199a-5p/Klotho to Promote the Growth and Metastasis of Intrahepatic Cholangiocarcinoma Cells. Front Med (Lausanne) 2021;8:680378.

373. Ito S, Kinoshita S, Shiraishi N, et al. Molecular cloning and expression analyses of mouse βklotho, which encodes a novel Klotho family protein. Mechanisms of Development 2000;98:115–119.

374. Gao L, Guo Y, Liu X, et al. KLF15 protects against isoproterenol-induced cardiac hypertrophy via regulation of cell death and inhibition of Akt/mTOR signaling. Biochem Biophys Res Commun 2017;487:22–27.

375. Hou Z, O'Connor C, Frühauf J, et al. Regulation of differential proton-coupled folate transporter gene expression in human tumors: transactivation by KLF15 with NRF-1 and the role of Sp1. Biochem J 2019;476:1247–1266.

376. Herraez E, Sanchez-Vicente L, Macias RIR, et al. Usefulness of the MRP2 promoter to overcome the chemoresistance of gastrointestinal and liver tumors by enhancing the expression of the drug transporter OATP1B1. Oncotarget 2017;8:34617–34629.

377. Yamasaki M, Makino T, Masuzawa T, et al. Role of multidrug resistance protein 2 (MRP2) in chemoresistance and clinical outcome in oesophageal squamous cell carcinoma. British Journal of Cancer 2011;104:707.

378. Chen X, Zhang Q, Dang X, et al. Targeting the CtBP1-FOXM1 transcriptional complex with small molecules to overcome MDR1-mediated chemoresistance in osteosarcoma cancer stem cells. Journal of Cancer 2021;12:482.

379. Mustafi SB, Chakraborty PK, Naz S, et al. MDR1 mediated chemoresistance: BMI1 and TIP60 in action. Biochimica et biophysica acta 2016;1859:983.

380. Zollner G, Wagner M, Fickert P, et al. Hepatobiliary transporter expression in human hepatocellular carcinoma. Liver International 2005;25:367–379.

381. Han S, Ray JW, Pathak P, et al. KLF15 regulates endobiotic and xenobiotic metabolism. Nat Metab 2019;1:422–430.

382. Fan L, Sweet DR, Prosdocimo DA, et al. Muscle Krüppel-like factor 15 regulates lipid flux and systemic metabolic homeostasis. J Clin Invest 2021;131:139496.

383. Aggarwal A, Costa MJ, Rivero-Gutiérrez B, et al. The circadian clock regulates adipogenesis by a Per3 crosstalk pathway to Klf15. Cell Rep 2017;21:2367–2375.

384. Fan L, Sweet DR, Fan EK, et al. Transcription factors KLF15 and PPARδ cooperatively orchestrate genome-wide regulation of lipid metabolism in skeletal muscle. Journal of Biological Chemistry 2022;298. Available at: https://www.jbc.org/article/S0021-9258(22)00366-0/abstract [Accessed June 15, 2022].

385. Prosdocimo DA, John JE, Zhang L, et al. KLF15 and PPARα Cooperate to Regulate Cardiomyocyte Lipid Gene Expression and Oxidation. PPAR Res 2015;2015:201625.

386. Nabatame Y, Hosooka T, Aoki C, et al. Kruppel-like factor 15 regulates fuel switching between glucose and fatty acids in brown adipocytes. J Diabetes Investig 2021;12:1144–1151.

387. Jeyaraj D, Scheer FAJL, Ripperger JA, et al. Klf15 orchestrates circadian nitrogen homeostasis. Cell Metab 2012;15:311–323.

388. Read JA, Winter VJ, Eszes CM, et al. Structural basis for altered activity of M- and H-isozyme forms of human lactate dehydrogenase. Proteins 2001;43:175–185.

389. Adachi K, Yamasawa S. Quantitative histochemistry of the primate skin. IX. Phosphoglycerate kinase and phosphoglycerate mutase. J Invest Dermatol 1967;49:22–30.

390. Fothergill-Gilmore LA, Watson HC. The phosphoglycerate mutases. Adv Enzymol Relat Areas Mol Biol 1989;62:227–313.

391. Hitosugi T, Zhou L, Elf S, et al. Phosphoglycerate mutase 1 coordinates glycolysis and biosynthesis to promote tumor growth. Cancer Cell 2012;22:585–600.

392. Christman JK. 5-Azacytidine and 5-aza-2’-deoxycytidine as inhibitors of DNA methylation: mechanistic studies and their implications for cancer therapy. Oncogene 2002;21:5483–5495.

393. Howell PM, Liu Z, Khong HT. Demethylating Agents in the Treatment of Cancer. Pharmaceuticals (Basel) 2010;3:2022–2044.

394. Hourigan CS, Karp JE. Development of therapeutic agents for older patients with acute myelogenous leukemia. Curr Opin Investig Drugs 2010;11:669–677.

395. Sharma S, Kelly TK, Jones PA. Epigenetics in cancer. Carcinogenesis 2010;31:27–36.

396. Momparler RL. Pharmacology of 5-Aza-2’-deoxycytidine (decitabine). Semin Hematol 2005;42:S9-16.

397. Gao C, Wang J, Li Y, et al. Incidence and risk of hematologic toxicities with hypomethylating agents in the treatment of myelodysplastic syndromes and acute myeloid leukopenia: A systematic review and meta-analysis. Medicine (Baltimore) 2018;97:e11860.

398. Gaudet F, Hodgson JG, Eden A, et al. Induction of tumors in mice by genomic hypomethylation. Science 2003;300:489–492.

399. Howard G, Eiges R, Gaudet F, et al. Activation and transposition of endogenous retroviral elements in hypomethylation induced tumors in mice. Oncogene 2008;27:404–408.

400. Ghaleb AM, Aggarwal G, Bialkowska AB, et al. Notch inhibits expression of the Krüppel-like factor 4 tumor suppressor in the intestinal epithelium. Mol Cancer Res 2008;6:1920–1927.

401. Rowland BD, Bernards R, Peeper DS. The KLF4 tumour suppressor is a transcriptional repressor of p53 that acts as a context-dependent oncogene. Nat Cell Biol 2005;7:1074–1082.

402. Erice O, Labiano I, Arbelaiz A, et al. Differential effects of FXR or TGR5 activation in cholangiocarcinoma progression. Biochim Biophys Acta Mol Basis Dis 2018;1864:1335–1344.

403. Santos-Laso A, Izquierdo-Sanchez L, Rodrigues PM, et al. Proteostasis disturbances and endoplasmic reticulum stress contribute to polycystic liver disease: New therapeutic targets. Liver Int 2020;40:1670–1685.

404. Lee-Law PY, Olaizola P, Caballero-Camino FJ, et al. Targeting UBC9-mediated protein hyper-SUMOylation in cystic cholangiocytes halts polycystic liver disease in experimental models. J Hepatol 2021;74:394–406.

Appendix

Publications during the PhD

1. Rodrigues, P.M., Olaizola, P., **Paiva, N.A.**, Olaizola, I., Agirre-Lizaso, A., Landa, A., Bujanda, L., Perugorria, M.J., Banales., J.M., 2020. Pathogenesis of Cholangiocarcinoma. Annu. Rev. Pathol. Mech. Dis. 2021;16:annurev-pathol-030220-020455.

2. Macias, R.I.R., Kornek, M., Rodrigues, P.M., **Paiva, N.A.**, Castro, R.E., Urban, S, Pereira, S.P., Cadamuro, M., Rupp, C., Loosen, S.H., Luedde, T., Banales, J.M., 2019. Diagnostic and prognostic biomarkers in cholangiocarcinoma. Liver International. 39 Suppl 1, 108-122. https://doi.org/10.1111/liv.14090

3. Rodrigues, P.M., Olaizola, P., **Paiva, N.A.**, Perugorria, M.J., Banales. 2019. Intrahepatic Cholangiocarcinoma – the emerging entity. *Therapy in Liver Diseases*, Elsevier. Spain.

4. Ruiz de Gauna, M., Biancaniello, F., González-Romero, F., Rodrigues, P.M., Lapitz, A., Gómez-Santos, B., Olaizola, P., Di Matteo, S., Aurrekoetxea, I., Labiano, I., Nieva-Zuluaga, A., Benito-Vicente, A., Perugorria, M.J., Apodaka-Biguri, M., **Paiva, N.A.**, Sáenz de Urturi, D., Buqué, X., Delgado, I., Martín, C., Azkargorta, M., Elortza, F., Calvisi, D.F., Andersen, J.B., Alvaro, D., Cardinale, V., Bujanda, L., Banales, J.M., Aspichueta, P., 2022. Cholangiocarcinoma progression depends on the uptake and metabolization of extracellular lipids. Hepatology. 0, 1-18. https://doi.org/10.1002/hep.32344